NOTICE: This is the author's version of a work that was accepted for publication in Marine and Petroleum Geology. Changes resulting from the publishing process, such as peer review, editing, corrections, structural formatting, and other quality control mechanisms may not be reflected in this document. Changes may have been made to this work since it was submitted for publication. A definitive version was subsequently published in Marine and Petroleum Geology, Vol. 44, 2013. DOI: http://dx.doi.org/10.1016/j.marpetgeo.2013.02.018

Development of a Papua New Guinean onshore carbonate reservoir: a comparative borehole image (FMI) and petrographic evaluation

Moyra E.J. Wilson[1*], Dale Lewis[2], O'Karo Yogi[3], David Holland[4], Louise Hombo[3, 5], & Adrian Goldberg[4, 6]

1 – Department of Applied Geology, Curtin University, GPO U1987, Perth WA 6845 Australia. E-mail: m.wilson@curtin.edu.au

2 – Schlumberger Oilfield Australia Pty. Ltd., Perth WA 6850 Australia

3 – SPI (208) Ltd., Port Moresby, Papua New Guinea

4 – InterOil Australia Pty. L–td., Cairns, QLD 4870, Australia

5 – Present address: National Petroleum Company, PNG (NPCP), PO Box 320, Port Moresby, NCD, Papua New Guinea

6 – Present address: Eni Australia, PO Box 6862 East Perth, WA 6862 Australia

* – corresponding author

Abstract

The depositional and diagenetic controls on carbonate platform evolution are notoriously heterogeneous and difficult to determine from standard subsurface wireline logging techniques. Here, a combined borehole image (FMI – Fullbore Formation MicroImager), and petrographic study allowed evaluation of depositional and diagenetic trends across an Australasian subsurface buildup that is a major recent gas discovery. The Elk and Antelope gas fields are hosted in Tertiary reefal, platformal and associated deepwater carbonates in the present day foothills region of the Fold and Thrust Belt in the Gulf Province of Papua New Guinea.

A full suite of FMI logs (> 2800 m), and 292 thin sections (mainly from sidewall cores and cuttings) from both platform flank and shallow water deposits were evaluated during this study. Despite the obvious scale differences between the datasets there was some correlation between the independent petrography and FMI studies for: a) picking major facies boundaries, and b) interpretation of depositional environments, the latter particularly for slope and deep water deposits. However, thin section petrography proved critical in understanding primary depositional textures and secondary alteration features through the shallow-water carbonates where complex diagenetic overprinting had strongly impacted original fabric, and/or in regions affected by "gas smearing". The petrographic study allowed more detailed examination of diagenesis and its impact on rock fabric (which links to the FMI textures). Component analysis and depositional textures identified in thin section are good indicators of original depositional environment. Full FMI coverage allowed textural definition on a dm/m scale, identification and characterisation of vertical changes, and likely large-scale variations in depositional environments and sequences. It was clear from combining the results of the two studies that diagenesis as well as depositional fabric had a strong impact on resultant FMI facies. The diagenetic overprinting would have been difficult to extract from the FMI data without the benefit of the petrographic work. This study shows the merits of selective petrographic analysis to calibrate the quality of facies interpretation from FMI images, and proved critical for enhancing and in places revising initial FMI interpretations.

Introduction

The depositional and diagenetic properties that control the reservoir quality of carbonate rocks are notoriously heterogeneous and difficult to predict from standard subsurface logging techniques (Nurmi *et al.,* 1990; Akbar *et al.,* 1995). In particular, many depositional and diagenetic facies are often not clearly defined by standard logs because of decimetre-scale averaging of many logging tools (Nurmi *et al.,* 1990). In recent years,

borehole imagery is being widely used to help evaluate reservoir properties and the influence that depositional and diagenetic factors have on the variability of porosity and permeability development in carbonate systems (Akbar *et al.,* 1995; 2000/2001; Russell *et al.,* 2002; Ahr *et al.,* 2005). Key to the interpretation of carbonate systems, electrical borehole imaging brings the advantages that: (a) many depositional and diagenetic facies have distinctive fabrics, (b) near complete, centimetre-scale 3-D imaging is produced around the borehole, (c) fabrics relating to facies may be quantified during processing, and (d) individual identifiable rock grains or pores may be delineated and quantified through advanced processing (Akbar *et al.,* 1995; Schlumberger, 2004). However, some have cautioned against the interpretation of borehole images in isolation from other subsurface data since this imagery: (a) only indirectly reflects porosity, fluid and mineralogical variations, (b) coalesces the combined response of depositional and diagenetic fabrics, (c) is commonly specific to wells drilled or filled with either water- or oil-based muds, (d) is sensitive to the rugosity of the borehole, and (e) may be adversely affected by factors such as gas-smearing or 'wash-out' (Nurmi *et al.,* 1990; Akbar *et al.,* 1995). Despite this, in uncored carbonate wells electrical images may be used as the primary interpretational tool, due to difficulties in evaluating standard wireline logs and because cuttings provide limited rock data over thick intervals. With the advent of quality rotary sidewall coring there is now the potential to calibrate and compare electrical images directly with depth-calibrated rock and petrographic data. Herein, we test to what extent a combined thin section and borehole imaging study of carbonate systems will allow enhanced definition of micro- to metre-scale variations in depositional and diagenetic character that in turn control reservoir properties. Also, it is inferred that through such a combined study it will be possible to draw meaningful interpretations about the depositional and post-depositional evolution of carbonate systems through distinguishing a wide range of carbonate deposits (from shallow to bathyal environments) affected by highly variable diagenetic alteration.

Here, a combined detailed FMI (Fullbore Formation MicroImager) and petrographic study allowed evaluation of depositional and diagenetic trends on rock properties across an Australasian subsurface buildup that is a major recent gas discovery. The Elk and Antelope gas fields are hosted in Tertiary reefal, platformal and associated deepwater carbonates in the present day foothills region of the Fold and Thrust Belt in the Gulf Province of Papua New Guinea (PNG: Figures 1 and 2). Four wells were drilled with near complete coverage of FMI (>2800 m) and thin sections (>250 from rotary sidewall core plugs) across shallow platform to reefal buildup (Antelope-1 and -2 wells) and deeper water platform slope and bathyal deposits (Elk-1 and -2 wells). It was particularly pertinent to fully characterise the depositional and diagenetic trends and their impacts on reservoir development in the Elk-Antelope system since: (a) PNG is an underexplored frontier area in which controls on reservoir development are poorly understood, (b) limited fullbore coring was conducted (Elk-2 and Antelope-2), (c) seismic imaging of the carbonate system in this structurally complex region produced results that were extremely challenging to interpret, and (d) standard wireline logs did not reveal the marked heterogeneities in the system (Goldberg and Holland, 2008; Goldberg *et al.,* 2010).

Geological setting

The Elk and Antelope gas fields are hosted in Tertiary reefal, platformal and associated deep water carbonates. The fields lie at the leading edge of the New Guinea Orogen (NGO) as defined by Pigram & Davies (1987), Struckmeyer *et al.* (1993) and Davies *et al.* (1996). The NGO is the collisional zone between the relatively stable Australian cratonic area in the southwest and the islands and ranges constructed by Cenozoic volcanic activity in the northeast. The Elk/Antelope fields are located at the junction of the two dominant fold belt trends with the Papuan Fold Belt to the west and the Aure Tectonic Belt to the east (Figure 1).

Extensive 2-D seismic coverage in combination with airborne gravity and magnetic surveys over the fields established the structures on which five wells were drilled. Currently, two wells have been drilled in the Elk Field (Elk-1 and Elk-2) and three in the Antelope Field (Figure 2; Elk-4, Antelope-1 and Antelope-2). Carbonates in the Elk Field consist of deep-water platform slope and bathyal deposits. Carbonate facies in the Elk-4 well are similar to those from the Elk Field. In comparison, the Antelope wells penetrate shallow platform to reefal-buildup deposits. The slope deposits encountered in the Elk wells originally flanked the contemporaneous shallow-water carbonate development of the Antelope wells. Post-deposition, carbonates in the Elk Field have been structurally separated, and displaced up-section, from those in the Antelope Field by a WSW-ENE trending, SSE verging thrust (Figure 2). The combined Elk/Antelope fields have approximate dimensions of 15 kilometres (9 miles; N to S) long by 5 kilometres (3 miles; E to W) wide with a gas column of >600 m (>2,000 ft) in the carbonate section (Harris *et al*., 2009). Carbonates penetrated by the wells are the Eocene to Lower Oligocene Mendi (Limestone) Group, Oligo-Miocene Darai Group equivalent (neritic with some reworking) and the Upper Oligocene to Miocene Puri Limestone Formation (bathyal to outer neritic: Pigram *et al.*, 1989; Goldberg and Holland, 2008). The thickness of shallow-water carbonates is at least 960 m (encountered in Antelope-1: the well with maximal stratal penetration).

The carbonates are overlain by a thick, clay-rich mudstone (Orubadi Formation (or Orubadi Beds); cf. Pigram *et al*., 1989; Goldberg and Holland, 2008) containing abundant planktonic foraminifera of latest Miocene to earliest Pliocene age. The known thickness of the Orubadi Formation in the vicinity of the fields varies from 1000 to around 2000 m, although there has been significant post-depositional erosion associated with fold and thrust belt development (Goldberg and Holland, 2008). In the Elk field, there is a gradational down-sequence change from mudstones of the Orubadi Formation to marls and then carbonate. In the Antelope field, no marl is present and the Orubadi Beds directly overlie the

carbonate. All wells were terminated in the carbonate section; and the lithology below the reservoir is therefore unknown.

Methodology

A full suite of FMI logs (2873 m) and 292 thin sections from shallow water, platform flank and basinal deposits of the Elk – Antelope system were evaluated. Limited fullbore core was also available from Elk-2 (Core 1: 2658–2661.16 m, Core 2: 2708.66–2710.0 m) and Antelope-2 (Core 1: 1835.06–1840.49 m, Core 2: 1846.09–1881.85 m, Core 3: 2184.0–2193.27 m, Core 4: 2337.9–2351.84 m). Petrographic and FMI analyses were undertaken independently since the FMI images were available before the thin sections, with the results then compared and integrated. FMI intervals studied and numbers of thin sections (TS) for each of the wells are: (a) Elk-1 – 1630–1840 m (210 m in total) & 7 TS, (b) Elk-2 – 2204–3325 m (1121 m in total) & 32 TS, (c) Antelope-1 – 1731–2455 m (724 m in total) & 130 TS, and (d) Antelope-2 – 1812–2450 m (818 m in 4 runs) & 123 TS. Additional geochemical and microscopy data from the Elk-Antelope system utilised in the full diagenetic interpretation will be published elsewhere.

Borehole image logs supply geoscientists with high-resolution records of rock properties and characteristics along the borehole wall (Lagraba *et al.,* 2010). They provide a computer generated image based on geophysical measurements of acoustic reflectivity or of electrical conductivity, and represent formation response at the borehole wall, giving a continuous vertical record of the borehole circumference (Rider, 2002). Wireline-based resistivity imaging tools are configured with various arms each of which consists of a pad (and possibly an associated flap) that contains sensors which when pressed against the borehole wall record electrical current that was emitted from the sensors of the tool into the formation (Lagraba *et al.,* 2010). Schlumberger's Fullbore Formation MicroImager (FMI) is a wireline-based microresistivity formation imager used in water-based muds, which uses 192 microresistivity buttons spaced along four pads and flaps to generate a high (0.2 inch)

resolution borehole image with an 80% borehole coverage in 8 inch wells (Schlumberger, 2004). During processing, borehole images are subjected to various stages of a processing workflow, the most important of which are speed correction and image orientation using high-resolution accelerometer and magnetometer data, the mapping of a colour scale to resistivity values, and the use of filtering/enhancements to remove non-geological artifacts. Image quality can be affected by the presence of artifacts related to logging activities (e.g., stick-slip effects), borehole wall conditions (e.g., rugosity, washout, breakouts), processing (e.g., pad mismatching) or the geological formation (e.g., halo effects around pyrite nodules; García-Carballido *et al.,* 2010). Borehole images are typically presented in "unwrapped borehole" format with the cylindrical borehole surface log unzipped at the north azimuth and unrolled to a flat strip, on which straight dipping surfaces are represented by sinusoids (Rider, 2002).

The interpretation of borehole image logs provides directional sedimentological and structural information which can provide high-resolution data to integrate into reservoir and geomechanical models (García-Carballido *et al.,* 2010). The sedimentary interpretation of electrical image logs tends to follow routines similar to those used in a purely sedimentological analysis, building up through lithology, texture, and sedimentary structures to facies and eventually sequences (Rider, 2002). It should, however, be recognised that any information from downhole images reflects the combined electrical response of downhole variations in mineralogy, textures, pore systems and fluids. In addition to their use in sedimentary interpretation, image logs have been used for various quantitative analyses in carbonate reservoir characterisation, particularly in porosity and permeability analysis of vuggy carbonate reservoirs (Nurmi *et al.,* 1990; Chitale *et al.,* 2010; Xu, 2010). With many productive carbonates having dual porosity systems, Newberry *et al.* (1996) developed a technique for transforming electrical images into porosity maps of the borehole, allowing partitioning into primary (matrix) and secondary (vuggy) porosity. Russell *et al.* (2002) developed a methodology using electrical image logs and conventional log data to

characterise and extrapolate geological heterogeneity that provided permeability prediction (via vug connectivity) when applied to the Shuaiba reservoir of Oman.

Following acquisition and loading, the FMI data used in this study underwent environmental quality control and correction (including depth correction). Processing and interpretation of the FMI image data was completed by D. Lewis at Schlumberger; initially in an automated (default settings) way and with further refinement to improve image quality. Image enhancement prior to graphical display was through optimisation of the usage of colours via two methods: (a) static normalisation that is a global optimisation, and (b) dynamic normalisation that is a local optimisation using a sliding window. Borehole wall conditions were also assessed as to how they may have affected FMI image quality. Although borehole washouts were common in the Elk and Antelope wells, only in Antelope-2 does this appear to have significantly affected image quality, though pad contact remained good. In the upper parts of the Antelope wells gas smearing had adversely affected the quality of the image logs, a problem for which there is no correction. This is caused by gas in the borehole obscuring the formation by increasing resistivity between the pads and the borehole wall.

On the FMI images geological features such as bed boundaries, unconformities, fractures and potential sedimentary structures were identified and where appropriate their dips evaluated. FMI facies were defined using: the visual appearance of the image, *BorTex*-calculated textural outputs, and associated *FEQL*-calculated petrophysical outputs. *BorTex* is a *Geoframe* borehole image texture analysis application that was used in this study to calculate: (a) the overall conductivity ("Background Conductivity") of the image, (b) bedding density ("Lamination Density") using vertical changes in conductivity, (c) heterogeneity of resistive and conductive spots/patches ("Resistive versus Conductive inclusions"), and (d) connectiveness of conductive spots/patches ("Connectivity Index Coefficient") that provide an indication of permeability. *FEQL* (Formation Evaluation Quick Look) is a Schlumberger

petrophysical process, which provided lithology, porosity and clay content information used to help define the FMI facies. *FEQL* does not use image data and was undertaken “in-house” at Schlumberger utilizing the petrophysical data obtained via wireline logging, either in tools run in the same tool string as the FMI, or in other runs (usually the first tool run collects the main petrophysical data). Gamma Ray, Resistivity, Density, Porosity, Sonic, PEF (Photoelectric Factor) data were combined from a number of different runs and correlated in depth for each well. Although *FEQL* is produced independently of the FMI image interpretation, “outputs” that include lithology, porosity, fluid- and clay-content data are often used as "inputs" for the FMI image interpretation.

For the FMI facies nomenclature, textural terms are subjective and based only on visual FMI image appearance. Fine-grained FMI textures refer to smooth image appearance in which grains are below image resolution pixel size (<1.5 cm); whereas, coarse-grained textures refer to granular image appearance with resolvable grains (>1.5 cm). “Conglomerate” refers to images in which individual “clasts” are visible with no internal order; whereas, “boundstone” refers to such conglomerate in which an internal fabric is also visible. Laminated or thinly-bedded facies have a “Lamination Density” of >10/m; whereas, for medium- to thickly-bedded facies it is <10/m. Since the borehole images are a combined response to mineralogy, porosity, fluid and textural variations, FMI facies were subdivided to best capture lithological, textural and petrophysical properties (although variations in reservoir quality are not addressed here). Following identification of individual FMI facies the logging sequence was divided into a number of composite facies or zonations based on a common assemblage or dominance of certain FMI facies.

Petrography of 292 thin sections, mainly from sidewall cores and cuttings, allowed determination of carbonate components, microfacies, environmental interpretations and diagenetic evaluations (Appendix 1). Samples were stained with Alizarin Red S and potassium ferricyanide to allow differentiation of ferroan and non-ferroan calcite, as well as dolomite (Dickson, 1965; 1966). Facies nomenclature follows the textural classification

scheme of Dunham (1962), modified by Embry and Klovan (1971), with components given in lithology names where they exceed 10–15%. Nomenclature on carbonate cement geometries follows Flügel (2004). Age dating of samples was undertaken via foraminiferal biostratigraphy and strontium isotope analysis, although these results are not discussed in detail here (Haig, pers. comm., 2010; Allan, pers. comm., 2011; following van der Vlerk and Umbgrove, 1927; Blow, 1969; 1979; Adams, 1970; McArthur *et al.,* 2001; Lunt and Allan, 2004; McArthur and Howarth, 2004). Initial interpretations of the FMI and petrology were compared, and the results of both datasets combined to provide an overall depositional and diagenetic evaluation.

Elk-1 and 2 wells: FMI facies and their downhole distribution

A similar suite of FMI facies were defined for the Elk-1 and 2 wells, for which all dating of samples yielded Miocene ages (Figures 3 and 4). Four FMI facies were common to both wells, with an additional two and three defined in just the Elk-1 and Elk-2 wells, respectively (see Table 1 for FMI-facies characteristics). Out of the FMI facies, marls are common at the top of the Elk-1 and -2 wells (Figure 3 and 4) and were defined as a limestone with >35 % clay content (from *FEQL*) that has high overall conductivity (Figure 5b)[1]. Overall the texture of the marls on the FMI images appears smoother than other facies, but subequal amounts of thin to medium conductive and resistive beds and faint

[1]In the Elk and Antelope wells the Gamma Ray response is not always a reflection of clay content, since locally the carbonates are “hot” (see directly below). In the Elk-1 well the Accelerator Porosity Sonde (APS – neutron porosity tool) Formation Capture Cross-Section (SIGF) results for clays is high and for carbonates and gas is low. Therefore the SIGF results, through *FEQL* processing, provided the data for clay volumes (Vclay), i.e. the output for the lithology column in Figure 3. Partly because of this anomalous Gamma Ray response the Photoelectric factor tool (PEF) was run in wells subsequent to Elk-1. PEF revealed that some of the high gamma response zones contain dolomite, and this was fully corroborated through thin section petrography (see Antelope wells results and interpretation). Spectral gamma response, from tools run in Elk-2 and the Antelope wells, revealed that dolomitised intervals are locally Uranium-rich (causing the “hot” response). Although not shown in the lithology column for the Elk-1 well (Figure 3), the high gamma response in the interval 1810-1819 m may correspond to dolomite content. Dolomite content as identified during *FEQL* processing is shown in the lithology columns for Elk-2, Antelope-1 and -2 wells in which the PEF tool was run (Figures 4, 8 and 9).

lamination were observed. Below, and interbedded with, the marls in the upper parts of the imaged Elk-1 and -2 successions argillaceous laminated thinly bedded limestone, and in the case of Elk-1 nodular and argillaceous limestones, predominate to depths of 1709 and 2671 m, respectively (Figures 3 and 4). The argillaceous laminated-thinly bedded limestone consists of laminated to thinly interbedded limestone, characterised by a lamination density usually >10 lamina/m, and a clay content >10 % (from *FEQL*), with moderate conductivity (Figure 5d). Subequal amounts of thin resistive beds and conductive laminations or thin beds have clearer definition than in the marls, but are less well-defined than in the laminated-thinly bedded limestone (see paragraph below). The nodular and argillaceous limestone FMI facies is similar to the argillaceous facies described directly above, although clay content may drop below 10 % and resistive beds with a nodular, irregular to wavy texture commonly outweigh conductive ones (Figure 6c).

Laminated-thinly bedded limestone FMI facies dominate in the middle part of the imaged section of both wells (1709–1792 m in Elk-1 and 2671–2925 m in Elk-2; Figures 3 and 4). This facies consists of thin resistive beds of limestone interbedded with very thin conductive laminations; overall conductivity is low and lamination density high (>10 lamina/m; Figure 6a). A clay content of <10 % has been used to artificially set the boundary between the laminated and argillaceous laminated-thinly bedded limestone and there is some interdigitation of the two facies in the upper part of Elk-2 (Figure 4). In the lower middle portion of Elk-1 minor units of the argillaceous and nodular facies, as well as a mottled bioturbated limestone are also present (Figure 3). The mottled/bioturbated limestone was only seen in Elk-1 and has a distinctive appearance consisting of thick to massive resistive limestone beds with a crushed ‘meshwork’ fabric (Figure 6g). Within the middle portion of Elk-2 beds of fine-medium or coarse limestone conglomerate/breccia and medium-thickly bedded limestone are also present (Figure 4). The fine-medium limestone conglomerate/breccia consists of ‘medium-sized’, well-defined resistive clasts that contrast markedly with a conductive matrix (Figure 7a). Clasts vary from granule to pebble grade, but

are mostly in the pebble grade, and vary from angular to rounded. Matrix-dominated textures predominate and layering via clast alignment may be visible.

The basal part of the imaged section of Elk-1 (1792–1822 m) consists of medium-thickly bedded limestone (Figure 3). This medium bedded FMI facies consists of medium to thick resistive limestone beds with fine conductive interlaminations, and a lamination density usually <10 lamina/m (although fracturing may artificially enhance lamination density; Figure 6e). This medium bedded facies is also present as minor interbeds in the middle portion of Elk-1 and the middle to lower imaged part of Elk-2 (Figures 3 and 4). The basal portion of Elk-2 consists predominantly of a coarse limestone conglomerate/breccia (2925–3241 m) and in its lowermost part a strongly dolomitised/altered limestone (3241-3310 m; Figure 4). The coarse conglomerate/breccia is similar to the fine-medium limestone conglomerate/breccia described above except that clasts vary from granule to cobble grade, but are mostly in the upper pebble to cobble grade, with some having blurred margins (Figure 7e). Matrix-supported textures are most common, although the ratio of clasts to matrix varies considerably and clast-supported textures are also locally seen. Minor interbeds of the coarse limestone conglomerate/breccia are also present in the middle imaged part of Elk-2. Units of the fine-medium limestone conglomerate/breccia, laminated and medium-thickly bedded limestone interbed with the coarse limestone conglomerate/breccia in the upper basal part of Elk-2 (Figure 4). The strongly dolomitised/altered limestone conglomerate/breccia is very similar to the coarse limestone conglomerate/breccia FMI facies described directly above except that the boundaries between clasts and matrix are blurred, and dolomite is usually indicated on *FEQL* (Figure 7h).

Elk-1 and 2 wells: Initial interpretation from FMI data

On the basis of their clay content, generally smooth appearance (and inferred fine grained nature) together with plane parallel lamination the marl, argillaceous and laminated-

thinly bedded limestone FMI facies are all interpreted as low energy deposits. Considering the regional context a deep water marine origin was likely for all these deposits, with the marl having the 'smoothest' texture and highest clay content being the deepest water deposit in the succession. Nodular limestones are also found in deep water settings, where the irregular fabric, if of primary depositional origin, commonly results from soft sediment deformation of coarser layers upon softer, finer-grained ones. The more resistive laminae noticeable in the argillaceous, nodular and particularly the laminated facies may represent layers of fine-grained limestone material that has been winnowed in, or transported into, the low-energy, deep-water setting. The medium-thickly bedded limestone was interpreted to represent fine to medium grained limestone, most likely deposited in shallower water depths than the laminated facies. The origin of the minor mottled/bioturbated facies is unclear. It is probable, however, that this facies represents medium-thickly bedded limestone that has been highly fractured, but which may have been altered to some extent, possibly by bioturbation or some other process.

The clasts within the fine-medium and coarse limestone conglomerate/breccia are both interpreted to be bioclasts or perhaps limestone clasts of variable size within a generally finer grained matrix. Where the conglomerate/breccias interbed with facies of inferred deep water origin, derivation of shallow bioclasts or limestone from an adjacent carbonate edifice, emplaced during storms or via sediment gravity flows is likely. Some of the conglomerate/breccia beds show upwards fining (of conductive patches/spots) and lamination towards the top of units consistent with structures common in calciturbidites (Figures 7a and c). Although the down-hole appearance of the conglomerate/breccia units may reflect increasing proximity to a carbonate platform margin where these facies predominate, particularly in the lower parts of the wells, and especially in Elk-2, shallowing of the depositional environment seems likely (Figure 4). The coarse limestone/breccias typically have less internal structure than the finer units and emplacement via debris flows or as downslope talus deposits seems likely. Although an interpretation of near in-place

shallow water deposits was a possibility for the lower part of Elk-2 a platform slope origin was preferred since none of the material was *in-situ* and because units of the same FMI facies interdigitate with the deeper water deposits in the middle portion of the well. The strongly dolomitised/altered limestone conglomerate/breccia facies probably has similar, or perhaps shallower-water origins to the coarse limestone breccia/conglomerate. The blurred boundaries between clasts and matrix in this facies, and to a lesser extent the coarse conglomerate/breccia, together with an indication of dolomite on *FEQL*, are probably due to dolomitisation, or some other alteration along clast margins, as pad contact is generally good.

The logging sequences were divided into a number of zones based upon a common assemblage or dominance of certain facies (Table 2). These zones give an indication of changes in depositional environment. On the basis of up-hole changes an overall transition from a lower-upper rimmed carbonate slope at the base of the imaged succession to a lower slope or basin floor environment at the top is inferred for both Elk-1 and -2 (Figure 3 and 4). The interval of dolomitised/altered and coarse limestone conglomerate/breccia at the base of Elk-2 is likely to be proximal gravity driven mass transport units from a nearby platform margin and an upper slope environment is inferred (Figure 4). Laminated-thinly bedded and medium-thickly bedded facies with limestone conglomerate/breccia interbeds are inferred to accumulate under low to moderate energy background conditions on the lower to upper slope (intermediate) with conglomerate/breccias emplaced during storms or gravity flow episodes. Zones of almost exclusively laminated-thinly bedded limestone are likely to be low energy deposits accumulated out of the range of proximal gravity-driven flow events, but perhaps still receiving distal flows on the lower slope. Interbedded clay-rich and none clay-rich facies including laminated-thinly bedded limestone are inferred to have accumulated under lower energy conditions of the deeper part of the lower slope. The zones of marls interbedded with argillaceous limestone are very low energy deposits attributed to deeper water conditions than the deep lower slope, moving out onto the basin floor environment.

On the basis of these changes within the overall deepening upward trend in each well, three and four potential large-scale deepening upwards sequences were identified in Elk-1 and -2, respectively (Figures 3 and 4).

Elk-1 and 2 wells: Petrology, comparison with FMI data and overall interpretation

A limited number of cutting samples (7) were available from Elk-1 between 1671 and 1692 m that span FMI facies of nodular and argillaceous laminated-thinly bedded limestone (Appendix 1). Good coverage of samples (28) predominantly from sidewall cores and core plugs were available from Elk-2 spanning the whole imaged section and covering all FMI facies. The only area of poor sample quality in Elk-2 was from the lower part of the well below 2969 m where drilling issues were encountered and the only 3 samples available are cuttings, that may be cavings. Age dating of these lower cutting samples from Sr isotope analysis in Elk-2 yielded anomalous results that appear younger than in the overlying samples, and for these reasons the cuttings attributed to the dolomitised/altered limestone conglomerate/breccia zone could not be confidently linked to this FMI facies. Overall, meaningful comparison was therefore possible for all FMI facies in Elk-1 and -2 with the exception of the minor mottled/bioturbated and dolomitised/altered facies. Depositional interpretations from original FMI analysis were generally corroborated following petrography. Due to better sample coverage most data is drawn from Elk-2 but the findings also hold for Elk-1, particularly in its upper section.

On the basis of petrology the marl, argillaceous and laminated FMI facies with high clay-size content (generally >50%) and abundant well-preserved planktonic foraminifera are low energy, deep marine deposits. The marl FMI facies corresponds to a planktonic foraminifera wacke/mudstone or marl. With the highest clay-sized content (>90%), mud/wackestone textures and planktonic foraminifera comprising >80–90% of allochems the marls accumulated in bathyal water depths and are the deepest water deposits (Figure 5). Three samples corresponding to argillaceous laminated-thinly bedded facies in Elk-2 and all

the samples in Elk-1 are (or in the case of the cuttings, include) planktonic foraminifera wacke/packstones (Figure 5e-g). These wacke/packstones contain less clay-sized matrix (60–80%) than the wacke/mudstone or marl, but again are dominated by generally well-preserved and usually whole, though sometimes crushed planktonic foraminifera. Bioturbation is common, with now compacted, mostly bed parallel burrows of a few millimetres in diameter infilled mainly with clay-sized matrix (Figure 5f). Slightly irregular, layer parallel anastomosing dissolution seams, some developed preferentially along burrows, along and around which insoluble matrix is concentrated are another common feature in the wacke/packstone that are not evident in the wacke/mudstone (Figure 5f). Within some of the planktonic foraminifera-rich wacke/packstones disseminated, or interbedded laminae richer in, shallow fragmented bioclasts are present (including larger benthic foraminifera and minor corals). At Elk-2 2659.5 m one of these lamina rich in shallow bioclasts is partly silicicified (Figure 5g). The laminated-thinly bedded limestone FMI facies corresponds to planktonic foraminifera packstones interbedded with planktonic foraminifera bioclastic packstones, containing up to 10% and 40% fragmented shallow water bioclasts, respectively (Figure 6b). This laminated facies includes some bioturbation, compaction and alignment of bioclasts parallel to bedding, and dissolution seams particularly developed along lithological boundaries. Successive changes from the marls to wacke/packstone and then packstone textures of the argillaceous and laminated FMI facies respectively, and the associated reduced clay-sized and planktonic foraminifera content are consistent with a shallowing, or more winnowed trend, but still within a deep marine context (Figure 6). Bioturbation in these three facies are indicative of oxic conditions at the sea bed. Petrology reveals that the laminations seen in a number of the FMI facies are likely to have multiple origins including: (a) bed parallel bioturbation, (b) development of dissolution seams and perhaps other compaction related features, (c) interlamination of units richer in reworked shallow bioclasts, and (d) layer parallel silicicification. The cutting sample in the nodular and argillaceous limestone zone in Elk-1 is the sample with the most coral material (Figure 6d) and it is probable that some of the nodular appearance may be due to compaction around

coral clasts. The presence of fragmented shallow-water bioclasts including larger benthic foraminifera and corals in the laminated and nodular facies indicate reworking from a nearby shallow platform into deeper water. In addition to dissolution seams, mechanical compaction, and rare partial silicicification, equant cements and sutured grain contacts are other diagenetic features present in all of the planktonic foraminifera-rich facies.

Abundant fragmented shallow water material together with lithified carbonate clasts of both shallow and deep water origin and well-preserved planktonic foraminifera in the two conglomerate/breccia facies are consistent with downslope shedding of platform top and slope material into deeper water (Figure 7). The fine-medium limestone conglomerate/breccia FMI facies were sampled 10 times in Elk-2 (Appendix 1). At 2709 and 2779 m the upper two fine-medium conglomerate/breccias that were sampled correspond to planktonic and larger benthic foraminifera bioclastic packstones. These packstones contain well preserved planktonic foraminifera, together with slightly fragmented, but commonly well preserved flattened or robust larger benthic foraminifera, echinoderm, coralline algae and bryozoa debris with very minor amounts of lithoclasts of planktonic foraminifera wackestones. Most other sampled sites, however, are coral, larger benthic foraminifera and carbonate lithoclastic pack/rudstone/breccias (Figures 7b and d). These rudstone/breccias include a range of fragmented or abraded shallow water bioclasts, including pebble-sized reworked coral material, well preserved planktonic foraminifera together with limestone clasts of bioclastic packstone (Figure 7d). The lower two fine-medium conglomerate/breccias sampled at 2925 and 2926 m correspond to dolomitised foraminifera and echinoderm bioclastic packstones, containing abundant fragmented benthic foraminifera and echinoderm debris, but only very rare planktonic foraminifera. One sample of the coarse limestone conglomerate/breccia FMI facies is an altered planktonic foraminifera pack/floatstone with pebble-sized coral fragments (Figure 7f). The other samples of this FMI facies are probably dolomitised breccias (Figure 7g). On the basis of the petrology it therefore appears that the conglomerate/breccia FMI facies represent a range of microfacies including bioclastic

packstones, coral floatstone, rudstones and breccias with clasts or bioclasts of variable sizes. In both conglomerate/breccia facies dolomitisation post-dates reworking of clasts, compaction, and some fracturing. Other diagenetic features present in both facies include syntaxial overgrowth cements on echinoderm debris, mechanical compaction, granular mosaic, blocky and equant cements. Cements such as the granular mosaic ones replacing corals have occurred prior to bioclast reworking, whereas most equant cement formation post-dates reworking.

The medium-thickly bedded limestone FMI facies was only sampled twice in Elk-2. In the upper part of the well one sample is a planktonic foraminifera bioclastic packstone including fragmented larger benthic foraminifera, coralline algae and well preserved planktonic foraminifera (Figure 6f). The sample at 2968 m falls within the medium-thickly bedded FMI facies, but is very close to a medium limestone conglomerate/breccia and it is difficult to tell which facies is represented. Sample 2968 m is a very heavily dolomitised carbonate lithoclastic & bioclastic pack/rudstone/breccia including fragmented larger foraminifera as well as clasts of bioclastic packstone and grainstone.

Overall, the comparative petrology and FMI data study yielded a consistent interpretation of depositional environments and sequence trends for Elk-1 and Elk-2. The apparent increase in abundance of planktonic foraminifera and decrease in shallow bioclastic material uphole is consistent with a deepening trend or increasing distance from a platform margin. On the basis of the petrology and FMI interpretations both Elk wells are interpreted to pass through slope and basinal facies with a general up sequence deepening trend (Figures 3 and 4). The interpretation of three to four smaller-scale deepening upwards sequences within each well also holds following the petrographic analysis (Figures 3 and 4), although greater sampling frequency would have allowed further evaluation of the smaller-scale trends inferred from FMI. A rimmed shelf margin setting to a partially erosional margin is inferred due to the amount of coarse coral debris, and lithified carbonate material reworked into deeper planktonic foraminifera-rich deposits. There has been some reworking

of a range of shallow-water clasts together with deeper-water planktonic foraminifera-rich packstones and wackestones. The data from petrology therefore provides enhanced knowledge on the nature of the platform margin indicating that erosion of previously lithified carbonate material was an additional feature of the rimmed margin initially inferred from FMI.

In general for both Elk wells, FMI facies strongly reflect original depositional fabrics with relatively minor diagenetic overprint. Exceptions are the mottled/bioturbated facies that is interpreted to be diagenetic (fracture/alteration). Also some of the laminations seen on FMI likely reflect compactional features in which insoluble material is concentrated along dissolution seams, and/or a compactional overprint of earlier primary depositional lamination. The majority of other diagenetic features in the Elk wells are also interpreted to be burial related, but have had little impact on FMI images. The dolomites that are locally important towards the base of the wells, post-date many of the compactional features and are also attributed a burial origin. The dolomites appear to have precipitated along more permeable zones, including along clast boundaries, in fractures, or within more permeable sediments. The presence of dolomites has resulted in some 'blurring' (of clast boundaries) and perhaps some of the more conductive 'patches' on the FMI images.

Antelope-1 and 2 wells: FMI facies and their downhole distribution

A similar suite of FMI facies were defined for the top and middle imaged part of Antelope-1 as for the middle and lower imaged sections in Antelope-2. FMI analysis was initially run prior to independent age dating or petrography. Extensive dolomitisation in the upper and middle imaged portions of Antelope-1 and -2, respectively, was evident from the *FEQL* plots (mainly through the PEF results). It was recognised from the outset that textures seen in the FMI images due predominantly to this dolomitisation, or other diagenetic overprints, were difficult to distinguish from what may have been primary depositional features. There was a tendency to attribute textures to potential depositional origins, unless

a later alteration texture (such as fracturing) was clear. Poor image quality in Antelope-2 (1938–2088 m and below 2123 m of the main pass and in the entire 6.125'' section between 2224 and 2450 m) and Antelope-1 (locally in the upper half of the imaged section), mainly due to uncorrectable gas smearing (Figure 11a) compounded the issue of data interpretation and facies correlation between the wells. Fortunately, in a repeat pass of Antelope-2 below 2100 m, the image log was not affected by gas smearing, allowing interpretation down to 2218 m (in the 8.5'' section). As discussed below thin section petrography subsequent to the FMI analysis proved critical in understanding primary depositional textures and secondary alteration features in the Antelope wells. Five FMI facies were common to both Antelope wells, with an additional four and two facies defined in just the Antelope-1 and -2 wells, respectively (see Table 3 for FMI-facies characteristics).

The upper part of Antelope-2 (1829–1939 m) consists of a vuggy mottled limestone conglomerate/boundstone FMI facies that was not present elsewhere in the well or in Antelope-1. This vuggy mottled facies has a generally distinct resistive or slightly conductive limestone fabric with common conductive vugs and holes, and a conductive mesh-like 'layering' (Figure 10a-c). The facies is massive to thickly bedded. 'Clasts' are visible, but these 'blur' into the overall fine to more medium grained fabric seen on the images and sometimes form an internal structure suggestive of boundstone.

The upper part of Antelope-1 (1732–1935 m) and middle section of Antelope-2 (1939–2211 m) consist almost exclusively of low-, moderate-, and high-conductivity vuggy dolomite conglomerate/boundstone FMI facies (Figure 11). High to moderate conductivity dolomites predominate in Antelope-1, whereas low to moderate conductivity dolomites predominate in Antelope-2. These dolomitised facies commonly have a slightly blurred appearance on the FMI images and are massive to thickly bedded, with bedding generally highly discrete yet visible as very thin conductive layers. The variably resistive to conductive dolomite facies contain variably abundant vugs and larger holes (Figure 11a-d). Clasts are sometimes visible, but may blur into the overall fabric on the image and form an internal

structure suggestive of boundstone. The background dolomite appears fine to medium grained. The highly conductive dolomite intervals in both Antelope-1 and -2 have significantly greater gamma readings than the other facies in these two wells (see footnote 1). Unlike the other two dolomite facies a limestone component is almost completely absent from the highly conductive dolomite in Antelope-2, and comprises <10% in all the dolomite FMI facies in Antelope-1. The dolomite content of the moderate- and low conductivity dolomites in Antelope-2 is >80% and >60%, respectively.

In the lower predominantly dolomitised middle section of Antelope-2 (2143.5–2211 m) there are gradational changes (defined from *FEQL*) from low-conductivity dolomite to three interspersed minor units of vuggy limestone conglomerate/boundstone FMI facies. Similarly in Antelope-1 below the almost completely dolomitised section, low conductivity dolomites (Figure 11b) grade into vuggy limestone conglomerate/boundstone facies within a partially dolomitised zone (Figure 8; 1935–1976.2 m). The vuggy limestone conglomerate/boundstone facies typically consists of a generally distinct resistive or slightly conductive limestone fabric containing abundant conductive vugs and holes (Figure 12a & b). Thick bedding is generally highly discrete yet visible because of very thin conductive layers that define probable bedding planes. Some 'clasts' are visible, but in places blur into the overall apparently fine to medium grained fabric on the image and form an internal structure suggestive of boundstone. Within this facies in Antelope-1 the more conglomeratic to fine to medium grained fabric prevails over the potential boundstone fabric. As seen on the FMI images the vuggy limestone conglomerate/boundstone has a similar character to the low conductivity dolomite, but is predominantly of limestone composition with up to 20–40% dolomite content.

The lowermost imaged portion of Antelope-2 (2211–2450 m) consists of vuggy limestone conglomerate with minor interbeds of fine-grained, thinly bedded limestone FMI facies (Figure 13a and b). The vuggy limestone conglomerate is similar to the vuggy limestone conglomerate/boundstone described directly above, but lacks any internal

structure suggestive of boundstone, contains fewer clasts, and has more distinct occasional thick bedding (Figure 13a). The fine, thinly bedded limestone facies consists of a thinly bedded limestone with a generally smooth appearance and low to medium overall conductivity (Figure 13b). Poor image quality in this lower portion of Antelope-2 commonly renders it difficult to distinguish the vuggy conglomerate facies from the fine, thinly bedded limestone with which it gradationally interbeds.

In Antelope-1 a generally resistive interval below the partially dolomitised zone consists of limestone conglomerate/boundstones in its lower half that generally grade upwards into fine mottled limestone FMI facies (Figure 14a; 1976.2–2060.3 m). The mottled limestone is imaged as massive to metre-scale beds of resistive spots and patches within a generally conductive mottled fabric. The limestone conglomerate/boundstone has a coarser texture than the mottled limestone with distinct resistive 'clasts' in a more conductive groundmass. An internal, wavy structure is common suggesting that boundstone is sometimes present. The interval between 2060.3 and 2246.6 m consists of six 'cycles' dominated by limestone conglomerate breccia occasionally gradationally interbedded with fine, medium-bedded limestone and limestone conglomerate/boundstone FMI facies (Figure 14b). Each cycle features an unconformity at its base, is upward coarsening, with resistive clasts more abundant towards the top, and capped by units with potential boundstone fabric (Figure 14b). The limestone conglomerate/breccia has elliptical resistive clasts, some with distinct conductive rims in a moderately conductive groundmass. The fine, medium-bedded limestones generally have a smooth, but sometimes brecciated appearance and are resistive to slightly conductive. The lower cycle (between 2126.4 and 2246.6 m) is highly resistive and includes a number of potential boundstone units.

At 2246.6 m in Antelope-1 there is a distinct unconformity and below this in the lower imaged section (to 2454 m) well-layered units are predominantly moderately conductive. Limestones conglomerate/breccia predominate between 2246.6 and 2347 m and are interbedded or gradationally bounded by fine, thinly bedded limestone FMI facies. *Vice*

versa, fine, thinly bedded limestones with more minor medium-thickly bedded clastic limestones predominate between 2347 and 2454 m. Limestone conglomerate/boundstones also feature between 2290.5 and 2300 m. The succession has been subdivided on the basis of predominance of fine, or medium-thickly bedded facies and the presence of unconformities at 2291, 2300, 2311, 2316.4, 2320, 2325.6, 2336.8, 2377, 2381, 2389.5 and 2402.6 m. The clastic limestones include subrounded resistive spots or clasts aligned parallel to bedding in a more conductive groundmass and are similar to those described above for the middle part of Antelope-1. In the lower Antelope-1 section, however, thin conductive layers are more common, and resistive clasts are generally smaller, less abundant, matrix- rather than clast-supported, and more elongate than in middle imaged section. The fine, thinly bedded facies are like those described above for the lower part of Antelope-2, but typically contain minor resistive clasts.

Antelope-1 and 2 wells: Initial interpretation from FMI data

The vuggy mottled limestone conglomerate/boundstone FMI facies that comprise the uppermost zone in Antelope-2 (1829–1939 m), due to its speckled appearance, presence of clasts and potential internal structure, was tentatively interpreted as fine-medium grained grainstone, with areas of potential boundstone and/or rudstone. The 'mottled' texture was related to layered micritic content, possibly in the form of algal laminations that may have been subject to stylolitisation/dissolution. An overall interpretation of shallow water reef deposit, from a possible reef flat, was on the basis of moderate to high energy (from the grainstones) together with the potential co-occurrence of algal laminae with coral boundstones and rudstones.

The almost completely dolomitised and underlying partially dolomitised zones in upper Antelope-1 (1732–1976.2 m) and middle Antelope-2 (1939–2211 m) have rudstone to boundstone fabrics with a fine-medium, potential grainstone, groundmass. This

interpretation holds for five FMI facies: the low, moderate and highly conductivity dolomites, as well as the (vuggy) limestone conglomerate/boundstones (Figure 11a-e). However, dolomitisation and gas smearing, particularly in the high conductivity dolomite, does strongly obscure original depositional features, rendering conclusive interpretations difficult. Some of the thin conductive features interpreted mainly as bed boundaries may also be stylolites or dissolution seams (Figure 11d). The common vugs and holes may reflect primary preservation of intergranular or shelter porosity, and/or significant dissolution associated with dolomitisation, and/or of corals (Figure 11a-e). The high gamma readings in the high conductivity dolomite is a result of a high uranium content, not uncommon for dolomite, and associated with these almost completely dolomitised intervals (see footnote 1). For similar reasons to those listed above for the upper section of Antelope-2, these dolomitised and partially dolomitised deposits are also interpreted to be shallow water reef, potentially reef flat, deposits. The potential boundstone textures in Antelope-1 in the interval between 1976.2 and 2060.3 m was also thought to potentially be of reef flat origin, although the less clastic-rich upper mottled facies was perhaps deposited in a calmer water setting than the intervals above and below (Figure 14a). The potential boundstones that cap each of the six cycles between 2060.3 and 2246.6 m are also inferred to have reefal origins (Figure 14b). The elliptical clasts in the cycles are likely branching corals, with those having distinct conductive rims probably encrusted with coralline algae. Each cycle is interpreted to be due to increasing energy, and/or proximity to a reef probably reflecting upwards shallowing or lateral changes on a reef flat perhaps passing upwards into a reef crest environment. Moderate to high energies are inferred for much of these cycles due to the abundance of clasts (or reworked corals). The lowermost two cycles with the thickest boundstone caps may be predominantly reef crest deposits, or very proximal to this environment.

The rounded or elliptical clasts in the vuggy limestone conglomerate that predominates in the lowermost imaged portion of Antelope-2 (2211–2450 m) are interpreted to be reworked corals (Figure 13a). Due to its speckled appearance the groundmass to this

facies is probably largely grainstone of fine to medium grain size. The absence of boundstone, but abundance of limestone conglomerate (or coral rudstone) are suggestive of an environment very proximal to a reef, but not part of the reef proper, i.e., reef fringe (of James, 1984). The majority of the facies could be considered coarse coral debris deposited in a reef fringe setting. The minor interbeds of fine, thinly bedded limestone within the lowermost interval of Antelope-2 were probably also deposited in a reef setting, albeit of less proximity to the reef, or during periods of less reworking from the reef. In Antelope-1 the interval between 2246.6 and 2347 m dominated by limestone conglomerate/breccias is also interpreted to predominantly represent a reef fringe environment with minor reefal development between 2291 and 2300 m. Within this zone facies dominated by clastic material are considered proximal debris to the reef, whereas the fine layered limestone facies are interpreted as more distal deposits. The predominance of fine, thinly bedded limestone in the lowermost imaged section in Antelope-1 (2347–2454 m) is inferred to represent a relatively quiet water environment or one distal from a reef. The minor limestone conglomerate/breccia interbeds are probably coral debris deposits derived from an adjacent reef (as in the overlying section). These may have been emplaced during storms or other periods of increased wave activity, but could in some cases also be channel deposits. Overall, a backreef lagoon or toe of forereef slope environment is inferred for this lowermost interval.

Antelope-1 and 2 wells: Petrology, comparison with FMI data and overall interpretation

Overall, the comparative petrology and FMI data study yielded some agreement in the interpretation of depositional environments and sequence trends for Antelope-1 and Antelope-2. Following petrography, however, there was a significant change in depositional interpretation for the lower section of Antelope-2 that was generally poorly imaged via FMI, and also the uppermost section of Antelope-2, the former resulting in correction of a miscorrelation between the wells. Most other discrepancies between the original

independent interpretations are attributable predominantly to diagenetic overprints that were not easily identifiable from the FMI logs alone. The petrology therefore proved critical in the Antelope wells to better understand depositional changes, complex diagenetic overprints, to provide calibration for the FMI data and in places to revise original FMI interpretations.

Upper Antelope-2 well: The upper part of Antelope-2 (1829–1939 m) had both whole cores (Core 1: 1835.06–1840.49 m, Core 2: 1846.09–1881.85 m) and 47 thin sections from core plugs and rotary sidewall cores available for comparison with the FMI logs (Figure 10). Following petrography the interpretation for this upper Antelope-2 interval changed from an overall shallow reef flat setting (original FMI interpretation) to moderate photic depths in an inter-reefal setting or one back from a reef crest, or perhaps less likely a forereef setting. The vuggy mottled limestone conglomerate/boundstone FMI facies comprising this upper part of Antelope-2 from both core and thin sections dominantly consists of bioclastic pack/grainstones and coral bioclastic rud/bound/pack/grainstones. Algal, coral and/or larger benthic foraminifera float/rud/pack/grainstones are subsidiary lithologies. The colour of the core varies from pale, to medium-grey with concentrations of dark grey insoluble material along dissolution seams and stylolites (Figure 10b, c, f, g & h). Changes in lithology are gradational (or occur across dissolution seams) and clear bedding surfaces are rare. In thin section the bioclastic (coralline) pack/grainstones are generally medium to coarse-grained, though often heavily recrystallised (Figure 10f & j). They include larger benthic, predominantly perforate, foraminifera, minor planktonic foraminifera, echinoderm, mollusc and coralline algal material. Many bioclasts are fragmented and abraded. Calcareous sponge spicules, bryozoa and barnacle material is also seen in some samples. The packstone matrix material includes micrite and non-carbonate material, possibly including very minor clays in darker grey areas. Packstone to wackestone textures are present in areas of dissolution seams and stylolites where fine matrix and insoluble material dominates. For the coral (& coralline algal bioclastic and/or larger benthic foraminifera) rud/bound/(float)/pack/grainstone corals and rhodoliths are up to 30 cm across (Figure 10c).

Corals include branching and massive forms, and most are heavily affected by recrystallisation and/or dissolution then cementation (Figure 10d, I, j, k & l). Laminar encrusting coralline algae encrust some of the corals (Figure 10h, I & j). Many corals are reworked (e.g., bed parallel branching corals), although it is difficult to ascertain if others may be in growth position. Circum-clast dissolution seams and stylolites have formed around and between many recrystallised corals (Figure 10g & h). The matrix to the rud/boundstones consists of bioclastic pack/grainstone as described directly above. Although medium to coarse grained pack/grainstone are recognisable much of the core has a crystalline appearance (and this is also evident in thin section; Figure 10). Early dissolution, fracturing, solution enhancement of fractures and infill by siliciclastic sediment and dolomite crystal silt are common (Figure 10d & e). Mosaic to blocky non-ferroan calcite cements are prevalent partially infilling pore space, and in part post-date some mechanical compaction features. Intervals of wavy, wispy and anastomosing dissolution seams present at decimetre- to metre-scale intervals, are between a centimetre to 30 cm thick, and may be cross-cut by jagged stylolites, with amplitudes of up to 4 cm. Dissolution seams and stylolites are mostly associated with finer intervals and orientated horizontally or inclined up to thirty degrees. Fractures are straight to irregular and typically oriented near vertical to 70 degrees and may have apertures up to 1 cm and be open, solution-enhanced, or closed and/or cemented. Minor late dolomite cements and a late phase of leaching is seen in many samples.

On the basis of the biota, their growth forms, common bioclast fragmentation and abrasion, as well as grain/rudstone textures deposition under normal marine, moderate to high energy conditions is inferred. Packstones and floatstones probably accumulated in lower energy areas, but still contain abundant fragmented and reworked shallow water biota. The setting was an area of, or in close proximity to, coral growth, i.e., reefal or near-reefal. As many of the corals are reworked, there is the possibility of an inter-reef, forereef or reef-flat (back from the reef crest) setting. Stratal orientations and orientations of recrystallised

corals were commonly difficult to obtain in the core. Reworked branching corals, dissolution seams and stylolites are commonly oriented perpendicular to the core axis and may therefore indicate, or enhance, near-horizontal bedding. However, not all surfaces that potentially relate to original bedding are horizontal, and there has been considerable structural deformation of the region and tilting of strata via thrusting since deposition (Goldberg and Holland, 2008). For these reasons, a forereef setting in which inclined bedding would normally be expected to prevail, cannot be ruled out. The thin sections do not have an abundance of biota distinctive of very shallow water depths such as common molluscs or imperforate foraminifera, and where present these are generally reworked. Foraminifera, such as robust (commonly abraded) *Amphistegina* are common. Spicules, bryozoa (and barnacles) are most common in current or tidal influenced areas with some nutrients, such as may occur in fore-, inter- or back-reef areas. The thick algal coating present on some of the corals would also be consistent, though not exclusive to, current swept areas with some nutrients. The observations of orientations, biota types and their preservation would be most consistent with moderate photic depths in an inter-reefal setting or one back from a reef crest, or perhaps less likely a fore-reef environment. The presence of planktonic foraminifera indicate open marine circulation. Influx of minor insoluble material could occur in both reef flat (possibly terrestrial-derived) or inter-reef and fore-reef settings (via currents). Most of the siliciclastic material was present as fissure fills (probably infilling karstic cavities) and/or concentrated along seams via compaction. It is likely that any karstification, fracturing and dissolution seam development may have enhanced the conglomeratic, brecciated or boundstone textures inferred from the FMI images.

Upper and middle Antelope-1, and middle and lower Antelope-2 wells: Results of petrography corroborated the overall predominant reef flat interpretation from the FMI for the upper pervasively dolomitised, partially dolomitised and middle predominantly undolomitised sections in Antelope-1 down to 2177.8 m, as well as the middle pervasively and predominantly dolomitised portion of Antelope-2 (1955–2211 m). Following petrography

the interpretation for much of the lower mainly undolomitised interval of Antelope-2, down to at least 2347 m, was also modified to a predominantly reef flat setting, rather than a reef fringe environment as was originally inferred from the initial FMI analysis. A reefal to reef flat origin was also possible for the pervasively dolomitised zones, although alteration rendered distinction of these environments difficult. The large range in FMI textures throughout these reef flat-interpreted intervals that span the middle imaged portion of Antelope-1 and much of Antelope-2 reflects a combination of considerable variation in depositional textures linked to local environmental change on the reef flat, varied diagenetic overprinting (including dolomitisation and karstification) as well as differences in petrophysical properties.

All samples within the middle interval of Antelope-2 between 1955 and 2193 m are pervasively dolomitised (Figure 11; 34 samples), as are those from the upper interval of Antelope-1 (1748–1938 m; 38 samples). In Antelope-2 the lower boundary of the dolomitised zone may extend deeper (as is apparent from the *FEQL*), but no samples were available between 2193 and 2231 m. Age diagnostic biota are generally absent from the dolomitised intervals in both wells, and Sr isotopic analysis yield unreliable ages (Allan, T., pers. com., 2011). From petrography, the dolomitised intervals in both wells show very similar depositional and diagenetic features. Although pervasive dolomitisation commonly overprints earlier textures and features, recognisable depositional textures are wackestones, packstones, grainstones, floatstones and rudstones (Figure 11f-j). Boundstones may also be present as inferred from the FMI images, but this texture is at a larger-scale than identifiable in individual thin sections. Bioclasts, where recognisable, include locally very common branching or massive corals, imperforate foraminifera and molluscs (Figure 11f-j). Less common elements include disseminated or encrusting coralline algae, and *Halimeda.* Many bioclasts show some fragmentation and/or abrasion and may be replaced by dolomite, or are more commonly seen as leached moulds, with some infilling by dolomite cement (Figure 11f-j). In both wells there is a tendency for high- and moderate-conductivity dolomite FMI facies to correspond to coral-rich pack/grain/rudstones, although this is not systematic

and there are also examples of wackestones with high-conductivity (Appendix 1). In terms of their diagenesis many samples show common micritisation of bioclasts, with micrite envelopes now outlining partially cemented biomoulds. Dissolution of aragonitic bioclasts occurred in some samples prior to 'dusty' dolomite rhombs pervasively replacing micritic matrix (Figure 11f-j). Early aragonite dissolution is associated with reddening and/or fine siliciclastic sediment infill (the later mainly in Antelope-2 samples) in a third of dolomitised samples from Antelope-1 and a lesser proportion of samples from Antelope-2. Sample 1964 m in Antelope-2 includes a laminated and matrix-supported breccia infill to a linear cavity within a reddened dolomitised mollusc bioclastic packstone (Figure 11h). Leaching of calcite bioclasts commonly follows 'dusty' dolomite formation, and in turn is often followed by a clear phase of dolomite cement partially infilling pores. A localised, late phase of coarse, non-ferroan poikilotopic calcite cement post-dates the clear dolomite cements (Figure 11g-i). Late leaching post-dates the clear dolomite cements and/or the poikilotopic calcite. Samples in Antelope-2 tend to have less leaching of calcitic bioclasts and/or the late calcite cements comprise a higher percentage (Figure 11i; up to 15–25%) of the sample than in Antelope-1. Consistent with the *FEQL* results, the presence of calcitic bioclasts and/or calcite cements is most common in the low and moderate conductivity dolomites in Antelope-2, makes up less than 10% of the high- and moderate-conductivity dolomites in Antelope-1 (typically as cements), and are generally absent from high-conductivity dolomites in Antelope-2.

Limited samples (6 between 2184 and 2193 m) were available for study from the lower predominantly dolomitised section in Antelope-2 (2143.5–2211 m). Nine samples were available from the partially dolomitised zone in Antelope-1. The low conductivity dolomite FMI facies within this zone in Antelope-2 correspond to dolomitised bioclastic wacke/packstones rich in molluscs and similar to some of the mollusc-rich lithologies in the overlying pervasively dolomitised zone (Figure 11h). Dolomitised coral bioclastic pack/floatstones correspond to low conductivity dolomites from the partially dolomitised interval in Antelope-1, and again resemble lithologies from the upper pervasively dolomitised

zone. Just below the pervasively dolomitised zone in Antelope-1 sample 1938.8 m is a recrystallised and fractured pack/floatstone with cavities that are partially infilled by fractured dolomitised micritic infill and dolomite cements (Figure 12c). The four samples corresponding to vuggy limestone conglomerate / boundstone FMI facies in Antelope-2 are partially dolomitised (coral) bioclastic wacke/pack/floatstones containing common coral, mollusc and some encrusting coralline algal material (Figure 12f-h). Disseminated coralline algal debris and imperforate foraminifera are also present in some samples. Corals are mostly branching forms and may be fragmented, or whole, with the latter showing little signs of abrasion. In comparison, vuggy limestone conglomerate / boundstones in Antelope-1 predominantly correspond to coral and coralline algae bioclastic grain/pack/rudstone showing common fragmentation and abrasion of bioclasts (Figure 12d-e). Bioclastic content is similar to that in the conglomerate / boundstones from Antelope-2 in also containing imperforate foraminifera and molluscs. In the partially dolomitised zones from both Antelope-1 and -2 dolomitisation and calcite cements follow the same trends as those of the pervasively dolomitised samples, but are more patchy. For example, some samples show partial dolomitisation of matrix, minor dolomite cements and late poikilotopic calcite cements, whereas other samples have common clear dolomite cements partially infilling pores between calcitic bioclasts (Figure 12e-h). Sample 2184.1 m in Antelope-2 includes a laminated dolomitised micritic infill to an earlier possible dissolution or shelter cavity between corals (Figure 12f).

The fine-grained, thinly bedded limestone FMI facies in the lowermost imaged portion of Antelope-2 (2211–2450 m) consist of imperforate foraminifera and mollusc or algal grain/packstones (Figure 13c-d; 11 samples). The interbedded vuggy limestone conglomerate FMI facies may also consist of these same grain/packstone lithologies (6 samples), but are more commonly recrystallised corals (6 samples) or coral-rich bioclastic grain/pack/float/rudstones (Figure 13e-f; 9 samples). Minor wackestones (2372 m) and breccias (Figure 13g; some partially dolomitised) or heavily fractured samples (4 samples)

are also present. Molluscs and imperforate foraminifera tend to be more common in the upper part of this lower imaged interval, and although corals are seen throughout they are abundant in the lower part of the interval. Perforate foraminifera, including *Miogypsina,* echinoderm debris and *Halimeda* are locally abundant within the lower imaged interval. Fragmentation and abrasion of bioclasts is seen in many, but not all samples. Two samples in this lower zone contain reworked carbonate lithic clasts (Figure 13g; 2289 and 2434 m). Samples in this lower Antelope-2 interval are predominantly undolomitised. Minor dolomitisation is seen of micritic matrix to a breccia (2289 m), and as late cement in fractures (2283, 2294.5 & 2422 m). Early micritisation was followed by isopachous cements (sometimes multiple phases) particularly in the lower coral-rich samples below 2347 m (Figure 13e-f). Mottled texture (glaebules, alveolar texture) and *Microcodium* are early features in samples from around 2300 & 2370 m (Figure 13g). Dissolution followed by extensive blocky cements and or neomorphic replacement of bioclasts plus blocky to drusy cements are extremely common (Figure 13c-d). Later diagenetic features include fracturing (sometimes multiple phases), further blocky to equant cementation, minor compaction and late dissolution plus rare dolomite cement precipitation.

In Antelope-1 from just below the partially dolomitised zone, the 3 samples corresponding to fine mottled limestone FMI facies are partially dolomitised coral float/rud/packstones or breccias (1983–1987.5 m). Dolomitisation has resulted in a 'network-like' fabric due to replacement of: (1) matrix between corals or molluscs, or (2) bladed cements between clasts in breccia (Figure 14c). Where dolomites replace the matrix of samples, the bioclasts have been leached out and their moulds infilled by poikilotopic calcite cements. Two more samples corresponding to fine mottled limestone FMI (2027 & 2035 m) are mollusc, imperforate foraminifera and coral bioclastic grain/packstones. Samples 1991–2189.79 m corresponding to limestone conglomerate/boundstones, massive, medium-bedded clastic and fine, medium bedded limestone FMI facies are all predominantly mollusc and imperforate foraminifera bioclastic pack/grainstones (Figure 14d-e). Corals are

present in some of the massive, medium-bedded samples and are common in the limestone conglomerate /boundstone samples (Figure 14f). Larger perforate foraminifera, echinoderm debris and coralline algae are all also locally present in the middle interval of Antelope-1, with many bioclasts fragmented and abraded. Although pack/grainstones textures predominate, wackestones were also present at 2055, 2070, 2084, 2095, 2109, 2122.6 and 2166.8 m corresponding to the massive and fine medium bedded limestone FMI facies. Planktonic foraminifera are present in the wacke/packstones corresponding to fine- and massive-, medium bedded limestone FMI facies at 2095 and 2109 m. Between 2200 and 2239.2 m samples are coral-rich grain/rudstones and floatstones in which *Halimeda,* larger perforate foraminifera and coralline algae are all common (Figure 14f), whereas imperforate foraminifera and molluscs are rare. A number of samples mostly corresponding to limestone conglomerate/boundstone FMI facies in the middle imaged interval of Antelope-1 contain reworked non-carbonate and carbonate lithic clasts, including chert (Figure 14c & f; Samples 1983, 2004, 2182 and 2228 m). Samples in this middle Antelope-1 interval are partially dolomitised, to predominantly undolomitised. Early micritisation was followed by dissolution, rare isopachous (1983–1991, 2041, 2180, 2200–2228 m), or common blocky cements, some compaction and neomorphic cements (Figure 14c-f). Reworked clasts show highly varied diagenetic histories, including mottling, fracturing, reddening and partial dolomitisation. Reworking of clasts is associated with fracturing, brecciation, dissolution, sediment infill and neomorphic cements. Some reworked clasts are coated in isopachous cements and there may be multiple phases of these as well as multiple dolomitising episodes. Glaebular structure, *Microcodium* and cavity infills are seen at 2004.5, 2012.5, 2018, 2041, 2055, 2155, 2180 and 2182 m, with most of these samples corresponding to limestone conglomerate /boundstones (Figure 14e). Later diagenetic features includes clear dolomite cement, chemical compaction, together with minor dedolomitisation, fracturing, late leaching and some sediment infiltration &/or micritisation of pore spaces.

Evidence for the reef flat interpretation of Antelope-1 down to 2177.8 m, as well as the middle of Antelope-2 (1955–2211 m) includes common reworked and potentially *in situ* corals, the latter inferred from FMI investigation, together with abundant imperforate foraminifera and molluscs that are very common shallow photic elements. There was local reworking of corals possibly from the inferred reef flat setting or a nearby reef crest, but it appears there was also some reworking of carbonate and non-carbonate clasts across the reef flat. Some of the resistive 'clasts' seen on FMI may therefore represent actual 'clasts' rather than being exclusively corals. Much of this reef flat experienced moderate to high energy conditions as indicated by the predominance of grainstone and rudstone textures. However less common wackestone and floatstones reveal that local areas, or periods, were affected by lower energy conditions. Although tentative energy regimes were assigned following the FMI analysis, there are a number of examples where these interpretations were modified after petrography. For example, a possible relatively calm water setting was inferred from predominantly 'clastic-free' mottled FMI textures in the upper part of the 1976.2–2060.3 m interval in Antelope-1. Following petrography many of the samples from this mottled interval were revealed to be cemented grainstones and breccias or conglomerates indicative of moderate to high energy conditions. Petrology also revealed that, at least in part, the mottled FMI texture is attributable to partial dolomitisation of cements, and/or matrix of a probable earlier karstified zone. Multiple samples in both Antelope wells from the reef flat zones show a range of features collectively indicative of subaerial exposure including *Microcodium,* alveolar and/or glaebular textures, early aragonite dissolution associated with reddening, and laminated micritic, siliciclastic, or brecciated infills to irregular dissolution cavities (Esteban and Klappa, 1983). This evidence for multi-phase exposure and karstification was not deciphered from the initial FMI analysis. Some of the brecciation, mottling and conglomeratic/ boundstone textures seen in FMI when compared with corresponding thin sections, were attributable, at least in part, to exposure-related features. The vuggy limestone conglomerate / boundstone and conglomerate FMI facies appear to have multiple origins as coral and/or lithoclastic rudstone, floatstones or

breccias, potential boundstones as well as corresponding to karstic features or zones. Following petrology there was some minor movement of internal facies zone boundary changes within the overall inferred reef flat deposits. Originally the change from predominantly reef flat to underlying reef flat cycles was picked at a prominent boundary at 2060.3 m on the FMI Antelope-1 images. After petrology a 'sequence' boundary was preferred at a prominent slightly irregular boundary at 2055.1 m. The conductive zone just above 2055.1 m contains planktonic foraminifera and probably reflects open marine and slightly deeper water conditions, i.e., localised evidence for marine incursion/flooding within the reef flat deposits, hence picking the boundary just below this. On the basis of textural evidence from samples the energy regime for the five reef flat cycles identified from FMI between 2055.1 and 2177.8 m varied, although moderate to high energies predominated. Cycles are interpreted to reflect changes in energy and or relative water depth with some of the cycles probably shallowing upwards to bound/rudstone textures and/or zones with evidence for subaerial exposure.

The highly resistive lowermost reefal-associated cycle in Antelope-1 identified during FMI analysis (2177.8–2246.6 m) is now interpreted predominantly as reef crest deposits due to the number of potential boundstone units (from FMI), abundance of corals, but paucity of common reef flat elements such as imperforate foraminifera or molluscs. Robust perforate foraminifera, coralline algae and *Halimeda* are all also consistent with, though not exclusive to, a reef crest setting. Samples from this interval are the main ones to show thick, isopachous or bladed cements rimming corals, or other bioclasts, a feature common in reef crest areas in which significant cementation is associated with flushing of marine waters through platform margin deposits (cf. Flügel, 2004). The lowermost imaged portion of Antelope-2 (2347–2450 m) is also rich in corals, *Halimeda,* perforate foraminifera, coralline algae and many samples also show the thick isopachous rimming cements. Some grainstone units rich in imperforate foraminifera also occur below 2347 m and overall these deposits are interpreted as reef crest to reef flat. Following petrology the lower

predominantly undolomitised imaged third of Antelope-2 (2211–2467 m) is now correlated with the middle (perhaps down to 2246.6 m), rather than lower imaged portion of Antelope-1 (the latter was originally inferred from the initial FMI interpretation). Subsequent dating via biostratigraphy and Sr isotope analysis also revealed that the lower imaged third of Antelope-2 is age equivalent to the middle imaged portion of Antelope-1, with both yielding Early to Middle Miocene ages (Tony Allan, pers. comm., 2011).

Lower imaged Antelope-1 well: Following petrography of samples from the lower imaged portion of Antelope-1 some modifications were made to the initial interpretation from FMI of a predominantly reef fringe environment (2246.6–2347 m) with minor reefal development (2290.5–2300 m), and backreef lagoon to toe of forereef slope environment (2347–2454 m). Below the unconformity at 2246.6 m the medium-thickly bedded clastic limestones mainly correspond to coarse-grained larger benthic foraminifera bioclastic packstones, with subsidiary grain- or floatstone textures. Larger benthic foraminifera commonly have thin, flattened morphologies, but abraded more robust forms are also seen. Echinoderm debris, coralline algae and bryozoa are also common components, and corals or carbonate lithoclasts (or fine carbonate infills to burrows) are more minor components (Figure 15b-c). Samples of the fine, thinly bedded limestone FMI facies include similar bioclasts to the medium-thickly bedded FMI facies, but are generally fine- to medium-grained echinoderm bioclastic packstones, with lesser amounts of larger benthic foraminifera, and in which abraded branching corals are very rare to absent (Figure 15d). Planktonic foraminifera are locally present in the lower imaged portion of Antelope-1, but are most common in fine, thinly bedded FMI facies at 2323.5 and 2409 m. From the biotic assemblages, and their morphologies, it was possible to infer relative depth within the photic zone for many of the deposits (thin flattened perforate foraminifera common in deeper photic depths and robust forms in shallower depths; Hallock & Glenn, 1986; van Gorsel, 1988; Beavington-Penney & Racey, 2004). Also, since many units lacked corals, and non-framework building bioclasts dominate, the deposits are described as platform deposits,

rather than being necessarily linked to reefal systems as in the original FMI interpretation. Between 2246.6 and 2454 m the environment is predominantly moderate to deeper photic depth deposits, with or without significant reworking of shallow bioclastic material, plus or minus reworked corals.

There was a change in interpretation of the limestone conglomerate/boundstones FMI facies between 2290.5 and 2300 m where three corresponding samples are coral, lithoclastic and larger benthic foraminifera rud/float/grainstone-breccias. A depositional breccia origin with a range of reworked lithified carbonate clasts and corals is now preferred for much of this unit (Figure 15e). Development of a coral boundstone over the breccia cannot be totally ruled out, although lithic clasts as well as corals are seen in thin section at the top of the interval. That moderate to deeper photic depth deposits underlie and overlie the breccia is consistent with a sediment gravity flow origin for the whole unit, and an upper boundstone cap is less likely. Resistive areas in the lower part of the unit may reflect highly cemented clasts rather than mudstone or wackestone lithologies.

Isopachous and equant as well as neomorphic calcite cement are present in the rudstone breccia samples. Very minor thin isopachous cements are also seen around selected bioclasts in a few samples, but are mainly absent from the lower imaged interval of Antelope-1. Minor micritisation of bioclasts is common throughout the lower imaged portion of Antelope-1, as are syntaxial overgrowths on echinoderm material. Mechanical and chemical compaction features in the form of grain deformation, breakage and suturing are common throughout the lower interval. Blocky to equant cements between bioclasts, fracturing, very minor dolomite replacement of matrix or clear dolomite cements and late leaching are all minor localised features in this lower interval. As with the Elk wells, the diagenetic features in the lower part of Antelope-1 are mainly burial related, and with the exception of the minor cements and compaction-enhanced lamination for the most part do not significantly affect the depositional fabrics imaged by FMI.

Final subdivision of the entire lower imaged portion of Antelope-1 into 5 environmentally distinct normal marine zones was on combined key FMI and petrographic characteristics (Figure 8). A faulted contact at 2347 m was no longer considered as a facies zone boundary. The key characteristics used for subdivision are: ratios or predominance of thinly bedded conductive (wacke/packstones) to more massive resistive units (pack/grainstones) with or without resistive patches (reworked cemented corals or clasts), and brecciated units. The predominant packstone depositional textures, together with some abrasion and fragmentation of disseminated bioclasts are indicative of mainly moderate energies on the platform. Less common grainstone textures may reflect some winnowing by wave-, storm-, or current-generated flow, or perhaps higher, local biotic productivity than micrite accumulation. Between 2290–2302 and 2396–2445 m there is evidence for reworking of previously lithified carbonate material. Between 2246.6 and 2449.5 m most deposits are interpreted as deep- to moderate-photic platform deposits. With a minor or localised component of reworked branching corals (and/or large resistive spots) deposits are largely inferred to be distal to any potential reefal development. The interval between 2340-2389.5 m is an exception being characterised by predominantly coral-rich bioclastic pack/grain/rudstone (clastic resistive FMI units) with subsidiary conductive, thinly bedded FMI units (probable bioclastic wacke/packstones). Deep to moderate, or perhaps shallower photic depths are inferred. There is general agreement in interpretation of depositional environment (proximal reef fringe with reworking of corals and other shallow bioclasts via storms or channels) from independent FMI and petrology studies. The interval between 2300 and 2340 m has evidence for punctuated shedding of bioclastic-rich material from shallower water, and/or localised shallowing of the environment, albeit still distal from any potential reefal development. Between 2389.5 and 2454 m resistive (wacke/pack/floatstones) interbed with conductive (pack/float/rudstone) units containing common resistive clasts. Some of the resistive patches may be lithified carbonate clasts (seen in thin section) as well as corals. A moderate- to deep-photic inner-, or outer-, platform margin/slope environment is inferred with reworking from higher energy, i.e., there

is good agreement with the backreef lagoon or toe of forereef slope from the original FMI study. There may be a facies boundary at 2449.5 m, into shallow photic deposits (inferred from petrology with samples extending down to 2668 m). However, since the FMI image only extends to 2454 m a basal boundary was not picked. Throughout the lower imaged interval of Antelope-1 identified bed surfaces may be depositional in origin, but compaction related dissolution seams formed during diagenesis probably enhance the thinly- to medium-bedded appearance seen on FMI. Results of biostratigraphy and strontium isotopic analysis both yielded Late Oligocene to Early Miocene ages for the lower imaged portion of Antelope-1.

Discussion

Akbar *et al.* (1995) stated that 'image [logs] are no substitute for core analysis, but rather a complement to them'. In this study, where very limited fullbore core was available, a FMI image analysis study was complemented by petrographic study predominantly of rotary sidewall cores. This combined study allowed enhanced definition of micro- to sequence-scale variations in depositional and diagenetic character than would have been possible from either 'stand-alone' study (Figure 16). On a centimetre- to sequence-scale, FMI analysis allowed evaluation of combined depositional and diagenetic textures, clasts, boundaries and stratal trends (of individual beds and sequences). On a micro- to grain-scale, petrography enabled analysis of components, depositional textures, microfacies, diagenetic overprints and their relative timing. In general, the petrography allowed detailed definition of depositional environments (from components and primary textures) and diagenetic alteration, albeit of multiple spot samples, whereas likely large-scale variations in depositional environments and sequences were assessable via image analysis.

Despite the obvious scale differences between the datasets there was adequate correlation between the independent petrography and FMI studies for: a) picking major

facies boundaries, and b) interpretation of depositional environment for the slope and basinal deposits. However, for the shallow water carbonates where diagenesis had strongly impacted the original fabric, and/or in regions of gas smearing petrology proved critical in enhancing or revising original interpretations based on FMI, and particularly for understanding diagenetic overprinting. In the case of picking, or adjustment of, more minor facies boundaries, such as defining those between potential reef-flat versus reef-crest deposits, or recognising minor platform-top flooding events, the follow-up petrography proved critical. In the Elk wells that penetrated platform slope and bathyal deposits there was generally moderate agreement in defining depositional environments and up-sequences changes from the independent FMI and petrology studies. From petrography it was apparent that the slope and bathyal deposits had mainly been affected by burial diagenesis, in which primary depositional fabrics had been unaltered, 'tightened' (such as via circum-clast stylolites in breccias), or enhanced (such as dissolution seam development along lithological boundaries). Petrology proved essential in unravelling non-unique origins for some of the features seen in FMI. Laminations seen in a number of the FMI facies from the Elk wells have multiple origins including: (a) bed parallel bioturbation, (b) development of dissolution seams and perhaps other compaction related features, (c) interlamination of units richer in reworked shallow bioclasts, and (d) layer parallel silicicification. Non-pervasive, patchy dolomitisation in deposits from the Elk wells resulted in minor blurring (of clast margins) and perhaps mottling on the FMI images.

In the shallow-water deposits penetrated by the Antelope wells although there was some agreement in defining depositional environments from the independent FMI and petrographic studies, differences were often due to diagenetic overprinting. The often complex cementation, replacement and compaction events affecting the shallow-water deposits discernable from petrography commonly had a strong impact on textures seen in FMI. This diagenetic overprinting due to marine, meteoric and burial diagenesis, as well as dolomitisation would have been difficult or impossible to extract from the FMI data without the benefit of the petrographic work. Other core-image analysis studies have allowed direct

correlation between FMI textures and Dunham's depositional carbonate textures (of mudstones, wackestones, packstone, grainstones and boundstones; Roestenburg, 1994; Akbar *et al*., 1995; Basu *et al*., 2002; Russell *et al.*, 2002). This was only possible, however, if the grains, matrix and primary pores have maintained their depositional character, and/or been affected by a systematic diagenetic overprint (Roestenburg, 1994; Russell *et al.*, 2002). In the Elk/Antelope wells it was commonly possible to pick depositional textures from the FMI fabrics particularly for coarser facies, such as rudstones or boundstone, or for finer slope or bathyal deposits, such as mud/wackestones or packstones. However, for the shallow-water deposits from the Antelope wells classifying mud-, wacke-, pack-, or grainstones from the FMI commonly proved difficult due to variable down-hole cementation, leaching, dolomitisation or karstification. For example, there were a number of cases where inferred calm water deposition from FMI analysis turned out to be predominantly high energy, but cemented, grainstone deposits during petrographic analysis. It may be that an iterative process of using the petrographic results to search for subtle differences in FMI textures may help differentiate the finer grained depositional textures (Russell *et al.*, 2002), but the significant down-hole variations in diagenesis in the Antelope wells are likely to hamper such studies. The significant number of thin sections evaluated for this study allowed understanding that individual FMI textures or facies may represent multiple depositional and/or diagenetic features (cf. Nurmi *et al*., 1990). This study highlights the requirement for thin section analysis to be undertaken in tandem with image analysis to evaluate potentially non-unique origins for carbonate FMI textures. For example, conglomerate/boundstone FMI facies in the Antelope wells had multiple origins as rudstones, floatstones, lithoclastic conglomerates, boundstones and karstified grainstones or packstones. Fine-medium and coarse conglomerate/breccias in the Elk wells had multiple origins as packstones, rudstone, breccias, floatstones or dolomitised packstones. Again it may be that iterative training of FMI interpretation through input of the petrographic results would help reveal subtle differences in FMI textures to differentiate varied origins.

Although not detailed here, the FMI and petrographic studies were both key analyses for characterising and understanding reservoir quality development. As with the depositional and diagenetic evaluation, the FMI and petrographic data complemented each other in allowing pore systems to be detailed on a variety of scales (Nurmi *et al.,* 1990; Chitale *et al.,* 2010; Xu, 2010), and the integrated study resulted in significantly increased understanding of reservoir quality development than was possible from the individual studies. Pores, and their morphologies, were characterised on grain- to cavern-scales. Porosity distribution, abundances and pore connectivity was assessed on micro- to sequence-scales. The origins of pores over one centimetre in size were tentatively inferred from the FMI study, and where possible corroborated from the limited fullbore core available. One of the advantages of running FMI was that pore system characterisation was possible in zones of high porosity and/or large pore systems, i.e., key reservoir intervals, in which recovery of fullbore, or sidewall, cores may be compromised. Greater certainty was possible in inferring controls on porosity development on the sub-centimetre scale from petrology, particularly when results were combined from geochemical and other microscopy studies (Wilson, pers.obs.). The combined outputs from the FMI and petrological reservoir evaluations were used as key inputs in defining petrophysical Reservoir Rock Types (RRTs), together with understanding and predicting their distribution for building reservoir models (Grötsch and Mercadier, 1999; Akbar *et al.*, 2000/1; Russell *et al.*, 2002; Ahr *et al.*, 2005). In summary, the combined FMI and petrographic analyses resulted in significantly enhanced understanding of deposition, diagenesis and reservoir development in the Elk/Antelope system than would have been possible from either of the individual 'stand-alone' studies (Figure 16).

Conclusions

A combined down-hole image analysis (FMI) and predominantly side-wall core petrographic study of the Elk/Antelope carbonate reservoir from Papua New Guinea allowed enhanced definition of micro- to metre-scale variations in depositional and diagenetic

character. Both shallow-water and platform flank deposits from this Tertiary carbonate buildup that is a major recent gas discovery were evaluated via a full suite of FMI logs (> 2800 m) and 292 thin sections.

Image analysis and petrographic comparisons: Studies of the two independent datasets allowed complementary enhanced evaluation of micro- to sequence-scale variations in depositional and diagenetic character of platform and reservoir development. Despite the obvious scale differences between the datasets there was some correlation between the independent petrography and FMI studies for: a) picking major facies boundaries, and b) interpretation of depositional environment, particularly of flank deposits. However, where diagenesis had strongly impacted original fabric, as is commonly the case in these and other ancient shallow-water carbonates, or where gas smearing affected image quality, petrography proved key to evaluate depositional and diagenetic trends and their impact on petrophysical properties. Component analysis and depositional textures best identified in thin section, but partially inferable from image logs, are good indicators of original depositional environment. The petrographic study allowed more detailed examination of diagenesis and its impact on rock fabric (which links to the FMI textures). Full FMI coverage allowed textural definition on a dm/m scale, identification and characterisation of vertical changes, and likely large-scale variations in depositional environments and sequences. By combining the results of the two studies it was clear that diagenesis as well as depositional fabric had a strong impact on resultant FMI facies, particularly for the shallow-water deposits. This study shows that selective petrographic analysis is critical to revise and/or enhance the quality of facies interpretation from FMI images.

Shallow-water carbonate buildup development and diagenesis: FMI logs and thin sections through the Antelope-1 and -2 wells allowed characterisation of close to 1000 m of much of the Oligo-Miocene development of the shallow-water buildup. Oligocene deposition was predominantly on a relatively open platform within the photic zone, and

perhaps not always associated with localised or more extensive reefal development. Echinoderm and larger benthic foraminifera packstones with or without minor reworked coral debris are imaged on FMI as 'conglomeratic' and 'fine' medium- and thinly-bedded limestones. By the latest Oligocene and into the Early Miocene coral–rich rudstones and boundstones attest to reefal development in a probable reef-crest environment. Most of the remaining Miocene deposits are probable reef-flat deposits rich in imperforate foraminifera and molluscs, with punctuated potential coral reefal development. These Miocene deposits are dominated by grainstones and rudstones indicative of high to moderate energies, although packstones and less commonly wackestones are also present. Miocene deposits were imaged on FMI as: (a) low-, (b) moderate-, and (c) high-conductivity vuggy dolomite conglomerate/boundstones, as well as (i) mottled limestones, (ii) vuggy, and (iii) non-vuggy limestone conglomerate/(iv) boundstones or (v) conglomerate/breccias together with (vi) fine, medium-bedded 'fine' limestones. There was generally good agreement in inferring reef-flat and crest environments from the independent FMI and petrographic studies, with the coarser textures such as boundstones and rudstones, and depositional cycles more easily identifiable from FMI. Where differences in interpretations from the datasets mainly occurred, such as in inferred depositional energies or attributing most FMI features to primary depositional fabrics, was mainly due to the complex and varied diagenetic overprints that were only mainly discernable from petrography. Diagenetic overprinting includes complex and varied calcite cements, early and late dissolution, karstification, replacement, dolomitisation and compaction. The uppermost carbonate section in Antelope-2 consists of vuggy mottled limestone conglomerate/boundstone FMI facies, corresponding to (coral) bioclastic pack/grain/rud/boundstones that were not present in Antelope-1. Moderate photic depth inter-, back-, or less likely fore-reef deposits are inferred for the uppermost Antelope-2 section, with some differences in interpretation from the two datasets again mainly attributable to diagenetic overprinting.

Platform flank and associated bathyal deposition and diagenesis: The combined FMI and petrographic study of the Elk-1 and -2 wells allowed characterisation of ~800 m of

Miocene carbonate slope and associated bathyal deposits flanking the Antelope buildup. There was generally strong agreement in interpreting an overall deepening-upwards upper-slope to bathyal depositional environment (and within this three smaller-scale deepening-upwards cycles) for both wells from the two independent datasets. FMI facies of (a) marls, (b) argillaceous-laminated, (c) laminated-, and (d) nodular thinly-bedded limestones correspond respectively to planktonic foraminifera-rich: (i) marls or mud/wackestones, (ii) wacke/packstones, (iii) (coral), and (iv) bioclastic packstones. From the marls to planktonic-foraminifera bioclastic packstones these all represent bathyal deposits, but sequentially reflect shallowing, and/or increasing proximity to, or periods of bioclast shedding from, the adjacent shallow-water carbonate buildup. (a) Fine-medium- and (b) coarse limestone conglomerate/breccia and (c) medium to thickly bedded limestone FMI facies as discrete beds or more continuous sections variably correspond to bioclastic (including coral and planktonic foraminifera) grainstones, packstone, rudstones, floatstones and lithoclastic breccias that were deposited as slope and/or sediment gravity flow deposits. Since these slope and bathyal deposits were mainly affected by burial diagenetic features that either had little affect on, or enhanced, primary depositional textures there was strong correspondence in depositional interpretation from FMI and petrography. FMI analysis best revealed bed and/or sequence trends, as well as coarser-scale fabrics, whereas petrography allowed determination of components, depositional textures and diagenesis. Petrography revealed that some imaged structures (e.g., fine lamination) and individual FMI facies (e.g., the limestone conglomerate/breccias) may have multiple origins.

As has been stated (Akbar *et al.,* 1995), ‘image [logs] are no substitute for core’, or in this case other sample (sidewall core petrography) ‘analyses, but rather a complement to them’. This study highlights the merits of selective petrographic analysis to revise and/or enhance the quality of facies interpretation from FMI images, whether this is for inferring depositional environments, particularly for understanding diagenetic overprinting, or the evaluation of reservoir quality.

Acknowledgements

We thank InterOil Australia Pty Ltd. and SPI (208) Ltd., Papua New Guinea for supporting this study and allowing publication. Initial FMI characterisation and analysis was undertaken by Dale Lewis at Schlumberger Oilfield Australia Pty. Ltd., Perth. Petrology and comparison of results with FMI was by Moyra Wilson. Scott Rothwell (InterOil) is thanked for his technical assistance in sample and data retrieval. Nigel Deeks is thanked for commenting on the draft manuscript. We thank Associate Editor and reviewers Alex MacNeil and Stephen Kaczmarek for their constructive comments during revision of this manuscript. This is for Megan – who loves life, with all its colours, textures and complexity!

References

Adams, C.G., 1970. A reconsideration of the East Indian Letter Classification of the Tertiary: British Museum of (Natural History), Geology 19, 87-137.

Ahr, W.H., Allen, D., Boyd, A., Bachman, H.N., Smithson, T., Clerke, E.A., Gzara, K.B.M., Hassall, J.K., Murty, C.R.K., Zubari, H. and Ramamoorthy, R. 2005. Confronting the carbonate conundrum. Schlumberger Oilfield Review 17, 18-29.

Akbar, M., Petricola, M., Watfa, M., Badri, M., Charara, M., Boyd, A., Cassell, B., Nurmi, R., Delhomme, J.-P., Grace, M., Kenyon, B. and Roestenburg, J. 1995. Classic interpretation problems: evaluating carbonates. Schlumberger Oilfield Review 7, 38-57.

Akbar, M., Vissapragada, B., Alghamdi, A.H., Allen, D., Herron, M., Carnegie, A., Dutta, D., Olesen, J.R., Chourasiya, R.D., Logan, D., Stief, D., Netherwood, R., Russell, S.D. and Saxena, K. 2000/2001. A snapshot of carbonate reservoir evaluation. Schlumberger Oilfield Review 12 (Winter 2000/2001), 20-41.

Basu, T., Dennis, R., Basu, D., Al Awadi, W., Isby, J.S. and Muherjee, R. 2002. Automated facies estimation from integration of core, petrophysical logs, and borehole images.

American Association of Petroleum Geologists Annual Meeting, Houston, USA. Extended Abstracts 7 p.

Beavington-Penney, S.J. and Racey, A., 2004. Ecology of extant nummulitids and other larger benthic foraminifera: applications in palaeoenvironmental analysis. Earth Science Reviews 67, 219-265.

Blow, W.H., 1969. Late Eocene to Recent planktonic foraminiferal biostratigraphy. Proceedings 1st Plankt. Conf., Geneva 1967, 1, 199-422.

Blow, W.H., 1979. The Cainozoic Globigerinida. Brill, E.J., Leiden, 1412 p.

Chitale, V.D., Johnson, C., Entzminger, D. and Canter, L. 2010. Application of a modern electrical borehole imager and a new image interpretation technique to evaluate the porosity and permeability in carbonate reservoirs. In: Pöppelreiter, M., García-Carballido, C., and Kraaijveld, M. (eds). Dipmeter and borehole image log technology. AAPG Memoir 92, 295-307.

Davies, H.L., Winn, R.D. and KenGemar, P. 1996. Evolution of the Papuan Basin – a View from the Orogen. In: Buchanan, P.G. (Ed). Petroleum Exploration, Development and Production in Papua New Guinea. Proceedings of the Third PNG Petroleum Convention, Port Moresby, 245-270.

Dickson, J.A.D., 1965, A modified staining technique for carbonates in thin section. Nature 205, 587.

Dickson, J.A.D., 1966. Carbonate identification and genesis as revealed by staining. Journal of Sedimentary Petrology 36, 491-505.

Dunham, R.J., 1962. Classification of carbonate rocks according to depositional texture. *In:* Ham, W.E. (Ed.), Classification of carbonate rocks. American Association of Petroleum Geologists, Memoir, 1, 108-121.

Embry, A.F. and Klovan, J.E. 1971. A late Devonian reef tract on northeastern Banks Island, Northwest Territories. Canadian Petroleum Geologist, Bulletin 19, 730-781.

Esteban, M., and Klappa, C.F., 1983. Subaerial exposure. In: Scholle, P.A., Bebout, D.G., and Moore, C.H., (Eds.), Carbonate Depositional Environments. American Association of Petroleum Geologists, Memoir 33, 1-55.

Flügel, E., 2004, Microfacies of carbonate rocks. Analysis, interpretation and application; Springer-Verlag, Berlin, 976 p.

García-Carballido, C., Boon, J., and Tso, N. 2010. Data management and quality control of dipmeter and borehole image log data. In: Pöppelreiter, M., García-Carballido, C., and Kraaijveld, M. (eds). Dipmeter and borehole image log technology. AAPG Memoir 92, 39-49.

Goldberg, A., and Holland, D. 2008. Inversion tectonics and the structural development of the Elk/Antelope Gas Field, Papua New Guinea. In: Blevin, J.E., Bradshaw, B.E., and Uruski, C., (Eds), Eastern Australasian Basins Symposium III, Petroleum Exploration Society of Australia, Special Publication, 247-258.

Goldberg, A. Wilson, M.E.J. and Sioni, S. 2010. Quantitative seismic interpretation for characterizing carbonate diagenesis – an Elk/Antelope Gas Field Study. ASEG extended abstracts. 4 p. DOI: 10.1071/ASEG2010ab128.

Grötsch, J., and Mercadier, C., 1999, Integrated 3-D reservoir modeling based on 3-D seismic: The Tertiary Malampaya and Camago buildups, offshore Palawan, Philippines. American Association of Petroleum Geologists, Bulletin 83, 1703-1728.

Hallock, P. and Glenn, E.C., 1986. Larger foraminifera: a tool for paleoenvironmental analysis of Cenozoic carbonate depositional facies. PALAIOS 1, 55-64.

Harris, D.G., Mahoney, R.J. and Braaten, K.M. 2009. InterOil Corporation resource assessment: Elk/Antelope. GLJ Petroleum Consultants, Calgary, (www.interoil.com/faq/Elk_Antelope_Gas_Field_2009_GLJ_-_FINAL.PDF -, accessed 30/04/2012). 51 p.

James, N.P., 1984, Reefs. In: Walker, R.G (Ed.), Facies Models, Geological Association of Canada, 229-244.

Lagraba, P., Hansen, S.M., Spalburg, M., and Helmy, M. 2010. Borehole image tool design, value of information, and tool selection. In: Pöppelreiter, M., García-Carballido, C. and Kraaijveld, M. (eds). Dipmeter and borehole image log technology. AAPG Memoir 92, 15-38.

Lunt, P. and Allan, T., 2004. A history and application of larger foraminifera in Indonesian biostratigraphy, calibrated to isotopic dating. GRDC Workshop on Micropalaeontology, 109 p.

McArthur, J.M. and Howarth, R.J., 2004. Strontium isotope stratigraphy. *In*: Gradstein, F.M., Ogg, J.G. and Smith, A.G. (Eds.), A Geologic Time Scale 2004, Cambridge University Press. pp. 96-105.

McArthur, J.M., Howarth, R. and Bailey, T.R., 2001. Strontium Isotope Stratigraphy: LOWESS version 3. Best fit line to the marine Sr-isotope curve for 0 to 509 Ma and accompanying look-up table for deriving numerical age. Journal of Geology 109, 155-169.

Newberry, B.M., Grace, L.M. and Stief, D.D. 1996. Analysis of Carbonate Dual Porosity Systems from Borehole Electrical Images. SPE paper no. 35158, p. 1-7.

Nurmi, R., Charara, M., Waterhouse, M. and Park, R. 1990. Heterogeneities in carbonate reservoirs: detection and analysis using borehole electrical imagery. In: Hurst, A., Lovell, M.A. and Morton, A.C. (Eds.). Geological Applications of Wireline Logs. Geological Society of London Special Publication 48, 95-111.

Pigram, C.J. & Davies, H.L. 1987. Terranes and the accretion history of the New Guinea Orogen. BMR Journal of Australian Geology & Geophysics. 10, 193-211.

Pigram, C.J., Davies, P.J., Feary, D.A. and Symonds, P.A. 1989. Tectonic controls on carbonate platform evolution in southern Papua New Guinea: Passive margin to foreland basin. Geology 17, 199-202.

Rider, M.H. 2002. The geological interpretation of well logs (2nd edition). Rider-French Consulting Ltd, Scotland, 280 p.

Roestenburg, J.W. 1994. Carbonate characterisation and classification from in-situ wellbore images. Proceedings of the Indonesian Petroleum Association, 23rd Annual Convention, Jakarta, Indonesia. 181-188.

Russell, S.D., Akbar, M., Vissapragada, B. and Walkden, G.M. 2002. Rock types and permeability prediction from dipmeter and image logs: Shuaiba reservoir (Aptian), Abu Dhabi. American Association of Petroleum Geologists, Bulletin 86, 1709-1732.

Schlumberger. 2004. Schlumberger WTA Marketing Service: FMI Fullbore Formation MicroImager: Houston, Texas, Schlumberger Educational Services, 2 p.

Struckmeyer, H.I.M., Yeung, M. and Pigram, C.J. 1993. Mesozoic to Cainozoic plate tectonic and palaeogeographic evolution of the New Guinea Region. In: Carman, G.J. and Carman, Z. (Eds). Petroleum Exploration and Development in Papua New Guinea, Proceedings of the Second PNG Petroleum Convention, Port Moresby, 261-290.

van de Vlerk, I.M., Umbgrove, J.H.F. 1927. Tertiaire gidsforaminifern van Nederlandsch Oost-Indiè. Wetenschappelijke Mededeelingen Dienst avn den Mijnbouw in Nederlandsch Oost-Indiè 6, 3-31.

van Gorsel, J.T., 1988. Biostratigraphy in Indonesia: Methods, pitfalls and new directions. Proceedings of the Indonesian Petroleum Association, 17th Annual Convention, Jakarta, 275-300.

Wilson, M.E.J. and Bosence, D.W.J. 1996. The Tertiary Evolution of South Sulawesi: A Record in Redeposited Carbonates of the Tonasa Limestone Formation. In: Hall, R. & Blundell, D.J. (eds.), Tectonic evolution of SE Asia. Geological Society of London, Special Publication 106, 365-389.

Xu, C. 2010. Porosity partitioning and permeability quantification in vuggy carbonates, Permian Basin, West Texas, U.S.A. *In:* Pöppelreiter, M., García-Carballido, C. and Kraaijveld, M. (eds). Dipmeter and borehole image log technology. AAPG Memoir 92, 309-319.

Figures and tables

Figure 1) Location of the Elk-Antelope gas fields in Papua New Guinea, and their tectonic context.

Figure 2) Plan-view, top-carbonate map of the Elk and Antelope Fields shown in time (TWT – two way time: from seismic). Carbonates in the Elk wells are topographically high due to thrusting, but were deposited in deeper water than those in the Antelope wells.

Figure 3) Elk-1 well: Downhole variations in FMI facies, FMI composite facies zones and inferred depositional environments plotted against FMI image, gamma and *FEQL* lithology logs. As noted in the text the Photoelectric Factor tool was not run in the wireline suite for the *FEQL* analysis of Elk-1 and dolomites are therefore not shown in the *FEQL* lithology column (see footnote 1 in text).

Figure 4) Elk-2 well: Downhole variations in FMI facies, FMI composite facies zones, inferred depositional environments, depositional and diagenetic features, plotted against FMI image, gamma and *FEQL* lithology logs.

Figure 5) Elk-1 and -2 wells – FMI facies: marl and argillaceous facies examples. (a) Header used for the FMI facies examples on this, and subsequent figures. (b) Example of marl FMI facies from Elk-1 well displaying mainly thin bedding. (c) Elk-2-2607.4 m – Photomicrograph of planktonic foraminifera mud/wackestone or marl equivalent to marl FMI facies. (d) Example of argillaceous laminated-thinly bedded limestone FMI facies from Elk-2 well displaying thin resistive beds and conductive laminations. The laminations appear much smoother, and sometimes fainter, than seen in the laminated-thinly bedded limestone. (e) Elk-1-1686 m – Photomicrograph of cutting sample equivalent to argillaceous laminated-thinly bedded limestone facies. (f) Elk-2-2658.1 m – Photomicrograph of planktonic foraminifera wacke/packstone showing irregular bed parallel dissolution seams developed along burrows equivalent to argillaceous laminated-thinly bedded limestone FMI facies. (g) Elk-2-2659.5 m - Photomicrograph of planktonic foraminifera wacke/packstone interbedded

with predominantly silicicified planktonic foraminifera bioclastic packstone equivalent to argillaceous laminated-thinly bedded limestone FMI facies.

Figure 6) Elk-1 and -2 wells – FMI facies: laminated-, nodular-, medium-thickly bedded and mottled/altered facies examples. (a) Example of laminated-thinly bedded limestone FMI facies from Elk-2 well, displaying mainly laminations. (b) Elk-2-2709.89 m – Planktonic foraminifera bioclastic packstone including well-preserved planktonic foraminifera and fragmented bioclasts (including larger benthic foraminifera, coralline algae and bryozoa). Mechanical and chemical compaction features present. (c) Example of very thinly interbedded nodular limestone and argillaceous limestone FMI facies from Elk-1 well. (d) Elk-1-1671 m – Range of cuttings including planktonic foraminifera bioclastic packstone and altered coral fragments equivalent to nodular and argillaceous laminated-thinly bedded limestone FMI facies. (e) Example of medium-thickly bedded limestone FMI facies from Elk-2 well. (f) Elk-2-2416 m – Photomicrograph of planktonic foraminifera bioclastic packstone equivalent to medium-thickly bedded limestone FMI facies. (g) Example of thinly mottled/bioturbated limestone FMI facies from Elk-1 well. The meshwork appearance is due to a combination of intense fracturing in addition to possible alteration.

Figure 7) Elk-1 and -2 wells – FMI facies: limestone conglomerate/breccia facies examples. (a) Example of fine-medium limestone conglomerate/breccia FMI facies from Elk-2 well (centre) with laminated-, and medium-thinly bedded limestone above and below, respectively. Fine-medium limestone conglomerate/breccia appears to fine upwards and has lamination towards the top of the unit. (b) Elk-2-2710.6 m – Photomicrograph of planktonic foraminifera bioclastic packstone (equivalent to medium limestone conglomerate/breccia FMI facies) overlying planktonic foraminifera packstone (equivalent to laminated-thinly bedded limestone FMI facies). An irregular dissolution seam closely follows the boundary between the two facies. (c) Analogue to the fine-medium limestone conglomerate/breccia imaged in (a): field photograph of calciturbidite from the Tonasa Limestone of South Sulawesi showing upwards fining and lamination towards the top of the

unit (from Wilson and Bosence, 1996). (d) Elk-2-2813.4 m – Photomicrograph of coral, larger benthic foraminifera and carbonate lithoclast (includes planktonic foraminifera and bioclastic wacke/packstone clasts) rudstone/breccia, with clasts predominantly of pebble grade, equivalent to fine-medium limestone conglomerate/breccia FMI facies. (e) Example of coarse limestone conglomerate/breccia FMI facies from Elk-2 well, showing mainly cobble grade clasts. (f) Elk-2-2756 m – Photomicrograph of altered planktonic foraminifera pack/floatstone with coral fragments equivalent to coarse limestone conglomerate/breccia FMI facies. (g) Elk-2-2756.4 m – Photomicrograph of dolomite between clasts or in fractures in partially dolomitised bioturbated planktonic foraminifera wackestone and planktonic and larger benthic foraminifera bioclastic wacke/packstone/breccia equivalent to coarse limestone conglomerate/breccia FMI facies (h) Example of the dolomitised/highly altered coarse limestone conglomerate/breccia FMI facies from Elk-2 well.

Figure 8) Antelope-1 well: Downhole variations in FMI facies, inferred depositional environments, depositional and diagenetic features, together with representative photomicrographs plotted against FMI image, gamma and *FEQL* lithology logs.

Figure 9) Antelope-2 well: Downhole variations in FMI facies, inferred depositional environments, depositional and diagenetic features, plotted against FMI image, gamma and *FEQL* lithology logs.

Figure 10) Antelope-2 well – FMI facies: vuggy mottled limestone conglomerate/boundstone facies examples. (a) Example of vuggy mottled limestone conglomerate/boundstone FMI facies. (b & c) Examples of vuggy mottled limestone conglomerate/boundstone FMI facies images compared to fullbore core. Note vugs, some after dissolved coral, coralline algal lamination (upper b) and rhodolith (lower c). (d & e) 1837.34 m – thin section photomicrographs of coral bioclastic float/rud/packstone with fractures and vugs enhanced by dissolution. Close-up (e) shows vugs partially infilled with non-ferroan blocky calcite crystals and then by siliciclastics and dolomite crystal silt. (f) 1859.83 m – thin section

photomicrograph showing bioclastic pack/grainstone with finer material concentrated along central possible burrow or seam, (g & h) 1859.40 and 1861.40 m – core photographs showing dissolution seams with dark insoluble material and some laminar coralline algae (white) around recrystallised corals and within recrystallised bioclastic matrix, (i) 1869.43 m – thin section photomicrograph showing coral (centre) affected by early dissolution and compaction, encrusted by coralline algae in a cemented bioclastic grainstone matrix. (j) 1879.03 m – thin section photomicrograph showing recrystallised coral encrusted by coralline algae in a cemented bioclastic grainstone matrix. Stylolite in lower field of view. (k) 1836.45m – thin section photomicrographs of recrystallised coral with micritic infill of original chambers, followed by dissolution and blocky non-ferroan calcite crystal precipitation. (l) 1862.55m – thin section photomicrograph of bioclastic pack/grainstone affected by dissolution of aragonite (coral) followed by cementation (blocky non-ferroan calcite) and compaction.

Figure 11) Antelope wells – FMI facies: low-, moderate-, and high-conductivity vuggy dolomite conglomerate/boundstone facies examples. (a) Example of high-conductivity vuggy dolomite FMI facies from pervasively dolomitised upper imaged interval of Antelope-1 showing gas smearing. (b) Example of low-conductivity vuggy dolomite FMI facies from partially dolomitised interval in Antelope-1 showing large vugs. (c & d) Examples of moderate-conductivity vuggy dolomite FMI facies from pervasively dolomitised middle interval in Antelope-2. The distinctive conductive layer in the centre of image ‘d’ was interpreted as possible clay or a dissolution seam. (e) Borabi-1-4623 ft core photograph: Dolomitised coral bioclastic bound/rudstone – analogue for Antelope dolomitised facies. (f-j) Thin section photomicrograph images of rotary sidewall core samples. (f) Antelope-1-1868 m – Dolomitised coral and mollusc bioclastic pack/floatstone. Dolomite has replaced micrite matrix and is present as a cement partially infilling moulds after leaching of aragonitic coral and mollusc fragments. (g) Antelope-1-1772 m – Dolomitised coral fragment. Micritic infill of coral has been dolomitised, then clear dolomite crystals partially infill biomouldic porosity

after leached-out coral followed by precipitation of large poikilotopic calcite crystals. (h). Antelope-2-1964 m – Possible karsted dolomitised mollusc bioclastic pack/floatstone with dark micritic filled ‘pipe’ through centre of sample. Calcite cements occlude porosity after dolomitisation and partially infill biomoldic voids after molluscs (I) Antelope-2-2115 m – Dolomitised bioclastic grainstone with moderate dolomite cement lined intergranular porosity. However, many of the calcitic bioclasts have been dolomitised (rather than dissolved) and late calcite cements occlude porosity after dolomitisation. (j) Antelope-2-2117 m – Dolomitised coral retaining excellent intragranular and some moldic porosity although much of the original coral skeleton has been replaced by dolomite. Pores are lined by dolomite cements.

Figure 12) Antelope wells – FMI facies: vuggy limestone conglomerate/boundstone facies examples. (a & b) Examples of vuggy limestone conglomerate/boundstone FMI facies from Antelope-2. (c-h) Thin section photomicrographs. (c) Antelope-1-1938.8 m – Highly altered, fractured and dissolution affected carbonate lithic and/or coral (may be subaerial exposure related). Infill of cavities by clay-size carbonate/siliciclastics & dolomite. (d) Antelope-1-1947.4 m – Coralline algal bioclastic grain/rudstone. (e) Antelope-1-1956 m – Coral/lithoclastic floatstone/breccia with multiple dolomite cements rimming pore space before precipitation of poikilotopic calcite crystals. (f) Antelope-2-2184.1 m – Recrystallised coral with dolomitised micritic cavity infill (layered dolomitised micrite infill may be shelter or possible karst infill) (g) Antelope-2-2189.36 m – Dolomitised bioclastic wacke/pack/floatstone with fabric replacive dolomite after micrite. Secondary porosity after dissolution of a coral fragment is partially occluded by dolomite cements. (h) Antelope-2-2184.45 m – Partially dolomitised bioclastic packstone with dolomite cements (colourless) infilling pores, some after dissolution of molluscs.

Figure 13) Antelope-2 well – Examples of vuggy limestone conglomerate (a) and fine-grained thinly bedded limestone (b) FMI facies from the lower imaged section of Antelope-2.

(c & d) Antelope-2 examples of thin sections corresponding to fine-grained thinly bedded limestone FMI facies. (c) Antelope-2-2240 m – Mollusc bioclastic grainstone with calcite cements occluding porosity. (d) Antelope-2-2363 m – Imperforate foraminifera bioclastic grainstone with drusy to blocky cements infilling most porosity (some after leached corals). (e & f) Antelope-2 examples of thin sections corresponding to vuggy limestone conglomerate FMI facies. (e) Antelope-2-2437 m – Cemented recrystallised coral rudstone with isopachous and blocky cements infilling pores. (f) Antelope-2-2388 m – Cemented recrystallised coral with isopachous and blocky cements infilling most porosity (after leached corals). (g) Antelope-2-2289 m – Limestone breccia with dolomitised matrix/cement infill - breccia may be karst related. (h) Antelope-2-2304 m – Close-up view of glaebular/alveolar texture in coral bioclastic pack/rudstone.

Figure 14) Antelope-1 well – (a) Example of limestone conglomerate/boundstone (lower part of image) and fine mottled limestone (upper part of image) from below partially dolomitised zone in Antelope-1. (b) FMI example of one of the 'cycle' boundaries (middle of image) in the middle imaged portion of Antelope-1. Lower part of image is a limestone conglomerate passing upwards into a conglomerate/boundstone FMI texture below the unconformable contact. Above the unconformity a fine, medium bedded limestone passes upwards into a massive-medium bedded clastic limestone FMI facies. (c) Antelope-1-1983 m – Limestone lithoclastic breccia with dolomitised isopachous cements. (d) Antelope-1-2076 m – Imperforate foraminifera (and mollusc) bioclastic grain/packstone. (e) Antelope-1- 2004.5 m – Reddened bioclastic grain/packstone (upper part of image) with alteration and glaebular texture in a dissolution cavity (lower part of image). Reddening, dissolution and the glaebular structure are all probably associated with karstification. (f) Antelope-1- 2228 m – *Halimeda*, coral (& larger benthic foraminifera) bioclastic rud/grainstone with isopachous cements.

Figure 15) Antelope-1 well lower imaged section – (a) Example of limestone conglomerate/breccia (highlighted by blue boxes) interdigitated with fine, thinly bedded

limestone FMI facies. (b). Antelope-1- 2238 m - Larger benthic foraminifera, (coralline algal & echinoderm) pack/grainstone corresponding to limestone conglomerate/breccia FMI facies. (c). Antelope-1-2402 m - Carbonate lithoclastic and larger benthic foraminifera bioclastic floatstone corresponding to limestone conglomerate/breccia FMI facies. (d) Antelope-1- 2323.8 m - Planktonic foraminifera (larger benthic foraminifera and echinoderm) pack/wackestone corresponding to fine, thinly bedded limestone FMI facies. (e) Antelope-1-2290.5 m - Coral & lithoclastic rudstone/breccia corresponding to limestone conglomerate/boundstone FMI facies.

Figure 16) Summary diagram showing depositional and diagenetic observations and inferences possible from a combined borehole (FMI) image analysis and petrography study together with implications for the characterisation, understanding and prediction of reservoir quality.

Table 1) Characteristics of the FMI facies from the Elk-1 and -2 wells, and their petrographic features.

Table 2) Table of composite FMI facies zones, their inferred characteristics and environment of deposition from Elk-1 and Elk-2 wells.

Table 3) Characteristics of the FMI facies from the Antelope-1 and -2 wells, and their petrographic features.

Appendix 1) Table sample locations, their lithologies from petrology, and the FMI facies defined from the image logs at the depth the sample was taken.

Well	Sample type	Depth (m)	Lithology - MW	FMI facies - DL
Elk-1	Cuttings	1671	Planktonic foraminifera (bioclastic/coral) Wacke/Packstone – richer in coral and other bioclastic-rich cuttings than other two samples studied	Argillaceous laminated-thinly bedded Limestone facies, but just below (<1670 m) Nodular Lm – Argillaceous Lm facies
	Cuttings	1674	Planktonic foraminifera (bioclastic/coral) Wacke/Packstone	Argillaceous laminated-thinly bedded Limestone
	Cuttings	1680	PF (bioclastic/coral) W/P	Argillaceous laminated-thinly bedded Limestone
	Cuttings	1683	PF (bioclastic) W/P	Argillaceous laminated-thinly bedded Limestone
	Cuttings	1686	Planktonic foraminifera (bioclastic/coral) Wacke/Packstone	Argillaceous laminated-thinly bedded Limestone
	Cuttings	1689	PF (bioclastic) W/P	Argillaceous laminated-thinly bedded Limestone within 1 m of Nodular Limestone & Argillaceous Limestone
	Cuttings	1692	PF (bioclastic) W/P	Nodular Limestone & Argillaceous Limestone

Well	Sample type	Depth (m)	Lithology - MW	FMI facies - DL
Elk-2	SWC	2355.80	PF (bioturbated) wacke/packstone with dissolution seam	Argillaceous laminated thinly bedded Limestone
	SWC	2409.00	Coral bioclastic grainstone	Fine limestone conglomerate/breccia
	SWC	2416.00	Bioturbated PF bioclastic packstone with dissolution seam	Medium thickly bedded limestone
	SWC	2607.40	PF wacke/mudstone or marl	Marl
	PfC?	2658.10	Bioturbated PF wacke/packstone with abundant dissolution seam	Argillaceous laminated thinly bedded Limestone
	PfC?	2659.50	PF wacke/packstone interbedded with partially silicified PF bioclastic packstone	Argillaceous laminated thinly bedded Limestone
	PfC?	2709.40	PF & LBF bioclastic packstone with well preserved shallow bioclasts	Medium limestone conglomerate/breccia
	PfC?	2709.82	PF & LBF bioclastic packstone with well preserved shallow bioclasts	Medium limestone conglomerate/breccias to laminated thinly bedded limestone
	PfC?	2709.89	Larger Benthic & planktonic foraminifera bioclastic packstone	Laminated thinly bedded limestone and fine limestone conglomerate/breccia
	PfC?	2710.35	LBF (coral) & PF bioclastic packstone	Medium limestone conglomerate/breccia
	PfC?	2710.60	PF packstone interbedded with PF bioclastic packstone	Laminated thinly bedded limestone
	SWC	2731.60	Coral, LBF, ?carb lithoclastic pack/rudstone/breccia	Medium limestone conglomerate/breccia
	SWC	2749.00	Fine Compacted partially dolomitised PF (bioclastic) packstone and coarse undolomitised (uncompacted) PF & LBF bioclastic packstone	Laminated thinly bedded limestone

	SWC	2756	Coral planktonic foraminifera bioclastic wacke/floatstone	Coarse limestone conglomerate/breccia
	SWC	2756.40	Partially dolomitised bioturbated PF wackestone and PF & LBF bioclastic wacke/packstone/ breccia	Coarse limestone conglomerate/breccia
	SWC	2779.00	PF wackestone and PF, LBF & coral bioclastic wacke/pack/floatstone	Medium limestone conglomerate/breccias and laminated thinly bedded limestone
	SWC	2812.60	Coral, LBF, ?carb lithoclastic pack/rudstone/breccia	Medium limestone conglomerate/breccia
	SWC	2813.40	Coral, LBF, ?carb lithoclastic pack/rudstone/breccia	Medium limestone conglomerate/breccia
	SWC	2858.70	Coral, coralline algae, LBF, ?carb lithoclastic pack/grain/rudstone/breccia	Medium limestone conglomerate/breccia
	Cutting	2910.00	PF (bioclastic) wacke/packstone	Laminated thinly bedded limestone
	PfC?	2925.00	Dolomitised (SB) foraminifera & echinoderm bioclastic packstone	Dolomitised medium limestone conglomerate/breccia
	SWC	2926	Dolomitised (SB) foraminifera & echinoderm bioclastic packstone	Dolomitised medium limestone conglomerate/breccia
	SWC	2936.50	Dolomitised bioclastic packstone	Dolomitised coarse limestone conglomerate/breccia
	SWC	2966.5	Dolomitised LBF & echinoderm bioclastic packstone/breccia	Dolomitised medium to coarse limestone conglomerate/breccia
	SWC	2968.80	Dolomitised carbonate lithoclastic & bioclastic pack/rudstone	Medium thickly bedded limestone to fine limestone conglomerate/breccia
	Cuttings (Cavings)	3240.00	PF wacke/packstone	Coarse limestone conglomerate/breccia
	Cuttings (Cavings)	3255.00	PF wacke/packstone	Strongly dolomitised/ altered limestone
	Cavings	3276	Planktonic foraminifera wacke/packstone and recrystallised lst (both/ ?either are unlikely to be representative of well lithology as caving)	Strongly dolomitised/ altered limestone

Well	Sample type	Depth (m)	Lithology - MW	FMI facies – DL & MW
Ant-1	SWC	1748.0	Dolomitized Coral bioclastic ?rud/floatstone	Moderate conductivity vuggy dolomite conglomerate/ boundstone
	SWC	1753.0	Dolostone	Moderate conductivity vuggy dolomite conglomerate/ boundstone
	SWC	1761.8	Dolomitized Coral bioclastic float/pack/grainstone	Moderate conductivity vuggy dolomite conglomerate/ boundstone
	SWC	1766.4	Dolomitized Coral (& CA) bioclastic float/pack/grainstone	Moderate conductivity vuggy dolomite conglomerate/ boundstone
	SWC	1770.5	Dolomitised coralline algae bioclastic ?packstone	Moderate conductivity vuggy dolomite conglomerate/ boundstone
	SWC	1772.0	Dolomitized coral	Moderate conductivity vuggy dolomite conglomerate/ boundstone
	SWC	1780.0	Dolomitized Coral bioclastic float/pack/grainstone	High conductivity vuggy dolomite conglomerate/ boundstone
	SWC	1786.0	Dolomitized Coral & CA bioclastic float/packstone	Moderate conductivity vuggy dolomite conglomerate/ boundstone
	SWC	1788.8	Dolomitized Halimeda bioclastic grain/packstone	Moderate conductivity vuggy dolomite conglomerate/ boundstone
	SWC	1793.8	Dolomitized coralline algae (&	High conductivity vuggy dolomite

			Halimeda) bioclastic packstone	conglomerate/ boundstone
	SWC	1796.0	Reddened coral (& mollusc/Halimeda) bioclastic packstone	High conductivity vuggy dolomite conglomerate/ boundstone
	SWC	1799.5	Dolomitised bioclastic grainstone	High conductivity vuggy dolomite conglomerate/ boundstone
	SWC	1800.0	Dolomitised & Reddened coral bioclastic float/packstone	High conductivity vuggy dolomite conglomerate/ boundstone
	SWC	1800.5	Dolomitised bioclastic grain/packstone	High conductivity vuggy dolomite conglomerate/ boundstone
	SWC	1804.0	Dolomitized Halimeda bioclastic wacke/packstone	High conductivity vuggy dolomite conglomerate/ boundstone
	SWC	1808.4	Dolomitised bioclastic grain/packstone	High conductivity vuggy dolomite conglomerate/ boundstone
	SWC	1815.0	Dolomitized Coral bioclastic rud/grainstone	High conductivity vuggy dolomite conglomerate/ boundstone
	SWC	1820.0	Dolomitized Mollusc bioclastic packstone	High conductivity vuggy dolomite conglomerate/ boundstone
	SWC	1820.6	Dolomitized (Mollusc) bioclastic packstone	High conductivity vuggy dolomite conglomerate/ boundstone
	SWC	1823.0	Dolomitized Coral bioclastic rud/grainstone	High conductivity vuggy dolomite conglomerate/ boundstone
	SWC	1827.0	Dolomitized coral	Moderate conductivity vuggy dolomite conglomerate/ boundstone
	SWC	1833.0	Dolomitised & Reddened coral bioclastic float/packstone	Moderate conductivity vuggy dolomite conglomerate/ boundstone
	SWC	1838.7	Dolomitised & Reddened bioclastic pack/grainstone	Moderate conductivity vuggy dolomite conglomerate/ boundstone
	SWC	1844.2	Dolomitised & Reddened coral & mollusc bioclastic packstone	Moderate conductivity vuggy dolomite conglomerate/ boundstone
	SWC	1854.0	Dolomitised & Reddened bioclastic packstone	Moderate conductivity vuggy dolomite conglomerate/ boundstone
	SWC	1858.0	Dolomitised (& Reddened) coral & mollusc bioclastic pack/floatstone	Moderate conductivity vuggy dolomite conglomerate/ boundstone
	SWC	1864.6	Dolomitised mollusc bioclastic packstone	Moderate conductivity vuggy dolomite conglomerate/ boundstone
	SWC	1868.0	Dolomitised coral & mollusc bioclastic pack/floatstone	Moderate conductivity vuggy dolomite conglomerate/ boundstone
	SWC	1873.0	Dolomitised bioclastic pack/grainstone	Moderate conductivity vuggy dolomite conglomerate/ boundstone
	SWC	1874.0	Dolomitised bioclastic pack/grainstone	Moderate conductivity vuggy dolomite conglomerate/ boundstone
	SWC	1895.6	Dolomitised & Reddened coral bioclastic float/packstone	Moderate conductivity vuggy dolomite conglomerate/ boundstone
	SWC	1900.0	Dolomitised bioclastic (mollusc) grainstone	Moderate conductivity vuggy dolomite conglomerate/ boundstone
	SWC	1902.6	Dolomitised & Reddened coral bioclastic float/packstone	Moderate conductivity vuggy dolomite conglomerate/ boundstone
	SWC	1905.6	Dolomitised & Reddened coral bioclastic float/packstone	Moderate conductivity vuggy dolomite conglomerate/ boundstone
	SWC	1913.6	Dolomitised bioclastic grainstone	Moderate conductivity vuggy dolomite conglomerate/ boundstone
	SWC	1920.8	Dolomitised & Reddened coral	Moderate conductivity vuggy dolomite conglomerate/ boundstone
	SWC	1933.2	Dolomite crystal	Low conductivity vuggy dolomite conglomerate/ boundstone
	SWC	1938.8	Recrystalised, fractured & partially dolomitised	Low conductivity vuggy dolomite conglomerate/ boundstone

			??pack/floatstone	
	SWC	1943.0	Recrystalised, fractured & partially dolomitised ??pack/floatstone	Vuggy limestone conglomerate/ boundstone
	SWC	1947.4	Partially dolomitised Coral & coralline algal bioclastic rud/grainstone	Vuggy limestone conglomerate/ boundstone
	SWC	1950.4	Partially dolomitised Coral & coralline algal bioclastic rud/grainstone	Vuggy limestone conglomerate/ boundstone
	SWC	1956.0	Recrystallised & partially dolomitised Coral/?lithic (& coralline algal) bioclastic pack/floatstone/breccia	Vuggy limestone conglomerate/ boundstone
	SWC	1957.4	Calcite crystal	Vuggy limestone conglomerate/ boundstone
	SWC	1960.0	Recrystalised & partially dolomitised ??packstone	Vuggy limestone conglomerate/ boundstone
	SWC	1964.2	Dolomitised coral ??bioclastic float/packstone	Low conductivity vuggy dolomite conglomerate/ boundstone
	SWC	1968.7	Dolomitised coral bioclastic float/packstone	Low conductivity vuggy dolomite conglomerate/ boundstone
	SWC	1983.0	Recrystalised, fractured & partially dolomitised ??pack/floatstone	Fine mottled limestone
	SWC	1984.0	Recrystalised & dolomitised ??coral (& bioclastic grainstone)	Fine mottled limestone
	SWC	1987.5	Recystalised, fractured & dolomitised coral bioclastic pack/grainstone	Fine mottled limestone
	SWC	1991.0	Coral, mollusc & imperforate bioclastic grainstone	Limestone conglomerate/ boundstone
	SWC	1995.4	Coral, mollusc & imperforate bioclastic grainstone	Limestone conglomerate/ boundstone
	SWC	2004.0	Dolomitised chert	Limestone conglomerate/ boundstone
	SWC	2004.5	Recrystalised coral, & mollusc bioclastic grain/packstone	Limestone conglomerate/ boundstone
	SWC	2012.5	Recrystalised lithoclastic bioclastic grainstone	Limestone conglomerate/ boundstone
	SWC	2017.0	Mollusc & imperforate foraminifera bioclastic pack/grainstone	Limestone conglomerate/ boundstone
	SWC	2018.0	Fractured Mollusc & imperforate foraminifera bioclastic pack/grainstone with cavity infill	Limestone conglomerate/ boundstone
	SWC	2027.0	Coral, Mollusc & imperforate foraminifera bioclastic grainstone	Fine mottled limestone
	SWC	2031.5	Coral, Mollusc & imperforate foraminifera bioclastic grain/packstone	Limestone conglomerate/ boundstone
	SWC	2035.0	Mollusc & imperforate foraminifera bioclastic grain/packstone	Fine mottled limestone
	SWC	2041.0	Fractured Mollusc & imperforate foraminifera bioclastic pack/grainstone with cavity infill	Limestone conglomerate/ boundstone
	SWC	2041.5	Mollusc (& peloid) bioclastic grainstone	Limestone conglomerate/ boundstone

	SWC	2046.0	Coral, Mollusc & imperforate foraminifera bioclastic grain/packstone	Limestone conglomerate/ boundstone
	SWC	2055.0	(Planktonic foraminifera) bioclastic wacke/packstone with clasts (or burrow fill??) of coral, mollusc & imperforate foraminifera bioclastic grainstone	Limestone conglomerate/ boundstone
	SWC	2070.0	(Planktonic foraminifera) bioclastic wacke/packstone	Massive-medium bedded clastic/ brecciated limestone
	SWC	2076.0	Imperforate foraminifera bioclastic grain/packstone	Massive-medium bedded clastic/ brecciated limestone
	SWC	2080.0	Imperforate foraminifera (& mollusc) bioclastic grain/packstone (cut thin)	Massive-medium bedded clastic/ brecciated limestone
	SWC	2084.0	(Coralline algae) Bioclastic wacke/packstone	Massive-medium bedded clastic/ brecciated limestone
	SWC	2084.4	Imperforate foraminifera bioclastic ?grain/packstone (cut very thin)	Massive-medium bedded clastic/ brecciated limestone
	SWC	2093.0	Imperforate/agglutinated foraminifera & mollusc bioclastic pack/grainstone	Fine medium-bedded limestone with brecciated appearance
	SWC	2095.0	Bioclastic wacke/packstone (cut thin)	Fine medium-bedded limestone with brecciated appearance
	SWC	2109.0	?Recrystallised Coral (& imperforate foraminifera) bioclastic wacke/packstone	Massive-medium bedded clastic/ brecciated limestone
	SWC	2111.5	Imperforate foraminifera (& mollusc) bioclastic pack/grainstone	Fine medium-bedded limestone with brecciated appearance
	SWC	2122.6	Recrystallised Coral & ?mollusc bioclastic wacke/pack/floatstone	Massive-medium bedded clastic/ brecciated limestone
	SWC	2133.0	Recrystalised ?Mollusc/coral bioclastic grainstone	Limestone conglomerate/ boundstone
	SWC	2146.0	Mottled mollusc & Imperforate foraminifera bioclastic pack/grainstone	Massive-medium bedded clastic/ brecciated limestone
	SWC	2155.0	Microcodium mottled (Imperforate foraminifera) bioclastic pack/grainstone	Massive-medium bedded clastic/ brecciated limestone
	SWC	2164.0	Mollusc & Imperforate foraminifera bioclastic pack/grainstone	Massive-medium bedded clastic/ brecciated limestone
	SWC	2166.0	Mollusc, coral, encrusting & Imperforate foraminifera bioclastic pack/grainstone	Massive-medium bedded clastic/ brecciated limestone
	SWC	2166.8	??Mollusc & Imperforate foraminifera bioclastic pack/wackestone (cut thin)	Massive-medium bedded clastic/ brecciated limestone
	SWC	2167.0	Mottled & brecciated coral bioclastic rud/packstone	Massive-medium bedded clastic/ brecciated limestone
	SWC	2180.0	Reddened/mottled coral bioclastic rud/packstone	Limestone conglomerate/ boundstone
	SWC	2182.0	Recrystallised coral, coralline algae & ?lithoclastic/bioclastic breccia/floatstone	Massive-medium bedded clastic/ brecciated limestone
	SWC	2186.0	Coral & coralline algal bioclastic	Limestone conglomerate/ boundstone

			floatstone	
	SWC	2189.79	Mollusc & Imperforate foraminifera bioclastic pack/grainstone (cut thin)	Massive-medium bedded clastic/ brecciated limestone
	SWC	2200.0	Recrystallised coral floatstone	Massive-medium bedded clastic/ brecciated limestone
	SWC	2211.8	Halimeda, larger benthic foraminifera (& coral) bioclastic rud/grainstone	Massive-medium bedded clastic/ brecciated limestone
	SWC	2218.5	Coral	Massive-medium bedded clastic/ brecciated limestone
	SWC	2228.0	Halimeda, coral (& larger benthic foraminifera) bioclastic rud/grainstone	Massive-medium bedded clastic/ brecciated limestone
	SWC	2239.2	Recrystalised fractured limestone (cut thin)	Limestone conglomerate/ boundstone
	SWC	2250.0	Larger benthic foraminifera (& coral) bioclastic packstone	Fine, thinly-bedded limestone
	SWC	2254.0	Bioclastic pack/wackestone	Fine, thinly-bedded limestone
	SWC	2255.6	Larger benthic foraminifera bioclastic packstone	Medium bedded clastic limestone
	SWC	2266.0	Larger benthic foraminifera, echinoderm, (coral & coralline algae) bioclastic packstone	Medium bedded clastic limestone
	SWC	2272.0	?Echinoderm, coralline algae & larger benthic foraminifera bioclastic packstone (cut thin)	Medium bedded clastic limestone
	SWC	2275.0	Echinoderm, larger benthic foraminifera (& coralline algae) bioclastic packstone	Medium bedded clastic limestone
	SWC	2288.0	Echinoderm (coralline algae & larger benthic foraminifera) bioclastic packstone	Fine, thinly-bedded limestone
	SWC	2290.0	Echinoderm (coralline algae & larger benthic foraminifera) bioclastic packstone	Fine, thinly-bedded limestone
	SWC	2290.2	Echinoderm (coralline algae & larger benthic foraminifera) bioclastic packstone	Fine, thinly-bedded limestone
	SWC	2290.5	Coral & lithoclastic rudstone / breccia	Limestone conglomerate/ boundstone
	SWC	2292.0	Coral and larger benthic foraminifera bioclastic rud/pack/grainstone	Limestone conglomerate/ boundstone
	SWC	2297.6	Coral and ?lithoclastic breccia/floatstone	Limestone conglomerate/ boundstone
	SWC	2302.8	Echinoderm (coralline algae & larger benthic foraminifera) bioclastic packstone	Fine, thinly-bedded limestone
	SWC	2316.0	Recrystallised planktonic & small benthic foraminifera (& echinoderm) bioclastic pack/grainstone	Fine, thinly-bedded limestone
	SWC	2322.8	Echinoderm (& coralline algae) bioclastic packstone	Fine, thinly-bedded limestone
	SWC	2323.5	Planktonic foraminifera (larger benthic foraminifera & Echinoderm) packstone	Fine, thinly-bedded limestone
	SWC	2329.0	Recrystallised Larger benthic	Fine, thinly-bedded limestone

			foraminifera (& Coralline algal) grainstone	
	SWC	2338.0	Larger benthic foraminifera, (Coralline algal & echinoderm) pack/grainstone	Medium bedded clastic limestone
	SWC	2353.0	Altered Larger benthic foraminifera & coral bioclastic rud/?grainstone (cut very thin)	Fine, thinly-bedded limestone containing clasts
	SWC	2372.6	Larger benthic foraminifera & coral bioclastic grainstone	Thickly bedded clastic limestone
	SWC	2394.0	Coral bioclastic rud/packgrainstone	Medium bedded clastic limestone
	SWC	2396.0	Carbonate ?lithoclastic and larger benthic foraminifera bioclastic floatstone	Medium bedded clastic limestone
	SWC	2401.0	Carbonate ?lithoclastic and larger benthic foraminifera bioclastic floatstone	Medium bedded clastic limestone
	SWC	2402.0	Carbonate lithoclastic and larger benthic foraminifera bioclastic floatstone	Medium bedded clastic limestone
	SWC	2409.0	Planktonic foraminifera bioclastic packstone (cut very thin)	Fine, thinly bedded limestone
	SWC	2445.0	Larger benthic foraminifera, (Coralline algal & echinoderm) pack/grainstone	Fine, thinly bedded limestone

Well	Sample type	Depth (m)	Lithology - MW	FMI facies – DL & MW
Ant-2	SWC	1832	Recrystallised coral bioclastic float/pack/grainstone	Vuggy Mottled Limestone Conglomerate / Boundstone
	SWC	1834	Recrystallised coral bioclastic pack/floatstone	Vuggy Mottled Limestone Conglomerate / Boundstone
	FCP	1835.24	Algal bioclastic pack/grainstone	Vuggy Mottled Limestone Conglomerate / Boundstone
	SWC	1836	Algal bioclastic grain/pacstone	Vuggy Mottled Limestone Conglomerate / Boundstone
	FCP	1836.45	Recrystalised coral	Vuggy Mottled Limestone Conglomerate / Boundstone
	FCP	1837.34	Recrystalised coral bioclastic rudstone	Vuggy Mottled Limestone Conglomerate / Boundstone
	FCP	1838.51	Recrystalised coral bioclastic rud/float/packstone	Vuggy Mottled Limestone Conglomerate / Boundstone
	FCP	1840.02	Coral bioclastic pack/grainstone	Vuggy Mottled Limestone Conglomerate / Boundstone
	SWC	1843	Recrystallised coral bioclastic grain/float/rudstone	Vuggy Mottled Limestone Conglomerate / Boundstone
	SWC	1845	(Coral) Algal bioclastic grain/packstone	Vuggy Mottled Limestone Conglomerate / Boundstone
	FCP	1846.35	(Coral) Algal bioclastic grain/packstone	Vuggy Mottled Limestone Conglomerate / Boundstone
	FCP	1848.74	Bioclastic pack/grainstone	Vuggy Mottled Limestone Conglomerate / Boundstone
	FCP	1849.64	Bioclastic pack/graintone	Vuggy Mottled Limestone Conglomerate / Boundstone
	SWC	1850	Recrystallised coral bioclastic grain/pack/rudstone	Vuggy Mottled Limestone Conglomerate / Boundstone
	FCP	1851.47	Recrystalised coral & mollusc	Vuggy Mottled Limestone

			biolcastic rud/packstone	Conglomerate / Boundstone
	SWC	1852	Recrystalised coral bioclastic ?rud/packstone	Vuggy Mottled Limestone Conglomerate / Boundstone
	FCP	1854.73	Recrystalised coral bound/rudstone	Vuggy Mottled Limestone Conglomerate / Boundstone
	FCP	1855.63	Recrystalised coral bioclastic rud/pack/grainstone	Vuggy Mottled Limestone Conglomerate / Boundstone
	FCP	1857.15	Bioclastic packstone	Vuggy Mottled Limestone Conglomerate / Boundstone
	SWC	1859	Bioclastic packstone	Vuggy Mottled Limestone Conglomerate / Boundstone
	FCP	1859.83	Recrystalised coral & algal bioclastic pack/rudstone	Vuggy Mottled Limestone Conglomerate / Boundstone
	SWC	1860.5		Vuggy Mottled Limestone Conglomerate / Boundstone
	SWC	1862.5	Bioclastic pack/grainstone	Vuggy Mottled Limestone Conglomerate / Boundstone
	FCP	1862.55	Bioclastic grain/packstone	Vuggy Mottled Limestone Conglomerate / Boundstone
	FCP	1864.63	(Coral/sponge) Bioclastic grainstone	Vuggy Mottled Limestone Conglomerate / Boundstone
	FCP	1867.96	Recrystalised coral bioclastic rud/grainstone	Vuggy Mottled Limestone Conglomerate / Boundstone
	SWC	1868	Bioclastic grainstone	Vuggy Mottled Limestone Conglomerate / Boundstone
	FCP	1869.43	Recrystalised coral & algal bioclastic grain/rudstone	Vuggy Mottled Limestone Conglomerate / Boundstone
	FCP	1870.96	Recrystalised (coral) bioclastic grainstone	Vuggy Mottled Limestone Conglomerate / Boundstone
	FCP	1874.23	(Coralline algal) bioclastic pack/grainstone	Vuggy Mottled Limestone Conglomerate / Boundstone
	SWC	1878.3 May be mislabel ed	Dolomitised coral & mollusc bioclastic pack/rudstone	Vuggy Mottled Limestone Conglomerate / Boundstone
	FCP	1878.30 May be mislabel ed	Dolomitised /recrystalised coral bioclastic rud/pack/grainstone	Vuggy Mottled Limestone Conglomerate / Boundstone
	SWC	1879	Coral bioclastic grain/rudstone	Vuggy Mottled Limestone Conglomerate / Boundstone
	FCP	1879.03	Recrystalised coral and coralline algal bioclastic rud/grainstone	Vuggy Mottled Limestone Conglomerate / Boundstone
	FCP	1879.33	Bioclastic grainstone	Vuggy Mottled Limestone Conglomerate / Boundstone
	FCP	1881.15	(Echinoderm & coralline algal) bioclastic grain/packstone	Vuggy Mottled Limestone Conglomerate / Boundstone
	FCP	1881.43	(Echinoderm &) coralline algal bioclastic grainstone	Vuggy Mottled Limestone Conglomerate / Boundstone
	SWC	1887	Larger benthic foraminifera & coralline algal bioclastic grainstone	Vuggy Mottled Limestone Conglomerate / Boundstone
	SWC	1900.00	Recrystalised coral bioclastic rud/pack/floatstone	Vuggy Mottled Limestone Conglomerate / Boundstone
	SWC	1902.5	Larger benthic foraminifera (& coralline algal) bioclastic grain/packstone	Vuggy Mottled Limestone Conglomerate / Boundstone
	SWC	1903	Algal bioclastic bind/pack/grainstone	Vuggy Mottled Limestone Conglomerate / Boundstone

	SWC	1903	Partially dolomitised coral & mollusc bioclastic pack/rudstone	Vuggy Mottled Limestone Conglomerate / Boundstone
	SWC	1904.5	Recrystalised coral bioclastic grain/rudstone	Vuggy Mottled Limestone Conglomerate / Boundstone
	SWC	1925.00	Recrystalised coral bioclastic rud/pack/grainstone	Vuggy Mottled Limestone Conglomerate / Boundstone
	SWC	1929	Larger benthic foraminifera & coral bioclastic grain/packstone	Vuggy Mottled Limestone Conglomerate / Boundstone
	SWC	1932	Larger benthic foraminifera (& coralline algal) bioclastic grain/packstone	Vuggy Mottled Limestone Conglomerate / Boundstone
	SWC	1937	Recrystalised coral & coralline algal bioclastic grain/rud/packstone	Vuggy Mottled Limestone Conglomerate / Boundstone
	SWC	1939	Bioclastic grain/packstone	Low conductivity vuggy dolomite conglomerate / boundstone
	SWC	1945	Recrystalised coral bioclastic pack/rud/grainstone	Low conductivity vuggy dolomite conglomerate / boundstone
	SWC	1955	Coralline algal bioclastic pack/grainstone	Low conductivity vuggy dolomite conglomerate / boundstone
	SWC	1959.00	Dolomitised bioclastic packstone	Low conductivity vuggy dolomite conglomerate / boundstone
	SWC	1960.5	Bioclastic grain/packstone	Low conductivity vuggy dolomite conglomerate / boundstone
	SWC	1964	Karsted (probable) dolomitised mollusc bioclastic pack/floatstone	Low conductivity vuggy dolomite conglomerate / boundstone
	SWC	1966	Dolomitised coral bioclastic pack/floatstone	Low conductivity vuggy dolomite conglomerate / boundstone
	SWC	1971.5	Dolomitised coralline algal & imperforate foraminifera bioclastic grain/packstone*	Low conductivity vuggy dolomite conglomerate / boundstone
	SWC	1974.5	Dolomitised bioclastic packstone	Low conductivity vuggy dolomite conglomerate / boundstone
	SWC	1989	Dolomitised coral bioclastic rud/packstone	Low conductivity vuggy dolomite conglomerate / boundstone
	SWC	1992	Dolomitised bioclastic pack/grainstone	Low conductivity vuggy dolomite conglomerate / boundstone
	SWC	1995	Dolomitised coral bioclastic rud/packstone	Low conductivity vuggy dolomite conglomerate / boundstone
	SWC	2002	Dolomitised (mollusc & Halimeda) bioclastic pack/grainstone	Low conductivity vuggy dolomite conglomerate / boundstone
	SWC	2005	Dolomitised mollusc bioclastic grain/packstone	Low conductivity vuggy dolomite conglomerate / boundstone
	SWC	2005.5	Dolomitised coral bioclastic float/rud/packstone	Low conductivity vuggy dolomite conglomerate / boundstone
	SWC	2011.5	Dolomitised mollusc bioclastic packstone	Low conductivity vuggy dolomite conglomerate / boundstone
	SWC	2011.50	Dolomitised bioclastic packstone	Low conductivity vuggy dolomite conglomerate / boundstone
	SWC	2017	Dolomitised coral & coralline algal bioclastic rud/packstone	Low conductivity vuggy dolomite conglomerate / boundstone
	SWC	2022	Dolomitised coralline algal bioclastic packstone	Low conductivity vuggy dolomite conglomerate / boundstone
	SWC	2024	Dolomitised coral & coralline algal bioclastic grain/rudstone	Low conductivity vuggy dolomite conglomerate / boundstone
	SWC	2037	Dolomitised mollusc bioclastic wacke/packstone	Low conductivity vuggy dolomite conglomerate / boundstone

	SWC	2037.00	Dolomitised bioclastic wacke/packstone	Low conductivity vuggy dolomite conglomerate / boundstone
	SWC	2048	Dolomitised mollusc bioclastic pack/wackestone	Low conductivity vuggy dolomite conglomerate / boundstone
	SWC	2052	Fractured & dolomitised coral & coralline algal bioclastic pack/rudstone	Low conductivity vuggy dolomite conglomerate / boundstone
	SWC	2062	Dolomitised coral & coralline algal bioclastic grain/rudstone	Low conductivity vuggy dolomite conglomerate / boundstone
	SWC	2062.00	Dolomitised bioclastic grainstone	Low conductivity vuggy dolomite conglomerate / boundstone
	SWC	2065	Dolomitised bioclastic grainstone	Low conductivity vuggy dolomite conglomerate / boundstone
	SWC	2070.5	Dolomitised coral bioclastic rud/grainstone	Low conductivity vuggy dolomite conglomerate / boundstone
	SWC	2093	Dolomitised coral (& imperforate foraminifera) bioclastic rud/grain/packstone	Moderate conductivity vuggy dolomite conglomerate / boundstone
	SWC	2100.5	Dolomitised coral bioclastic pack/float/grainstone	Moderate conductivity vuggy dolomite conglomerate / boundstone
	SWC	2100.50	Dolomitised coral bioclastic pack/float/grainstone	Moderate conductivity vuggy dolomite conglomerate / boundstone
	SWC	2115	Dolomitised coral bioclastic rud/grainstone	High conductivity vuggy dolomite conglomerate / boundstone
	SWC	2117	Dolomitised coral	High conductivity vuggy dolomite conglomerate / boundstone
	SWC	2124	Dolomitised bioclastic wackestone	High conductivity vuggy dolomite conglomerate / boundstone
	SWC	2124.00	Dolomitised bioclastic wacke/packstone	High conductivity vuggy dolomite conglomerate / boundstone
	FCP	2184.10	Recrystalised coral with dolomitised micritic cavity infill (layered dolomitised micrite infill may be shelter or ?karst infill)	Vuggy Limestone Conglomerate /Boundstone
	FCP	2184.45	Partially dolomitised bioclastic packstone	Vuggy Limestone Conglomerate /Boundstone
	FCP	2189.36	Dolomitised coral bioclastic pack/floatstone	Vuggy Limestone Conglomerate /Boundstone
	FCP	2189.76	Dolomitised bioclastic wacke/pack/floatstone	Vuggy Limestone Conglomerate /Boundstone
	FCP	2192.82	Dolomitised mollusc bioclastic wacke/packstone	Low conductivity vuggy dolomite conglomerate / boundstone
	FCP	2193.02	Dolomitised bioclastic packstone	Low conductivity vuggy dolomite conglomerate / boundstone
	SWC	2231	Coral & mollusc bioclastic pack/floatstone	Vuggy Limestone Conglomerate
	SWC	2240.00	Mollusc bioclastic grainstone	Fine, thinly bedded limestone
	SWC	2253.00	Mollusc & coral bioclastic grain/rud/packstone	Vuggy Limestone Conglomerate
	SWC	2264	Mollusc & foraminifera bioclastic pack/grainstone	Fine, thinly bedded limestone
	SWC	2274.00	Mollusc & imperforate foraminifera bioclastic grainstone	Vuggy Limestone Conglomerate
	SWC	2283	Foraminifera bioclastic packstone	Vuggy Limestone Conglomerate
	SWC	2289.00	Limestone breccia with dolomitised matrix/cement infill	Vuggy Limestone Conglomerate
	SWC	2294.5	Echinoderm & foraminifera	Vuggy Limestone Conglomerate

			bioclastic packstone	
	SWC	2302.00	Bioclastic pack/grainstone	Vuggy Limestone Conglomerate
	SWC	2304	Glaebular/alveolar coral bioclastic pack/rudstone	Vuggy Limestone Conglomerate
	SWC	2312.00	Recrystalised coral (predominantly) bioclastic pack/floatstone	Vuggy Limestone Conglomerate
	SWC	2321.5	(Fenestral) Coral bioclastic floatstone	Vuggy Limestone Conglomerate
	SWC	2329	Mottled mollusc bioclastic wacke/pack/grainstone	Fine, thinly bedded limestone
	SWC	2329.00	Bioclastic (mollusc & imperforate foraminifera) packstone	Fine, thinly bedded limestone
	SWC	2332	Mollusc & imperforate foraminifera bioclastic wack/packstone	Fine, thinly bedded limestone
	SWC	2338.40	Imperforate foraminifera (& algal) grainstone	Fine, thinly bedded limestone
	SWC	2340.5	(Imperforate) Foraminifera bioclastic grainstone	Fine, thinly bedded limestone
	SWC	2341.40	Imperforate foraminifera (& algal) grainstone	Fine, thinly bedded limestone
	SWC	2343	Imperforate foraminifera bioclastic grainstone	Fine, thinly bedded limestone
	SWC	2347.57	Calcite cemented cavity infill or coral replacement in (coral) bioclastic pack/floatstone	Vuggy Limestone Conglomerate
	SWC	2357.00	Calcite cemented recrystalised coral	Vuggy Limestone Conglomerate
	SWC	2361	Calcite cemented recrystalised coral	Vuggy Limestone Conglomerate
	SWC	2363.5	Imperforate foraminifera & mollusc bioclastic grainstone	Fine, thinly bedded limestone
	SWC	2372	Bioclastic wackestone	Vuggy Limestone Conglomerate
	SWC	2374	Cemented recrystalised coral (?floatstone)	Vuggy Limestone Conglomerate
	SWC	2383.00	Mollusc bioclastic wacke/packstone	Vuggy Limestone Conglomerate
	SWC	2387	Mollusc bioclastic grain/packstone	Vuggy Limestone Conglomerate
	SWC	2388	Cemented recrystalised coral	Fine, thinly bedded limestone
	SWC	2401.5	Recrystalised coral & foraminifera bioclastic rud/pack/grainstone	Vuggy Limestone Conglomerate
	SWC	2413.00	Coral & Halimeda bioclastic pack/floatstone	Vuggy Limestone Conglomerate
	SWC	2415	Fractured cemented recrystalised coral	Vuggy Limestone Conglomerate
	SWC	2422	Halimeda & mollusc bioclastic pack/grainstone	Vuggy Limestone Conglomerate
	SWC	2430	Fractured cemented recrystalised coral	Vuggy Limestone Conglomerate
	SWC	2434	Brecciated cemented recrystalised ?coral bioclastic rud/packstone	Vuggy Limestone Conglomerate
	SWC	2437	Cemented recrystalised coral rudstone	Vuggy Limestone Conglomerate

FMI Facies	Occurrence in wells	Texture seen on FMI image	Conductivity (from FMI)	Clay % (from FEQL)	Inclusions (from FMI)	Lamination Density (from FMI)	Connectivity Index Coefficient (from FMI)	Lithology (from samples)	Sedimentary features (from samples)	Diagenetic features (from samples)
Marl	Elk-1: upper imaged section. Elk-2: upper imaged section & upper part of upper 2 sequences.	Subequal thin-medium conductive and resistive beds (faintly laminated)(smooth appearance)	Very high (>22)	>35%	Sub-equal resistive & conductive inclusions	Intermediate	Medium	Planktonic foraminifera wacke/mudstone or marl	>90% clay-sized matrix (both carbonate and siliciclastic) and well-preserved planktonic foraminifera	Mechanical compaction of foraminifera. Minor equant calcite cement in bioclast chambers.
Argillaceous Laminated-thinly bedded limestone	Elk-1: mainly upper imaged section & upper part of all 3 sequences. Elk-2: upper imaged section & upper part of upper 2 sequences.	Sub-equal thin resistive beds & conductive laminations-thin beds (can have smooth appearance)	Medium (>22)	10-35%	Resistive patches and spots abundant. Conductive inclusions	High (>10)	Low	Planktonic foraminifera wacke/packstone	Abundant clay-sized matrix (60-80%) and well preserved planktonic foraminifera. Bioturbation is common. Disseminated, or interbedded laminae richer in, shallow fragmented bioclasts	Mechanical compaction of foraminifera. Anastomosing dissolution seams. Silicicfication of bioclastic rich laminae. Minor equant calcite cement in bioclast chambers.
Nodular Limestone & Argillaceous Limestone	Elk-1: mainly upper imaged section & upper to middle part of all 3 sequences.	Nodular resistive beds with thin conductive beds or laminations	Low (<10)	<10%	Resistive patches and spots abundant. Conductive inclusions	High (>10)	Low-medium	Planktonic foraminifera wacke/packstone plus probable coral bioclastic rud/packstones	Planktonic foraminifera rich cuttings plus fragemted corals and larger benthic foraminifera.	Blocky to equant cements. Mechanical compaction features and sutured grain contacts. Some cement may have formed prior to reworking of bioclasts, but most features are probably burial related.
Laminated-thinly bedded limestone	Elk-1: present in all 3 sequences, most common in middle imaged section. Elk-2: present in all 4	Thin resistive beds separated by conductive laminations	Usually low (<22)	<10%	Resistive patches and spots abundant. Conductive inclusions	High (>10)	Very low	Planktonic foraminifera packstones interbedded with planktonic foraminifera	Abundant whole and fragmented planktonic foraminifera with 10% and 40% fragmented shallow	Mechanical compaction of bioclasts and sutured grain contacts. Dissolution seams

	sequences, most common in middle imaged section.							bioclastic packstones	water bioclasts. Some bioturbation.	(common along lithological boundaries). Equant cements in bioclasts.
Mottled/bioturbated limestone	Elk-1: minor facies, most common in middle imaged section.	Medium-thickly bedded limestone highly fractured and possibly altered (possibly bioturbated)	Low (<10)	<10%	Resistive patches and spots abundant. Conductive inclusions	Low-medium (>10 due to skewing by fractures)	Very low	None available	N/A	N/A
Fine-medium limestone conglomerate/ breccia	Elk-2: present in lower 3 sequences, most common in middle imaged section.	Resistive clasts (angular-rounded) (usually up to granule to pebble) within a conductive matrix	Usually high (>22)	V.low - nil	Conductive patches and spots abundant; Resistive inclusions very low	Very Low (<<10)	Low to medium	Most samples are coral, larger benthic foraminifera and carbonate lithoclastic pack/rudstone/breccias, but also includes planktonic and larger benthic foraminifera bioclastic packstones, and dolomitised foraminifera and echinoderm bioclastic packstones	Well-preserved planktonic foraminifera, together with fragmented larger benthic foraminifera, coral, echinoderm coralline algae and bryozoa debris. Lithoclasts include planktonic foraminifera wackestones and bioclastic packstones.	Mechanical breakage of grains, sutured contacts and minor equant cements. Some samples contain significant post-depositional dolomite. Syntaxial overgrowths on echinoderm material
Medium-thickly bedded limestone	Elk-1: middle to lower imaged section & making up the lower part of the lower 2 sequences. Elk-2: most common in middle imaged section.	Subequal medium to thick resistive & conductive interbeds; or medium to thick resistive beds with conductive lamina	Usually low (<22)	<10%	Variable, yet usually resistive patches and spots abundant. Conductive inclusions	Low (<10)	Very low	Planktonic foraminifera bioclastic packstone and ? dolomitised carbonate lithoclastic & bioclastic pack/rudstone/breccia	Fragmented larger benthic foraminifera, coralline algae and well preserved planktonic foraminifera	Dolomitisation, sutured grain contacts, mechanical compaction, syntaxial overgrowths on echinoderm material and equant cements.
Coarse limestone conglomerate/ breccia	Elk-2: present in lower 3 sequences, most common in lower imaged section.	Resistive clasts (angular-rounded) (usually up to pebble to cobble) within a conductive matrix	High (>22)	V.low - nil	Conductive patches and spots abundant; Resistive inclusions very	Very Low (<<10)	Low to medium	Coral and planktonic foraminifera pack/floatstone and dolomitised breccias.	Corals in micritic matrix and in breccias clasts include planktonic foraminifera wackestone and planktonic	Compaction, fractures, granular, mosaic and equant cements. Dolomitisation between clasts or in fractures

					low				foraminifera bioclastic wacke/packstone	
Strongly dolomitised/ altered limestone	Elk-2: lower imaged section.	Resistive clasts (angular-rounded) (usually upper pebble/cobble) within a conductive matrix. Blurred boundaries between clasts and matrix.	Very high (>>22)	V.low - nil	Conductive patches and spots abundant; Resistive inclusions very low	Very Low (<<10)	Medium	None available	N/A	N/A

Table 1: Characteristics of the FMI facies from the Elk-1 and -2 wells, and their petrographic features.

Zone/composite facies	Probable sedimentology	Environment of deposition	Water depth/energy conditions
Marl & Argillcaeous Limestone	Clay-rich fine limestone sediments	Basin Floor	Very deep marine, very low energy conditions
Argillaceous Lm & nodular/laminated-thinly bedded Lm	Clayey and non-clayey fine limestone sediments	Deep lower slope	Deep marine, Low energy conditions
Mainly laminated-thinly bedded Lm	Non-clayey fine limestone sediments	Lower slope	Deep marine, Low energy conditions
Laminated-thickly bedded Lm & Limestone conglomerate/breccia	Fine –medium limestone sediments w/ debris flow limestone breccia/conglomerate deposits	Lower - Upper Slope	Intermediate marine depth. Generally low-moderate energy with gravity driven flow events
Mainly medium-thickly bedded Lm	Fine-medium limestone sediments	Lower - Upper Slope	Intermediate marine depth. Generally low – moderate energy w/ gravity driven flow events
Coarse Lm conglomerate/breccia, minor medium-thickly bedded Lm	Debris flow and/or storm-derived limestone breccia/conglomerate deposits, w/ minor fine-medium limestone sediments	Upper Slope	Shallow marine. Generally high energy conditions
Coarse Lm conglomerate/breccia	Debris flow and/or storm-derived limestone breccia/conglomerate deposits	Upper Slope	Very shallow marine. Generally high energy conditions
Dolomitised/strongly altered Limestone	Debris flow and/or storm-derived limestone breccia/conglomerate deposits	Upper Slope	Very shallow marine. Generally high energy conditions

FMI Facies	Occurrence in wells	Texture seen on FMI image	Conductivity (from FMI)	Composition (from FEQL)	Bedding or laminations (from FMI)	Connectivity Index Coefficient (from FMI)	Lithology (from samples)	Sedimentary features (from samples)	Diagenetic features (from samples)
Vuggy mottled limestone conglomerate/ boundstone	Antelope-2: upper imaged section.	Conductive vugs & holes & mesh-like layering within a generally distinct resistive conglomeratic/boundstone fabric.	Low-Medium	>70% limestone (predominantly >95% limestone) with minor dolomite	Massive to thickly bedded	Low	Coral, larger benthic foraminifera and/or coralline algal bioclastic grain/pack/rudstone	Massive corals many reworked, coralline algae (including rhodoliths),fragmented larger benthic foraminifera, echinoderm debris, bryozoa, barnacles and planktonic foraminifera. Grainy rudstone units gradationally interbed with more micritic algal laminated units	Heavily recrystallised. Early dissolution, fracturing, solution enhancement of fractures and infill by siliciclastic sediment and dolomite crystal silt are common. Mosaic to blocky calcite cements prevalent. Stylolites and dissolution seams common in micritic intervals.
Vuggy limestone conglomerate/ boundstone	Antelope-1: partially dolomitised lower part of upper imaged section. Antelope-2: predominantly dolomitised lower part of middle imaged section.	Abundant conductive vugs & holes within a generally distinct resistive conglomeratic/boundstone fabric	Low	Predominantly limestone with up to 20-40% dolomite	Thick bedded	Low	Coral and mollusc bioclastic pack/grainfloatstone	Common coral, mollusc and some encrusting coralline algal material. Disseminated coralline algal debris and imperforate foraminifera are also present.	Localised micritisation, aragonite dissolution, reddening . Some dolomite replacing matrix and as cement. Late leaching, poikilotopic calcite cements.
Highly conductive vuggy dolomite conglomerate/ boundstone	Antelope-1: upper pervasively dolomitised imaged section. Antelope-2: middle pervasively dolomitised imaged section.	Abundant conductive vugs & holes within a highly conductive, conglomeratic/boundstone fabric.	High	>90-95% dolomite with minor limestone	Massive to thickly bedded	High	Dolomitised (coral) bioclastic wacke/pack/floatstone	Dolomitised coral-rich units with common molluscs, and imperforate foraminifera. Less common coralline algae and *Halimeda*.	Bioclast micritisation, aragonite dissolution and reddening . Dolomite replacing matrix and as cement. Late leaching, poikilotopic calcite cements.

Moderately conductive vuggy dolomite conglomerate/ boundstone	Antelope-1: upper pervasively dolomitised imaged section. Antelope-2: middle pervasively dolomitised imaged section.	Abundant conductive vugs & holes within a moderately conductive or slightly resistive, conglomeratic/boundstone fabric.	Medium	>80% dolomite with more minor limestone	Massive to thickly bedded	Medium	Dolomitised coral bioclastic pack/float/grainstone	Dolomitised coral-rich units with common molluscs, and imperforate foraminifera. Less common coralline algae and *Halimeda.*	Bioclast micritisation, aragonite dissolution and reddening . Dolomite replacing matrix and as cement. Late leaching, poikilotopic calcite cements.
Low conductivity vuggy dolomite conglomerate/ boundstone	Antelope-1: upper pervasively and partially dolomitised imaged section. Antelope-2: middle pervasively and predominantly dolomitised imaged section.	Conductive vugs & holes within a generally resistive, usually blurred conglomeratic/boundstone fabric.	Low	>60% dolomite with more minor limestone	Massive to thickly bedded	Low	Dolomitised (coral) bioclastic (mollusc) wacke/pack/grain/rudstone	Dolomitised coral-rich units with common molluscs, and imperforate foraminifera. Less common coralline algae and *Halimeda.*	Bioclast micritisation, aragonite dissolution and reddening . Dolomite replacing matrix and as cement. Late leaching, poikilotopic calcite cements.
Vuggy limestone conglomerate	Antelope-2: lower imaged section.	Abundant conductive vugs & holes within a generally distinct resistive conglomeratic fabric (no obvious boundstone or internal fabric)	Low-Medium	>98% limestone with occasional very minor clay or dolomite	Occasional thick bedding	Medium	Coral bioclastic (mollusc, *Halimeda,* foraminifera) pack/grain/float/rudstone and/or limestone breccia	Coral-rich, other locally common elements include molluscs, *Halimeda*, perforate and imperforate foraminifera, echinoderm debris and carbonate lithoclasts.	Grain micritisation, isopachous cements (multiple phases). Glaebules, alveolar texture and *Microcodium.* Dissolution, common blocky and neomorphic cements. Fracutres, minor compaction and minor dolomite cements.
Fine, thinly bedded limestone	Antelope-1: lower imaged section. Antelope-2: lower imaged section.	Fine grained, typically thinly bedded limestone with smooth appearance. May include minor resisitive clasts.	Low-Medium	>98% limestone with occasional very minor clay or dolomite	Thin bedding	Medium	Bioclastic (mollusc and imperforate foraminifera) wacke/pack/ grainstone	Abundant molluscs and imperforate foraminifera. Less common *Halimeda*, coralline algae, perforate foraminifera and minor corals. Many bioclasts fragmented.	Grain micritisation, glaebules, alveolar texture and *Microcodium.* Dissolution, common blocky and neomorphic cements. Fracutres, minor compaction and minor dolomite

									cements.
Limestone conglomerate/ boundstone	Antelope-1: middle imaged section and minor interbeds in lower imaged section.	Coarse texture with distinct resistive clasts in a more conductive groundmass. Some internal, wavy (boundstone) fabric.	Low-Medium	Predominantly >90% limestone	Massive to thickly bedded	Low	(Coral), mollusc and imperforate foraminifera bioclastic pack/ grainstones	Common corals, carbonate lithoclasts, molluscs and imperforate foraminifera. Coralline algae, echinoderm debris larger benthic foraminifera and *Halimeda* also present. Many components fragmented and abraded	Micritisation, isopachous cements, dissolution, common blocky and neomorphic cements and compaction. Glaebular and alveolar structure as well as cavity infills present.
Fine mottled limestone	Antelope-1: upper part of middle imaged section.	Resistive spots and patches within a generally conductive mottled fabric	Medium	Predominantly >95% limestone	Massive to metre-scale bedding (?thick bedding)	Low	Partially dolomitised coral float/rud/packstones or breccias and mollusc, imperforate foraminifera and coral bioclastic grain/ packstones	Common corals, carbonate lithoclasts, molluscs and imperforate foraminifera. Many components fragmented and abraded	Dolomite may replace matrix and or earlier calcite cements. Late dolomite cements. Micritisation, isopachous cements, dissolution, common blocky and neomorphic cements and compaction.
Limestone conglomerate/ breccia	Antelope-1: middle and lower imaged sections.	Elliptical resistive clasts, some with distinct conductive rims in a moderately conductive groundmass	Medium-Low	>98% limestone	Massive to medium or thickly bedded	Low	(Coral), mollusc and imperforate foraminifera bioclastic pack/ grainstones, also minor wackestones in middle section. In lower imaged section larger benthic foraminifera bioclastic packstones with subsidiary grain- and floatstones.	Middle section: common corals, carbonate lithoclasts, molluscs and imperforate foraminifera. Coralline algae, echinoderm debris, larger benthic foraminifera and *Halimeda* also present and more common in lower section. Planktonic foraminifera locally present. Corals, carbonate lithoclasts and/or burrow infills and bryozoa all locally present in	Middle section: Micritisation, isopachous cements, dissolution, common blocky and neomorphic cements and compaction. Lower section: micritisation, syntaxial overgrowths compaction-related grain deformation, breakage and suturing common. Throughout: minor, localised

								lower section. Many components fragmented and abraded.	blocky to equant cements dolomite replacement of matrix or clear dolomite cements and late leaching.
Fine, medium-bedded limestone	Antelope-1: middle imaged section.	Generally has a smooth, but sometimes brecciated appearance and is resistive to slightly conductive.	Medium-Low	>98% limestone	Medium bedded	Low	Middle section: Mollusc and imperforate foraminifera bioclastic pack/ grainstones and wackestones. Lower section: Fine to medium grained echinoderm (and foraminifera) bioclastic packstones.	Molluscs and imperforate foraminifera common in middle section. Coralline algae, echinoderm debris larger benthic foraminifera and *Halimeda* also present and common in lower section. Planktonic foraminifera locally present. Many components fragmented and abraded.	Middle section: Micritisation, isopachous cements, dissolution, common blocky and neomorphic cements and compaction. Lower section: micritisation, syntaxial overgrowths compaction-related grain deformation, breakage and suturing common. Throughout: minor, localised blocky to equant cements dolomite replacement of matrix or clear dolomite cements and late leaching.

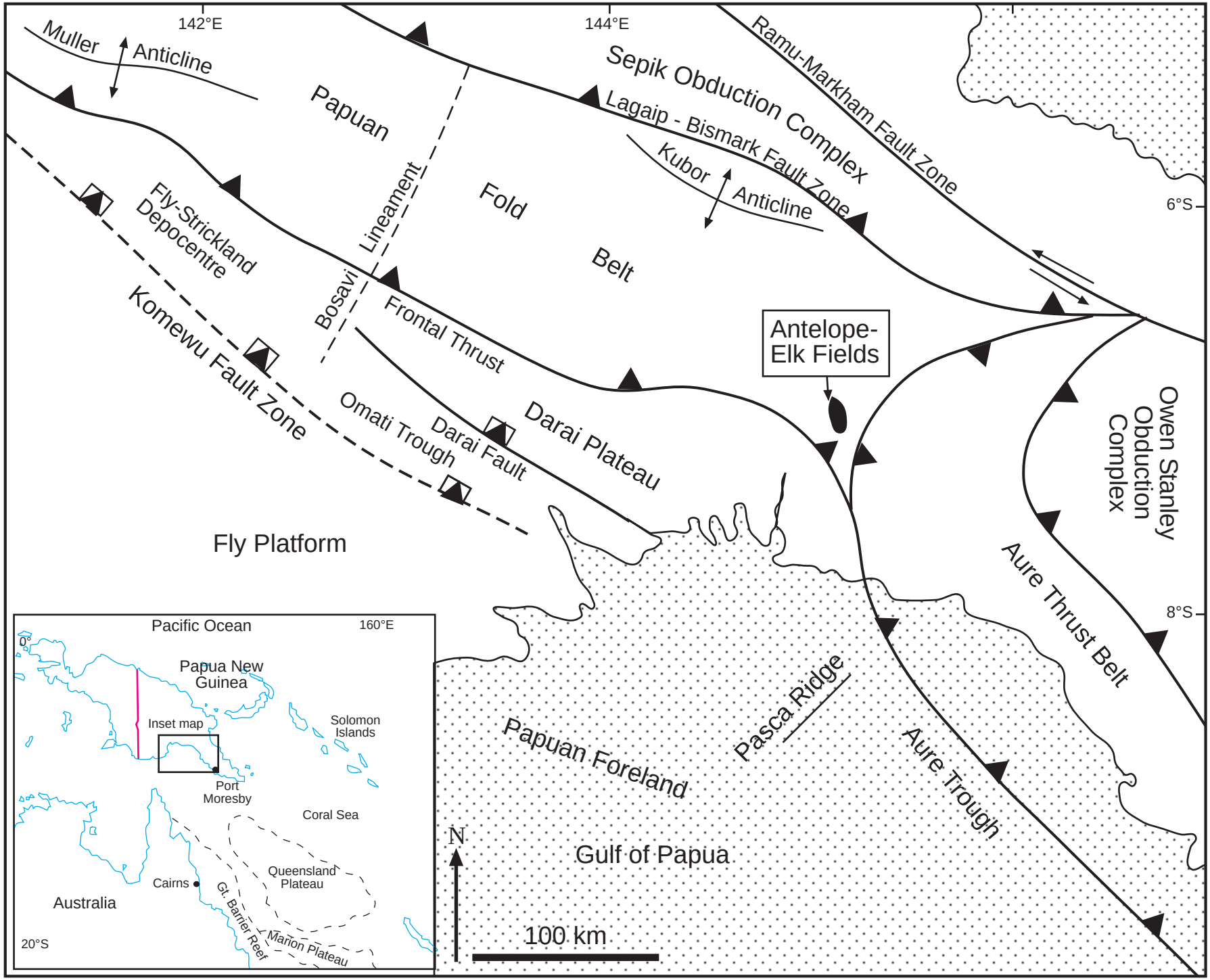
142°E
144°E
6°S
8°S
Muller Anticline
Papuan Fold Belt
Lineament
Sepik Obduction Complex
Lagaip - Bismark Fault Zone
Ramu-Markham Fault Zone
Kubor Anticline
Fly-Strickland Depocentre
Bosavi
Frontal Thrust
Komewu Fault Zone
Omati Trough
Darai Fault
Darai Plateau
Antelope-Elk Fields
Owen Stanley Obduction Complex
Aure Thrust Belt
Fly Platform
Pasca Ridge
Papuan Foreland
Aure Trough
Gulf of Papua
N
100 km
Pacific Ocean
160°E
0°
Papua New Guinea
Inset map
Solomon Islands
Port Moresby
Coral Sea
Queensland Plateau
Cairns
Gt. Barrier Reef
Marion Plateau
Australia
20°S

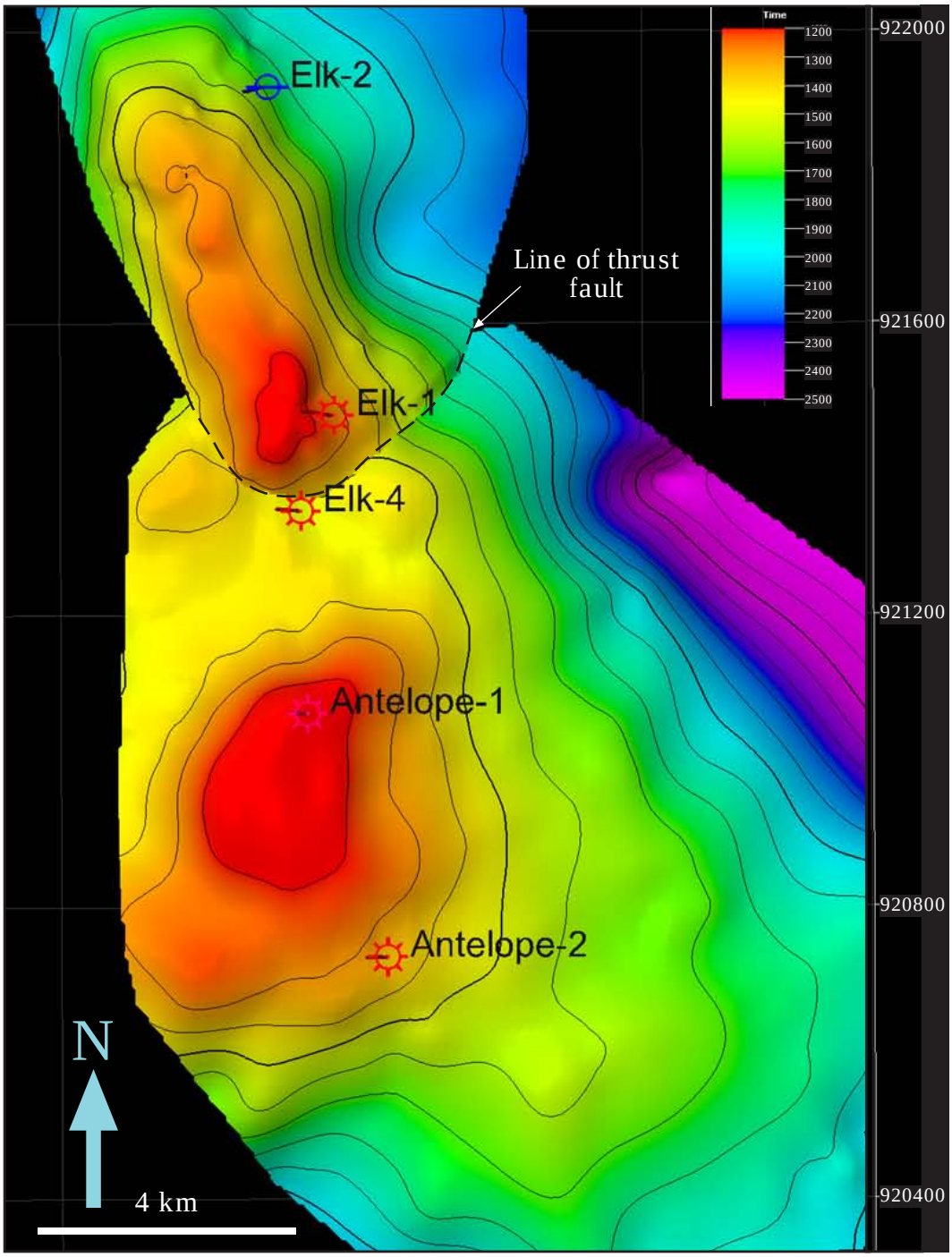
Time
1200
1300
1400
1500
1600
1700
1800
1900
2000
2100
2200
2300
2400
2500
922000
921600
921200
920800
920400
Elk-2
Line of thrust fault
Elk-1
Elk-4
Antelope-1
Antelope-2
N
4 km

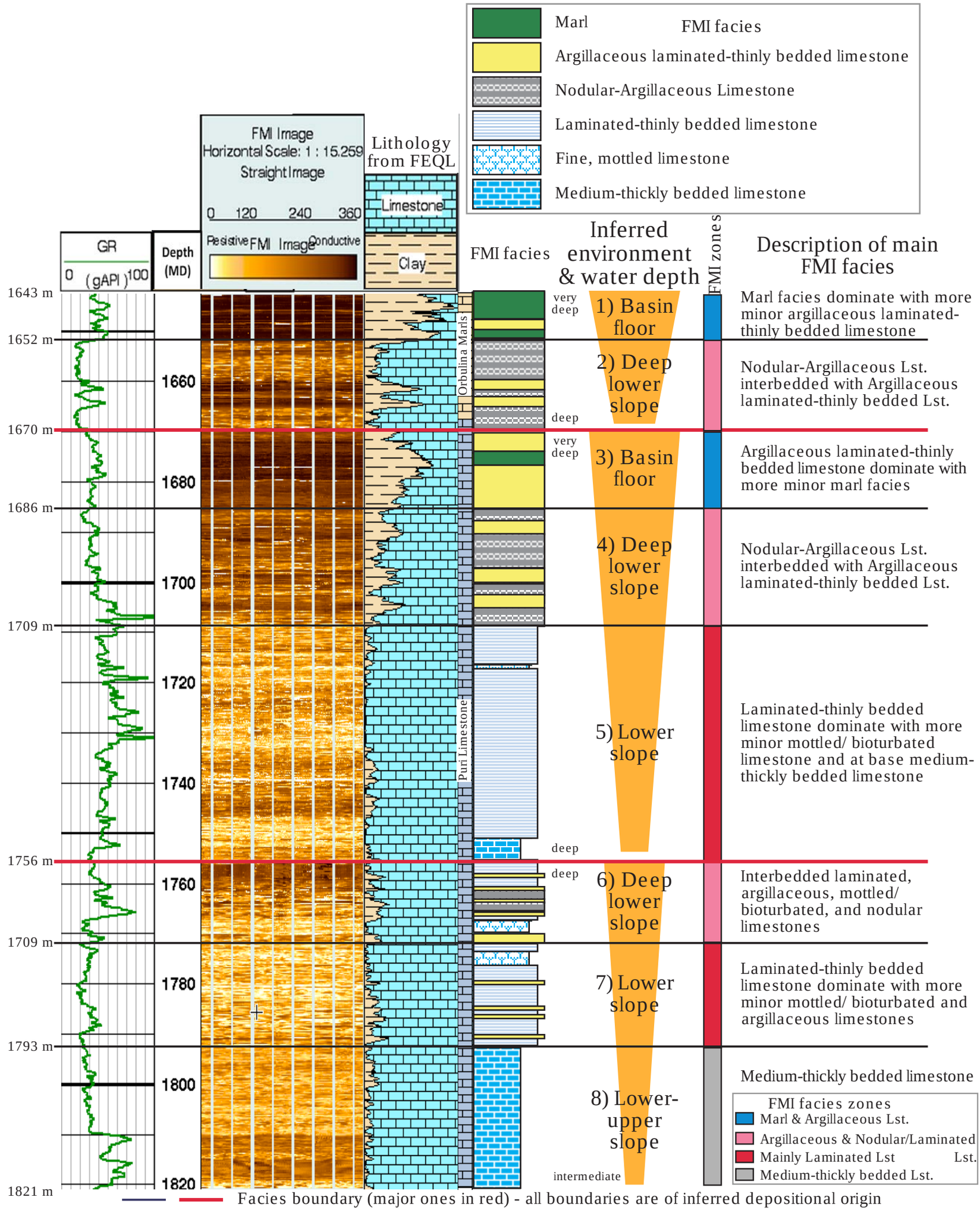
FMI facies
Marl
Argillaceous laminated-thinly bedded limestone
Nodular-Argillaceous Limestone
Laminated-thinly bedded limestone
Fine, mottled limestone
Medium-thickly bedded limestone
FMI Image
Horizontal Scale: 1 : 15.259
Straight Image
0 120 240 360
Resistive FMI Image Conductive
Lithology from FEQL
Limestone
Clay
GR
0 (gAPI) 100
Depth (MD)
FMI facies
Inferred environment & water depth
FMI zones
Description of main FMI facies
Orbulina Marls
Puri Limestone
1643 m
1652 m
1660
1670 m
1680
1686 m
1700
1709 m
1720
1740
1756 m
1760
1709 m
1780
1793 m
1800
1820
1821 m
very deep
deep
very deep
deep
deep
deep
intermediate
1) Basin floor
2) Deep lower slope
3) Basin floor
4) Deep lower slope
5) Lower slope
6) Deep lower slope
7) Lower slope
8) Lower-upper slope
Marl facies dominate with more minor argillaceous laminated-thinly bedded limestone
Nodular-Argillaceous Lst. interbedded with Argillaceous laminated-thinly bedded Lst.
Argillaceous laminated-thinly bedded limestone dominate with more minor marl facies
Nodular-Argillaceous Lst. interbedded with Argillaceous laminated-thinly bedded Lst.
Laminated-thinly bedded limestone dominate with more minor mottled/ bioturbated limestone and at base medium-thickly bedded limestone
Interbedded laminated, argillaceous, mottled/ bioturbated, and nodular limestones
Laminated-thinly bedded limestone dominate with more minor mottled/ bioturbated and argillaceous limestones
Medium-thickly bedded limestone
FMI facies zones
Marl & Argillaceous Lst.
Argillaceous & Nodular/Laminated
Mainly Laminated Lst
Lst.
Medium-thickly bedded Lst.
Facies boundary (major ones in red) - all boundaries are of inferred depositional origin

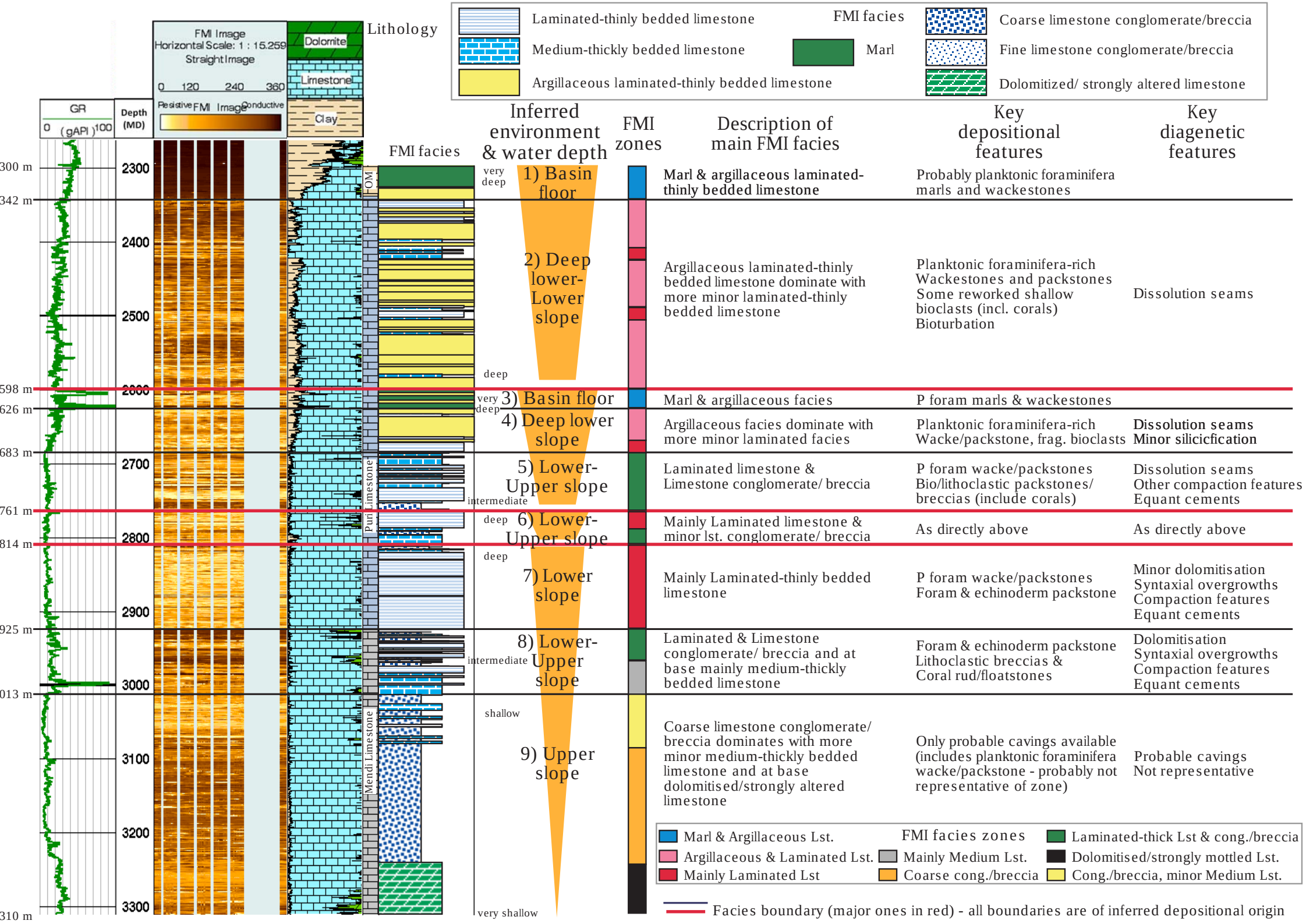
FMI Image
Horizontal Scale: 1 : 15.259
Straight Image
0 120 240 360
Resistive FMI Image Conductive
GR
0 (gAPI) 100
Depth (MD)
Lithology
Dolomite
Limestone
Clay
FMI facies
Laminated-thinly bedded limestone
Medium-thickly bedded limestone
Argillaceous laminated-thinly bedded limestone
Marl
Coarse limestone conglomerate/breccia
Fine limestone conglomerate/breccia
Dolomitized/ strongly altered limestone
Inferred environment & water depth
FMI zones
Description of main FMI facies
Key depositional features
Key diagenetic features
300 m
342 m
598 m
626 m
683 m
761 m
814 m
925 m
013 m
310 m
2300
2400
2500
2600
2700
2800
2900
3000
3100
3200
3300
OM
Puri Limestone
Mendi Limestone
very deep
deep
intermediate
shallow
very shallow
1) Basin floor
Marl & argillaceous laminated-thinly bedded limestone
Probably planktonic foraminifera marls and wackestones
2) Deep lower-Lower slope
Argillaceous laminated-thinly bedded limestone dominate with more minor laminated-thinly bedded limestone
Planktonic foraminifera-rich Wackestones and packstones
Some reworked shallow bioclasts (incl. corals)
Bioturbation
Dissolution seams
3) Basin floor
Marl & argillaceous facies
P foram marls & wackestones
4) Deep lower slope
Argillaceous facies dominate with more minor laminated facies
Planktonic foraminifera-rich Wacke/packstone, frag. bioclasts
Dissolution seams
Minor silicicfication
5) Lower-Upper slope
Laminated limestone & Limestone conglomerate/ breccia
P foram wacke/packstones
Bio/lithoclastic packstones/ breccias (include corals)
Dissolution seams
Other compaction features
Equant cements
6) Lower-Upper slope
Mainly Laminated limestone & minor lst. conglomerate/ breccia
As directly above
As directly above
7) Lower slope
Mainly Laminated-thinly bedded limestone
P foram wacke/packstones
Foram & echinoderm packstone
Minor dolomitisation
Syntaxial overgrowths
Compaction features
Equant cements
8) Lower-Upper slope
Laminated & Limestone conglomerate/ breccia and at base mainly medium-thickly bedded limestone
Foram & echinoderm packstone
Lithoclastic breccias &
Coral rud/floatstones
Dolomitisation
Syntaxial overgrowths
Compaction features
Equant cements
9) Upper slope
Coarse limestone conglomerate/ breccia dominates with more minor medium-thickly bedded limestone and at base dolomitised/strongly altered limestone
Only probable cavings available (includes planktonic foraminifera wacke/packstone - probably not representative of zone)
Probable cavings
Not representative
FMI facies zones
Marl & Argillaceous Lst.
Argillaceous & Laminated Lst.
Mainly Laminated Lst
Mainly Medium Lst.
Coarse cong./breccia
Laminated-thick Lst & cong./breccia
Dolomitised/strongly mottled Lst.
Cong./breccia, minor Medium Lst.
Facies boundary (major ones in red) - all boundaries are of inferred depositional origin

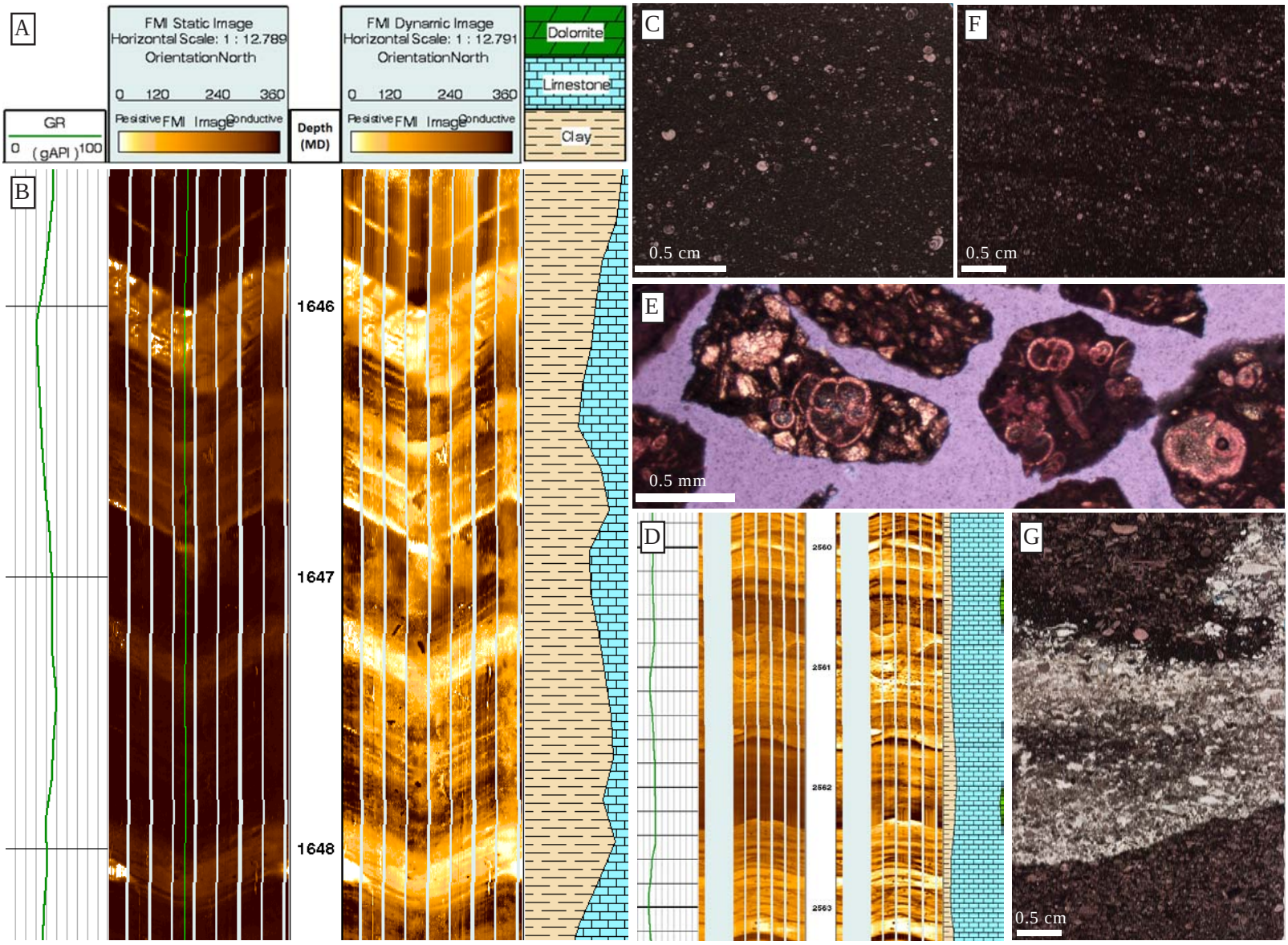
A
FMI Static Image
Horizontal Scale: 1 : 12.789
OrientationNorth
0 120 240 360
Resistive FMI Image Conductive
FMI Dynamic Image
Horizontal Scale: 1 : 12.791
OrientationNorth
0 120 240 360
Resistive FMI Image Conductive
GR
0 (gAPI) 100
Depth (MD)
Dolomite
Limestone
Clay
B
1646
1647
1648
C
0.5 cm
F
0.5 cm
E
0.5 mm
D
2560
2561
2562
2563
G
0.5 cm

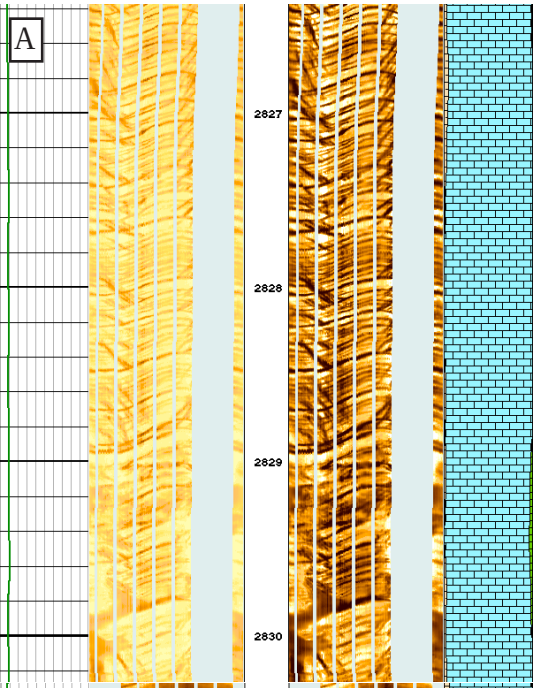
A
2827
2828
2829
2830

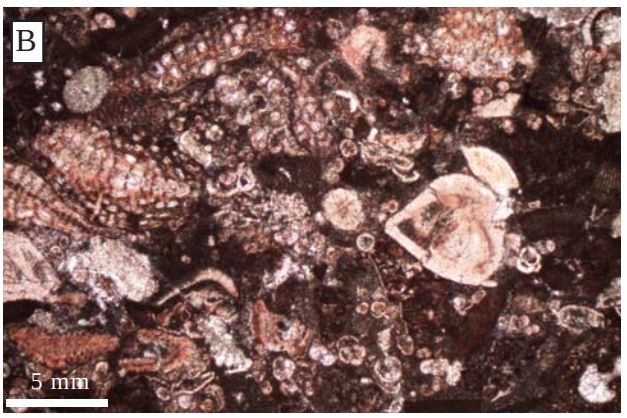
B
5 mm

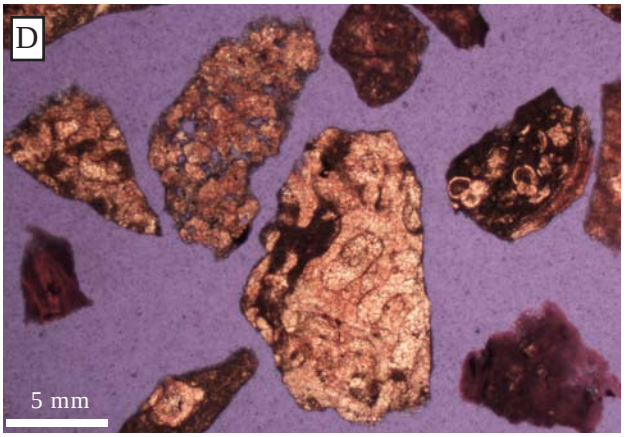
D
5 mm

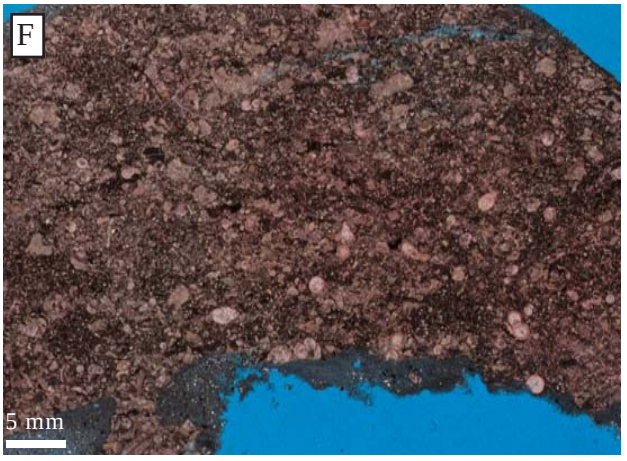
F
5 mm

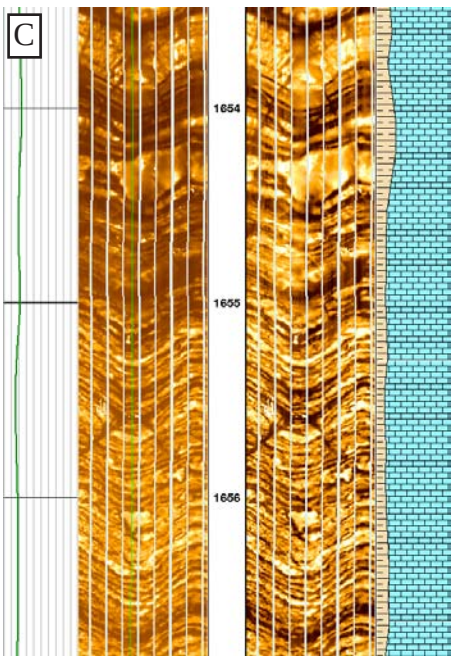
C
1654
1655
1656

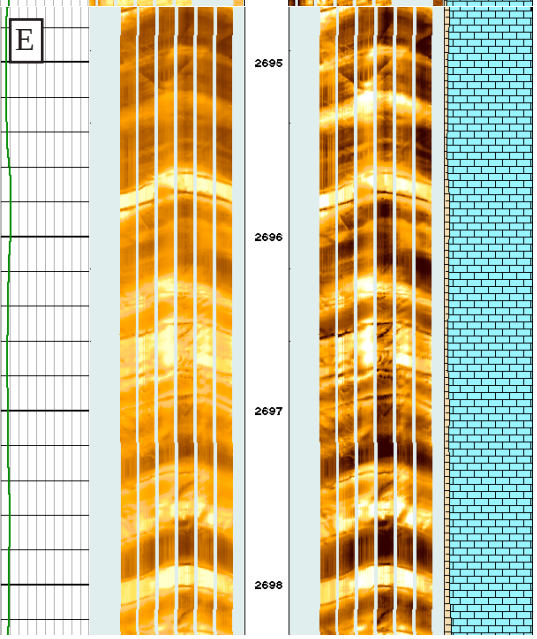
E
2695
2696
2697
2698

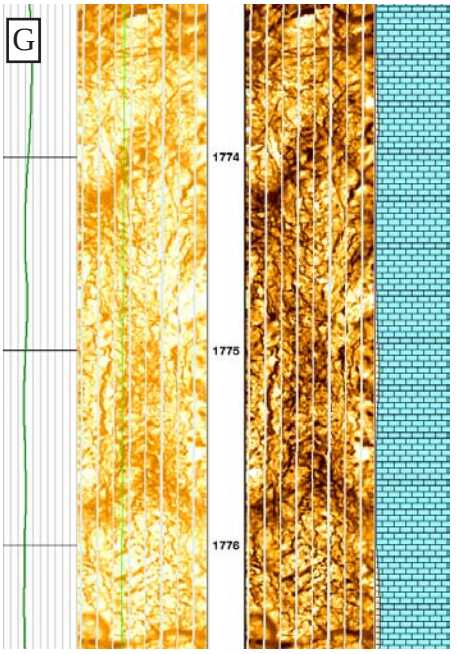
G
1774
1775
1776

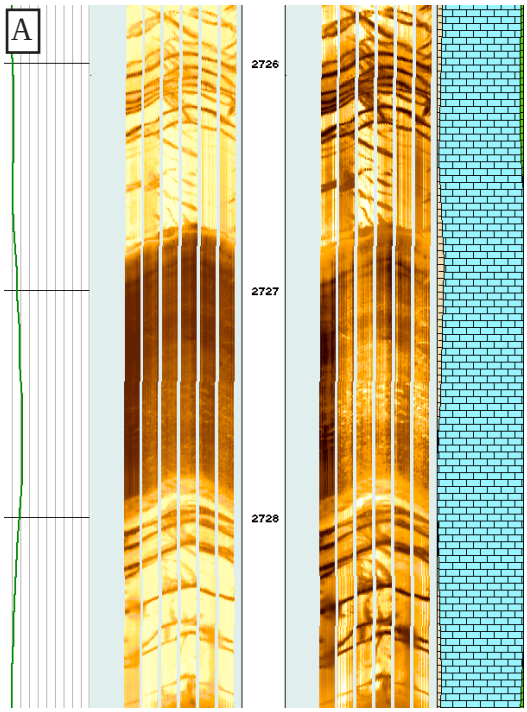
A
2726
2727
2728

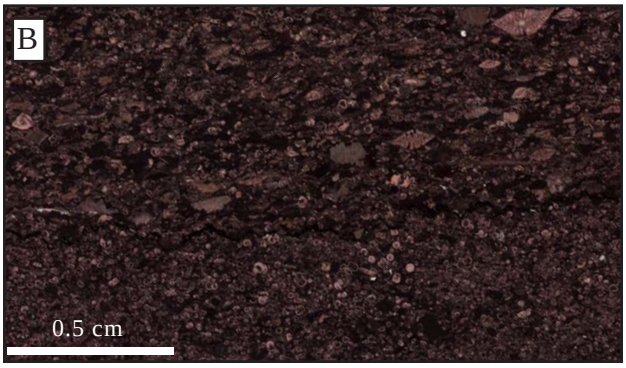
B
0.5 cm

C

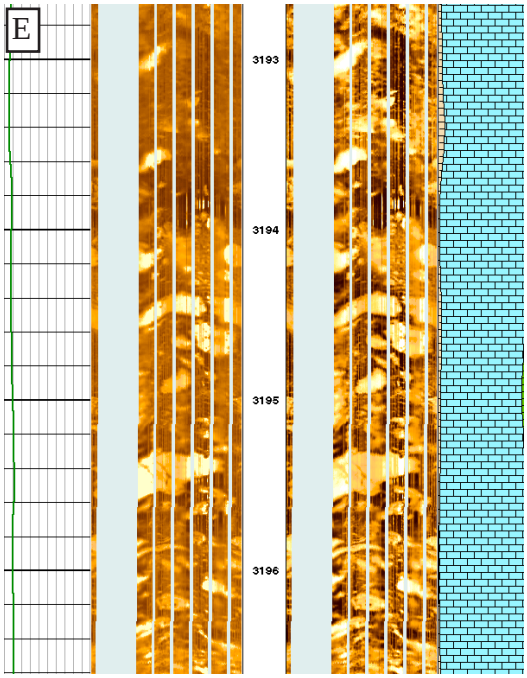
E
3193
3194
3195
3196

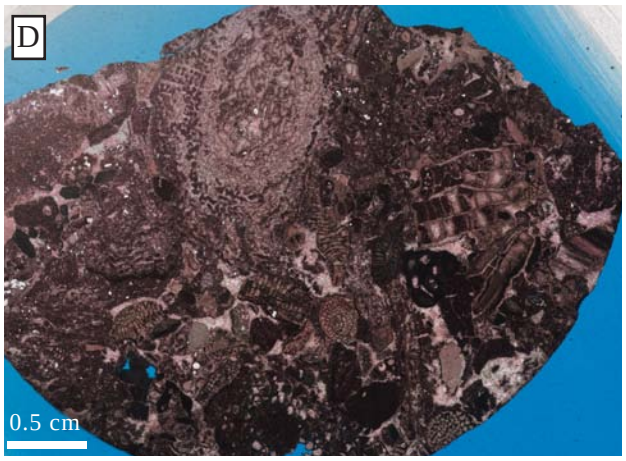
D
0.5 cm

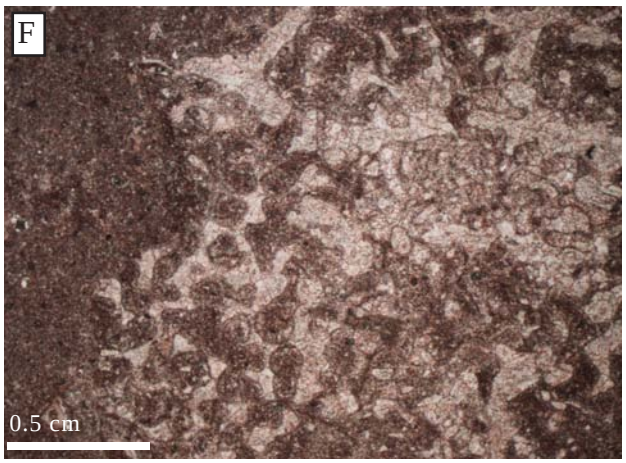
F
0.5 cm

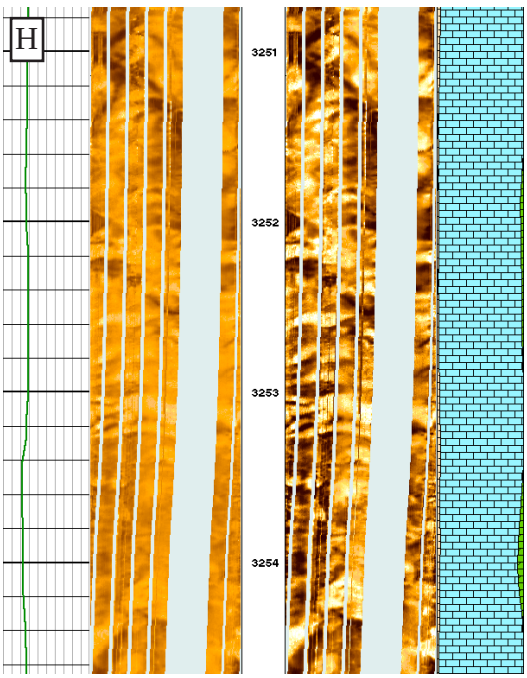
H
3251
3252
3253
3254

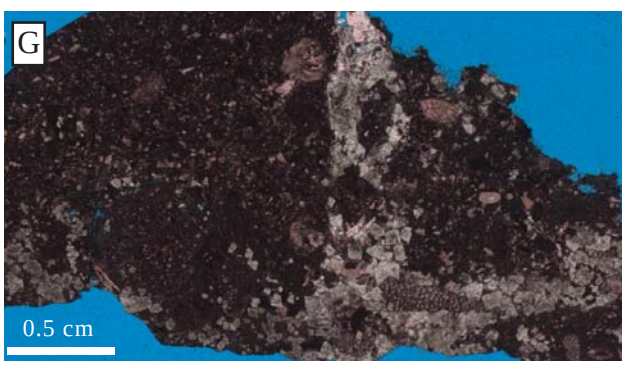
G
0.5 cm

Combined petrology-FMI facies or 'sequence' boundary depths

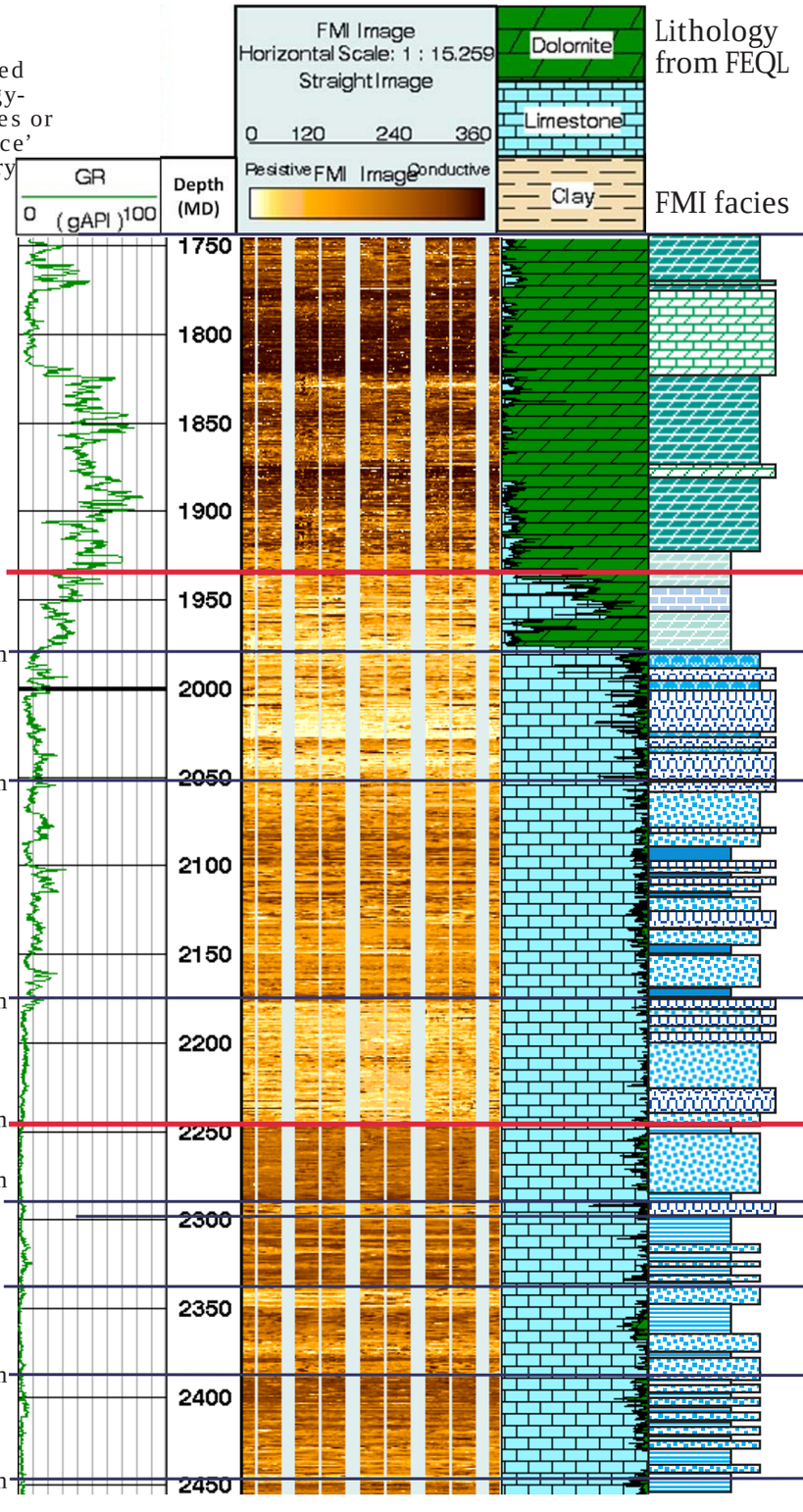

Lithology from FEQL

FMI facies

Probable environment

1) Completely dolomitised reef, possibly reef flat

2) Partially dolomitised reef flat (Di)

3) Cemented reef flat (D/D)

4) Reef flat cycles (D/D)

5) Reef crest to poss. margin/flat (D/D)

6) Deep to moderate photic platform (D/D)

7) Breccia/Conglomerate (De)

8) Deep to moderate photic platform (D/D)

9) Shallow to deep photic platform (D/D)

10) Deep to moderate photic platform (D/D)

Description of main FMI facies	Key depositional features	Key diagenetic features		Thin section photomicrograph
			1740 m	
Predominantly high- and moderate-, with minor low conductivity vuggy dolomite conglomerate/boundstone	Corals Boundstone Float/rudstone	Complete dolomitisation Leaching Partial infill pores by dolomite cement	1772 m	
			1935 m (Di)	
Predominantly low conductivity vuggy dolomite conglomerate/boundstone and vuggy limestone conglomerate/boundstone	Corals Imperforate forams Pack/grainstone Float/rudstone Breccias	Karstification Complex diagenesis Varied cements Partial dolomitisation Brecciation, leaching	1938.8 m	
			1976.2 m (Di)	
Limestone conglomerate/ boundstone grading upwards into fine, mottled limestone	Corals, Molluscs Imperforate forams Pack/grainstone Float/rudstone Breccias	Karstification Complex diagenesis Varied cements Brecciation, leaching Minor dolomitisation	1983 m	
			2055.1 m (De)	
5 cycles of fine, medium bedded lst, passing up into massive-medium bedded clastic limestone, then limestone conglomerate/boundstone	Corals, Molluscs Imperforate forams Pack/grainstone Float/rudstone 'Cyclic' deposits	Karstification Subaerial exposure Blocky & neomorphic cements Minor dolomitisation	2164 m	
			2177.8 m (De)	
1 cycle of fine, medium bedded lst, passing up into massive-medium bedded clastic limestone, then dominated by limestone conglomerate/boundstone	Corals, Algae Robust larger forams Pack/grainstone Float/rudstone More massive, breccias	Breccias, fracturing Isopachous & blocky cements Subaerial exposure Minor dolomitisation	2228 m	
			2246.6 m (De)	
Predominantly medium, thickly bedded clastic limestone	Larger forams, *Halimeda*, Echinoderm, Minor corals Wacke/packstones Planktonic forams	Compaction Syntaxial overgrowths Neomorphic/equant cement Dissolution seams	2275 m	
			2290.5 m (De)	
Limestone conglomerate/boundstone	Breccia, Range of carbonate clasts Corals, ??possible boundstone	Sedimentary breccia Varied clast history Fracturing Isopachous & blocky cements	2290.5 m	
			2300 m (De)	
Medium, thickly bedded clastic limestone and fine, thinly bedded limestone	Larger forams, Algae Echinoderm, Minor corals Reworked bioclasts Wacke/pack/grainstones Planktonic forams	Compaction Syntaxial overgrowths Neomorphic/equant cement Dissolution seams	2323.8 m	
			2340 m (De)	
Near equal medium, thickly bedded clastic limestone and fine, thinly bedded limestone	Larger forams, Corals Grain/rudstones Minor wacke/packstone Significant reworking of shallow bioclasts	Minor isopachous cements Neomorphic/blocky cement Compaction	2353 m	
			2389.5 m (De)	
Fine, thinly bedded limestone dominates with minor medium, thickly bedded clastic limestone.	Larger forams, Algae Echinoderm, Minor corals Reworked clasts Wacke/pack/floatstones Planktonic forams	Compaction Syntaxial overgrowths Equant cement Dissolution seams	2445 m	
			2449.5 m (De)	

Facies boundary (major ones in red) Nature of facies and facies boundaries: De - Depositional, D/D - Depositional/Diagenetic, Di Diagenetic

FMI facies

- High conductivity vuggy dolomite conglomerate / boundstone
- Moderate conductivity vuggy dolomite conglomerate / boundstone
- Low conductivity vuggy dolomite conglomerate / boundstone
- Vuggy limestone conglomerate / boundstone
- Fine, mottled limestone
- Limestone conglomerate / boundstone
- Medium / thickly bedded clastic limestone
- Fine, medium bedded limestone
- Fine, thinly bedded limestone

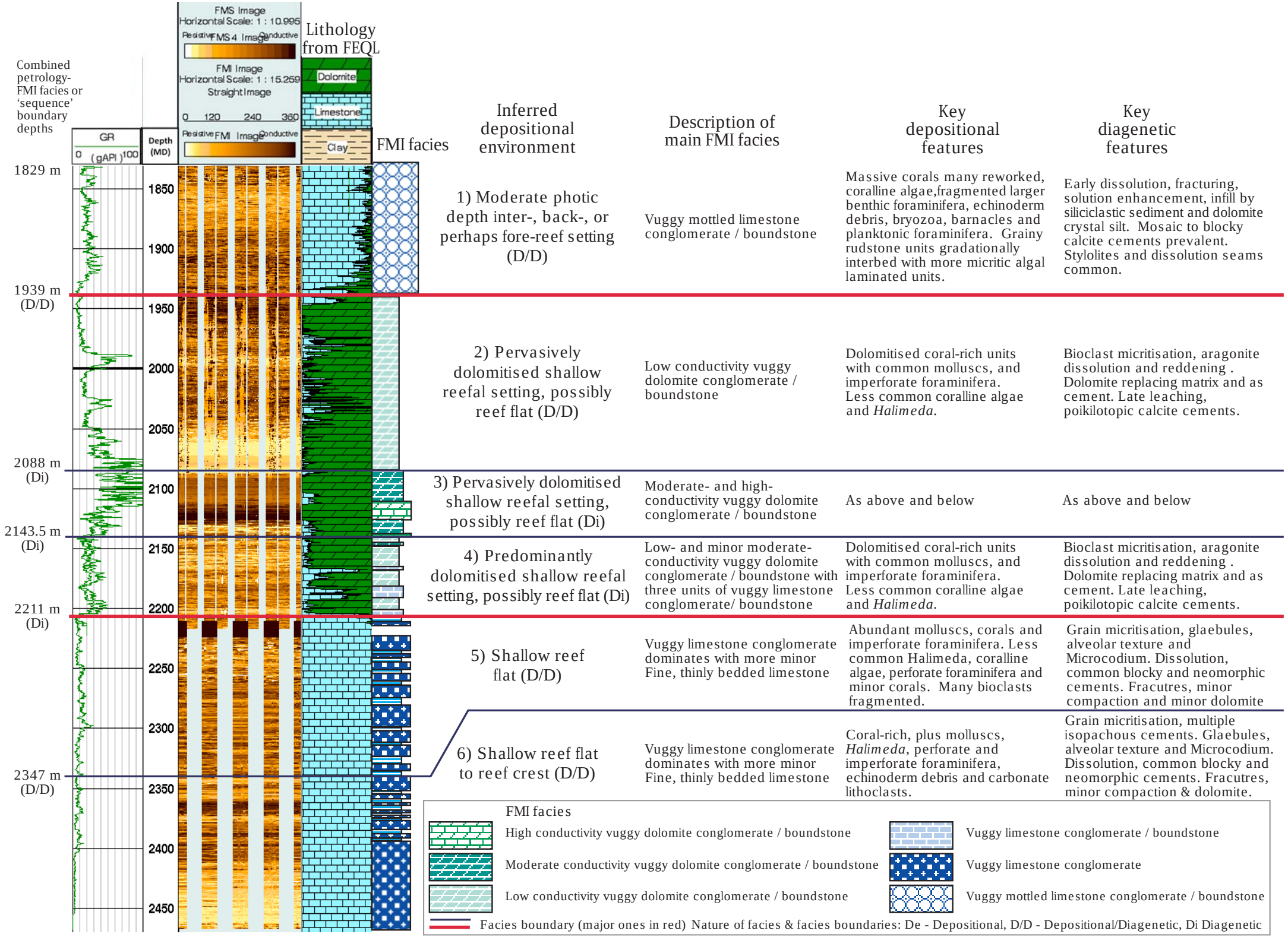
Combined petrology-FMI facies or 'sequence' boundary depths
FMS Image
Horizontal Scale: 1 : 10.995
Resistive FMS 4 Image Conductive
FMI Image
Horizontal Scale: 1 : 15.259
Straight Image
0 120 240 360
Resistive FMI Image Conductive
Lithology from FEQL
Dolomite
Limestone
Clay
GR
0 (gAPI) 100
Depth (MD)
1829 m
1850
1900
1939 m (D/D)
1950
2000
2050
2088 m (Di)
2100
2143.5 m (Di)
2150
2200
2211 m (Di)
2250
2300
2347 m (D/D)
2350
2400
2450
FMI facies
Inferred depositional environment
Description of main FMI facies
Key depositional features
Key diagenetic features
1) Moderate photic depth inter-, back-, or perhaps fore-reef setting (D/D)
Vuggy mottled limestone conglomerate / boundstone
Massive corals many reworked, coralline algae,fragmented larger benthic foraminifera, echinoderm debris, bryozoa, barnacles and planktonic foraminifera. Grainy rudstone units gradationally interbed with more micritic algal laminated units.
Early dissolution, fracturing, solution enhancement, infill by siliciclastic sediment and dolomite crystal silt. Mosaic to blocky calcite cements prevalent. Stylolites and dissolution seams common.
2) Pervasively dolomitised shallow reefal setting, possibly reef flat (D/D)
Low conductivity vuggy dolomite conglomerate / boundstone
Dolomitised coral-rich units with common molluscs, and imperforate foraminifera. Less common coralline algae and Halimeda.
Bioclast micritisation, aragonite dissolution and reddening . Dolomite replacing matrix and as cement. Late leaching, poikilotopic calcite cements.
3) Pervasively dolomitised shallow reefal setting, possibly reef flat (Di)
Moderate- and high-conductivity vuggy dolomite conglomerate / boundstone
As above and below
As above and below
4) Predominantly dolomitised shallow reefal setting, possibly reef flat (Di)
Low- and minor moderate-conductivity vuggy dolomite conglomerate / boundstone with three units of vuggy limestone conglomerate/ boundstone
Dolomitised coral-rich units with common molluscs, and imperforate foraminifera. Less common coralline algae and Halimeda.
Bioclast micritisation, aragonite dissolution and reddening . Dolomite replacing matrix and as cement. Late leaching, poikilotopic calcite cements.
5) Shallow reef flat (D/D)
Vuggy limestone conglomerate dominates with more minor Fine, thinly bedded limestone
Abundant molluscs, corals and imperforate foraminifera. Less common Halimeda, coralline algae, perforate foraminifera and minor corals. Many bioclasts fragmented.
Grain micritisation, glaebules, alveolar texture and Microcodium. Dissolution, common blocky and neomorphic cements. Fracutres, minor compaction and minor dolomite
6) Shallow reef flat to reef crest (D/D)
Vuggy limestone conglomerate dominates with more minor Fine, thinly bedded limestone
Coral-rich, plus molluscs, Halimeda, perforate and imperforate foraminifera, echinoderm debris and carbonate lithoclasts.
Grain micritisation, multiple isopachous cements. Glaebules, alveolar texture and Microcodium. Dissolution, common blocky and neomorphic cements. Fracutres, minor compaction & dolomite.
FMI facies
High conductivity vuggy dolomite conglomerate / boundstone
Moderate conductivity vuggy dolomite conglomerate / boundstone
Low conductivity vuggy dolomite conglomerate / boundstone
Vuggy limestone conglomerate / boundstone
Vuggy limestone conglomerate
Vuggy mottled limestone conglomerate / boundstone
Facies boundary (major ones in red) Nature of facies & facies boundaries: De - Depositional, D/D - Depositional/Diagenetic, Di Diagenetic

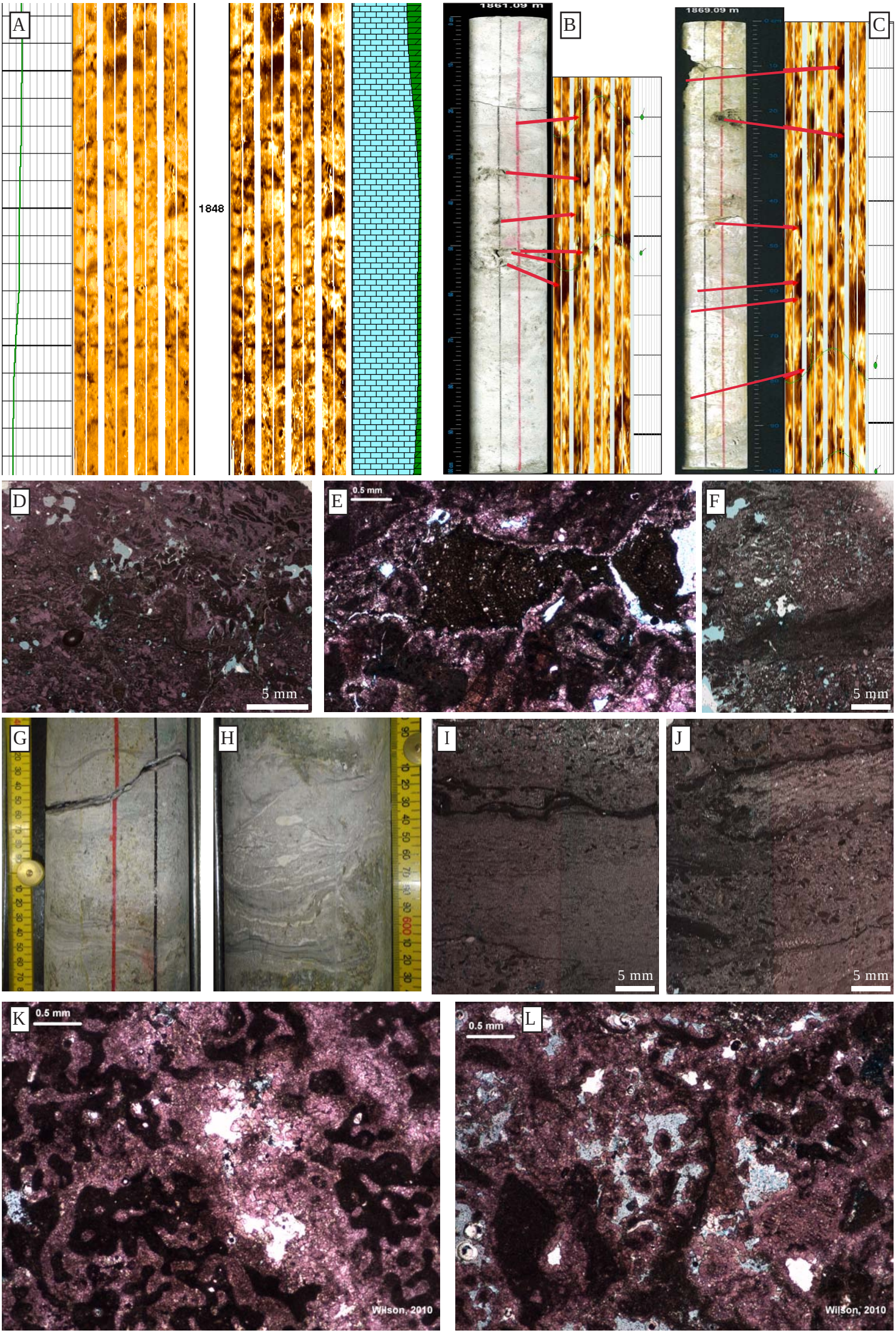
A
1848
B
1861.09 m
C
1869.09 m
D
5 mm
E
0.5 mm
F
5 mm
G
H
I
5 mm
J
5 mm
K
0.5 mm
Wilson, 2010
L
0.5 mm
Wilson, 2010

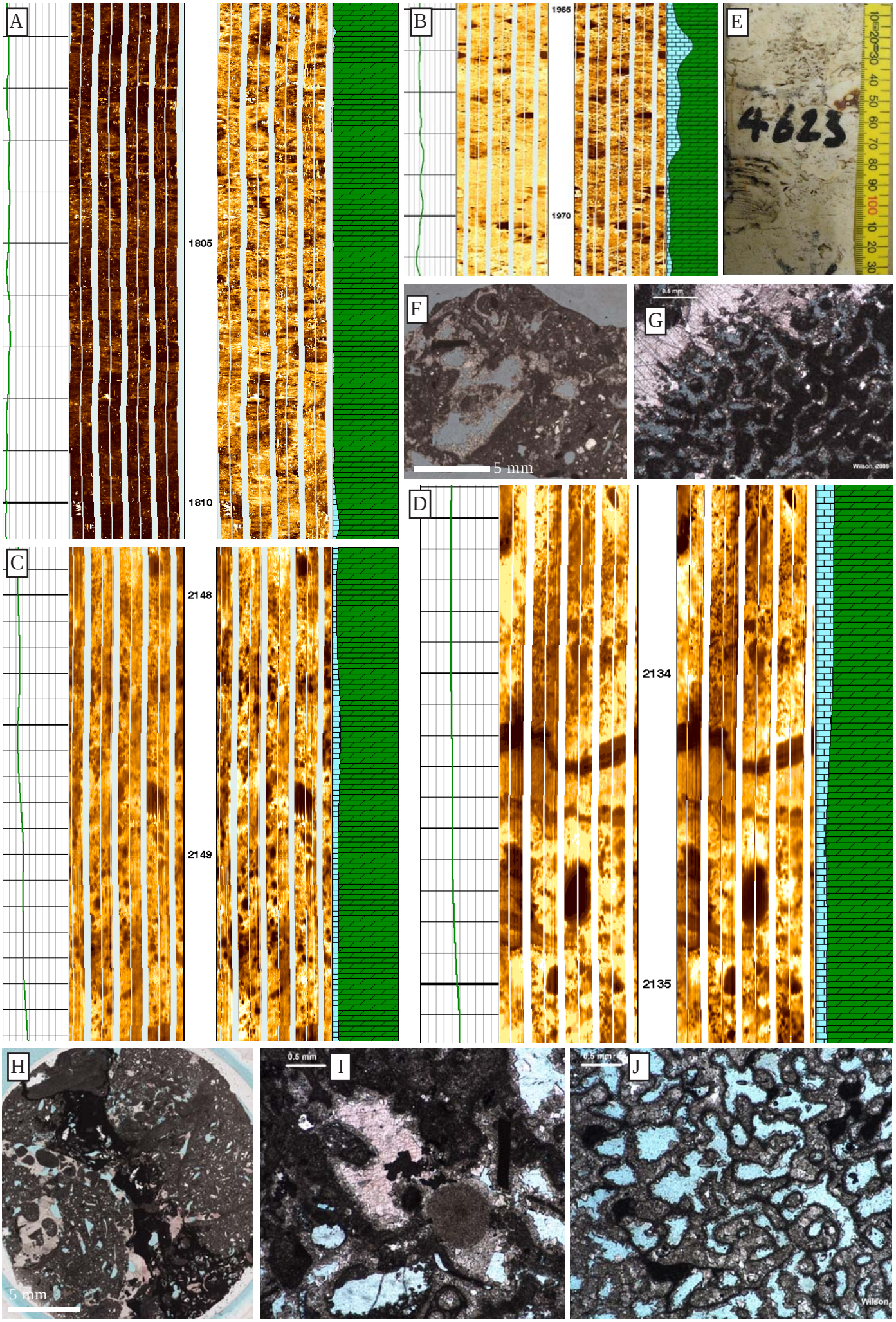
A
1805
1810
B
1965
1970
E
4623
F
5 mm
G
0.5 mm
Wilson, 2009
C
2148
2149
D
2134
2135
H
5 mm
I
0.5 mm
J
0.5 mm
Wilson

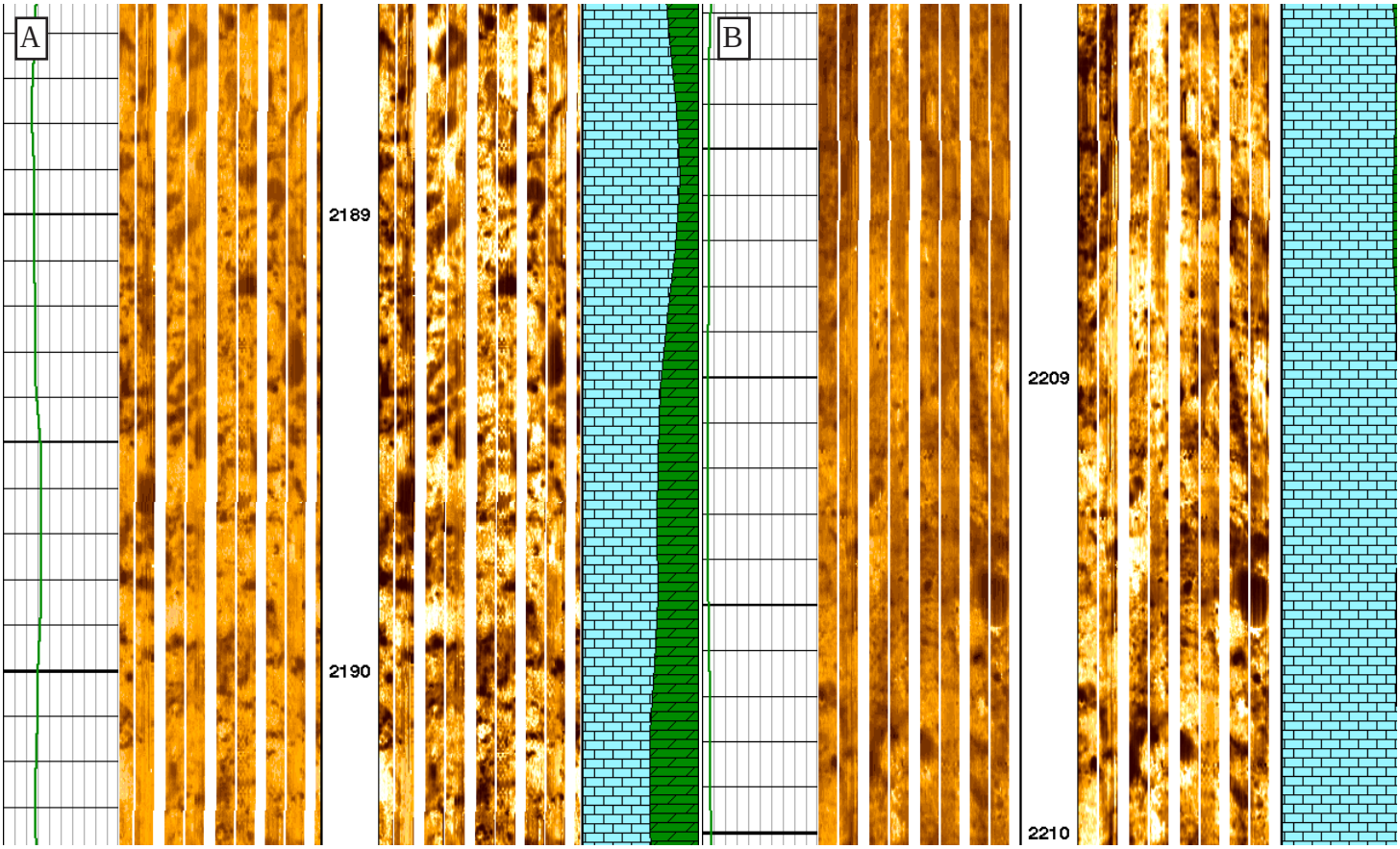
A
2189
2190
B
2209
2210

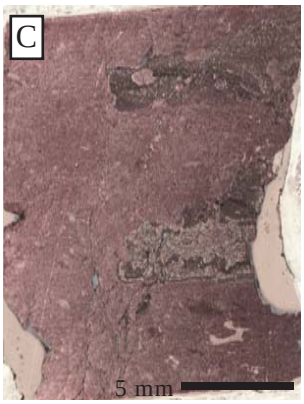
C
5 mm

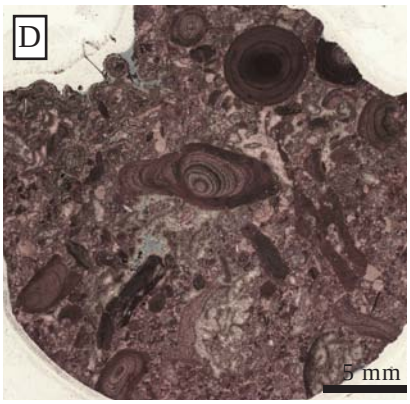
D
5 mm

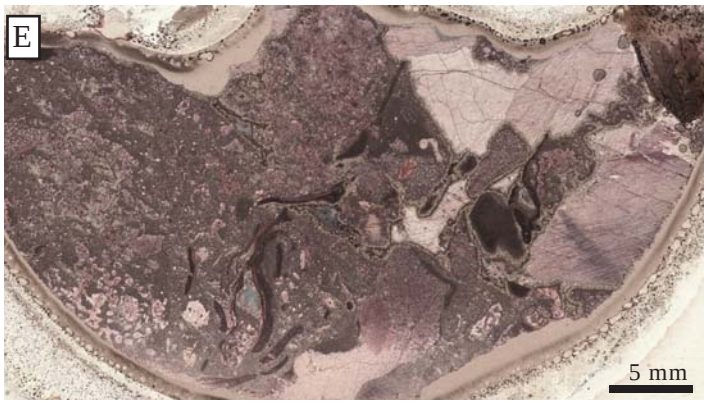
E
5 mm

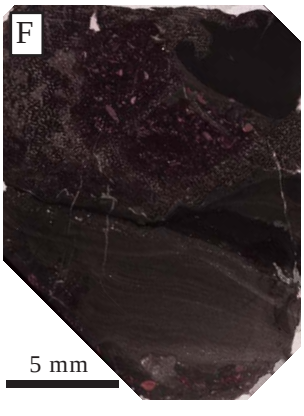
F
5 mm

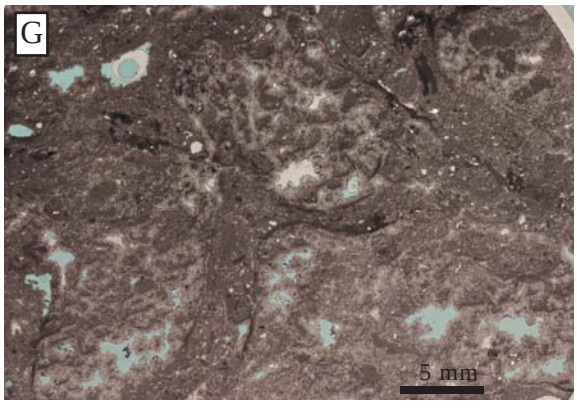
G
5 mm

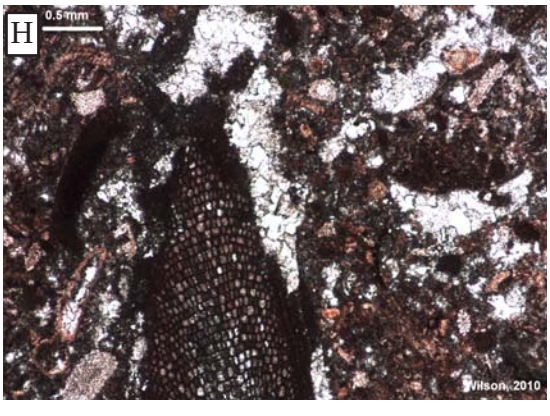
H
0.5 mm
Wilson, 2010

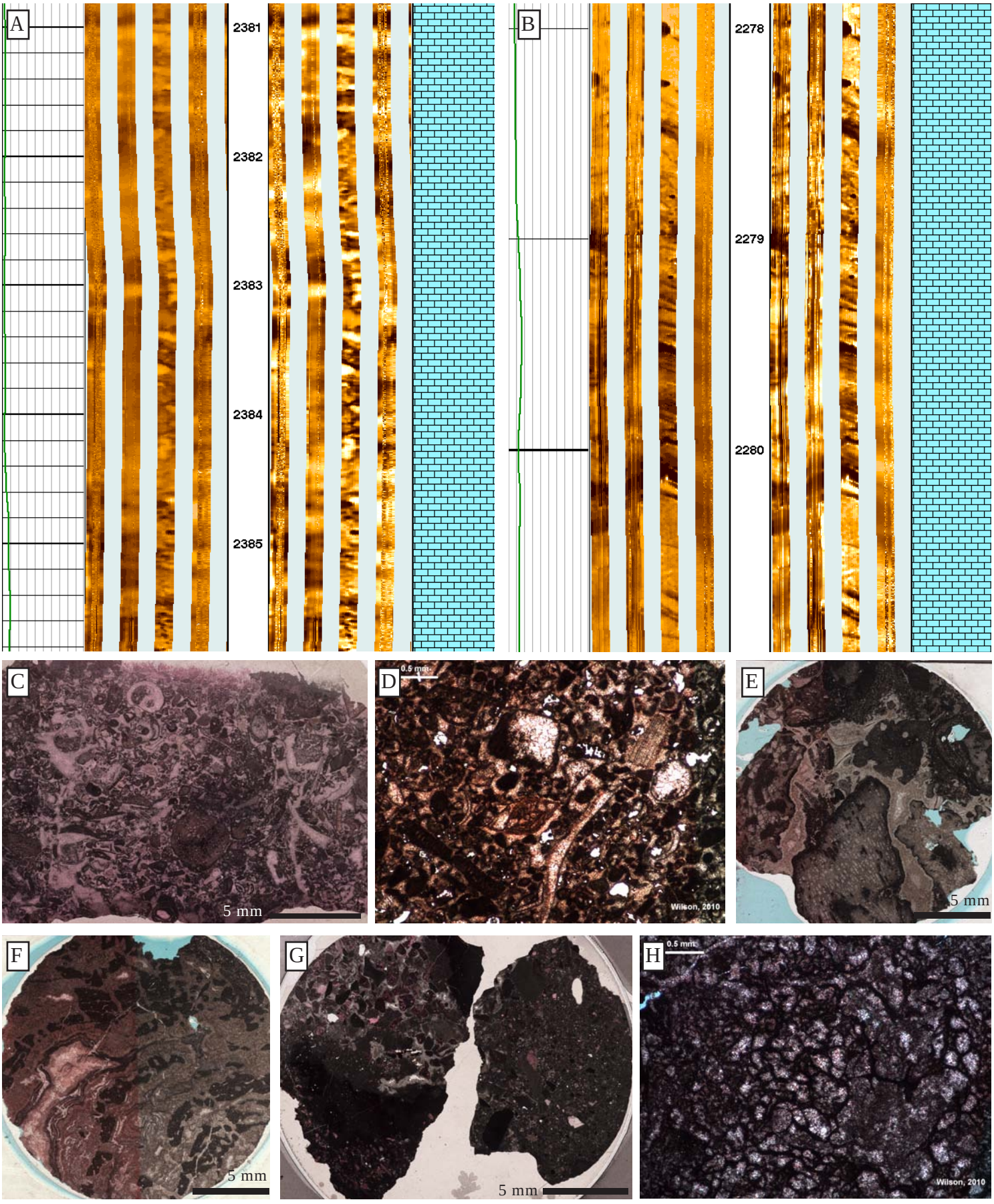
A
2381
2382
2383
2384
2385
B
2278
2279
2280
C
5 mm
D
0.5 mm
Wilson, 2010
E
5 mm
F
5 mm
G
5 mm
H
0.5 mm
Wilson, 2010

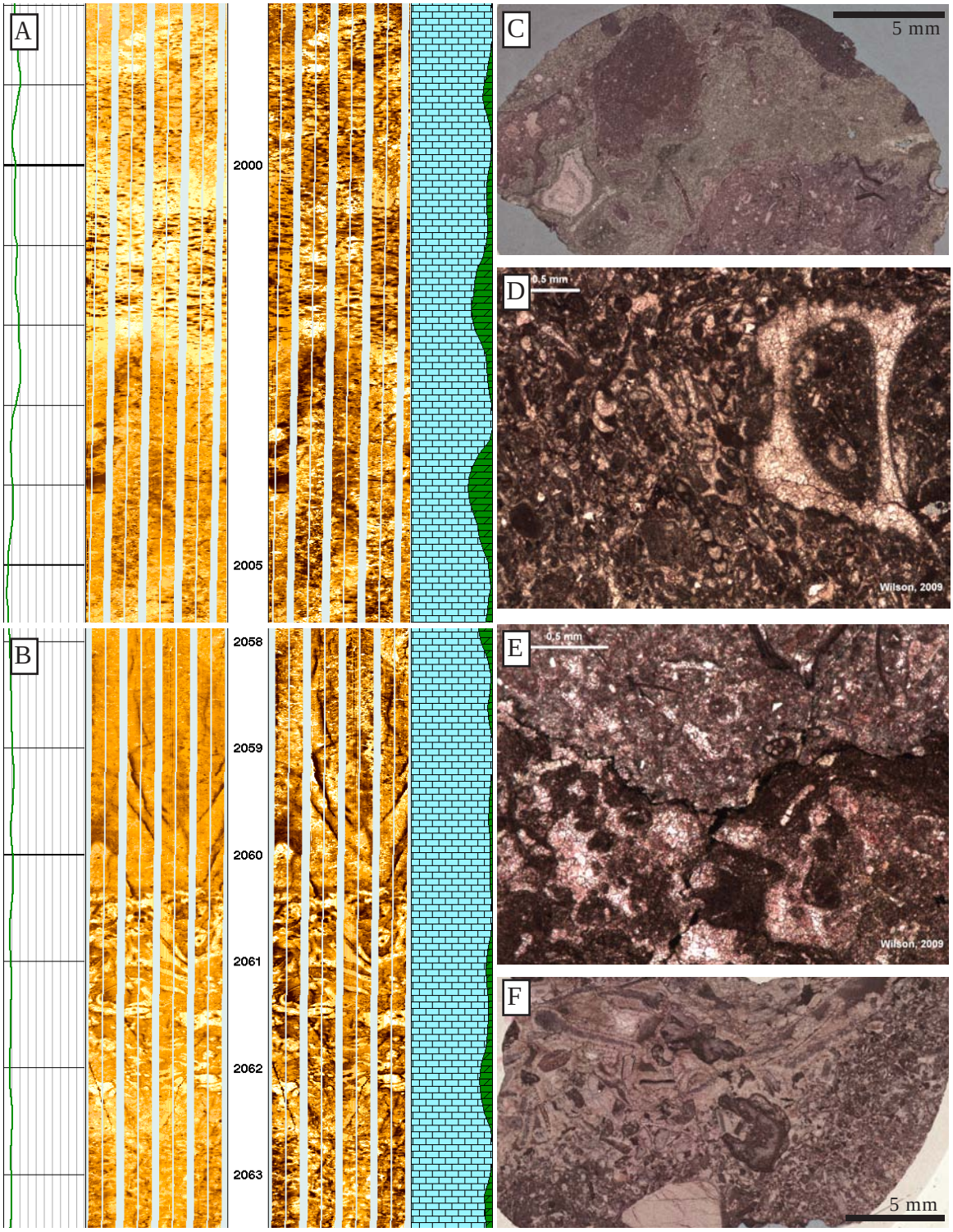
A
2000
2005
B
2058
2059
2060
2061
2062
2063
C
5 mm
D
0.5 mm
Wilson, 2009
E
0,5 mm
Wilson, 2009
F
5 mm

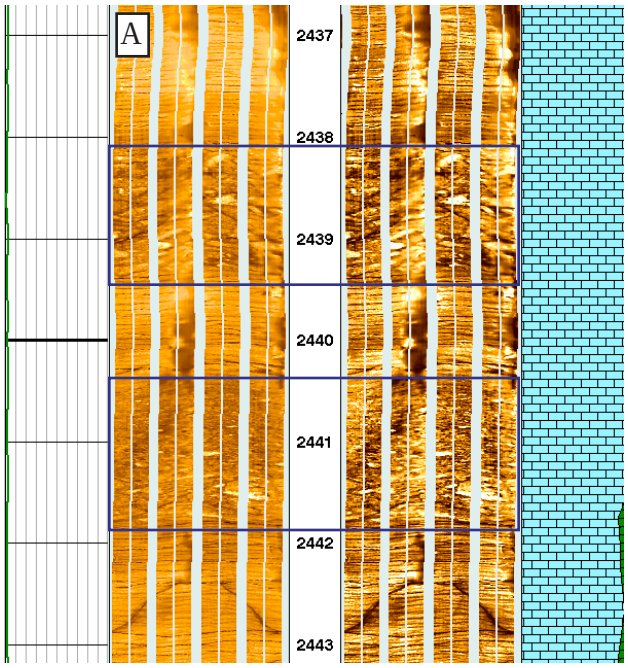
A
2437
2438
2439
2440
2441
2442
2443

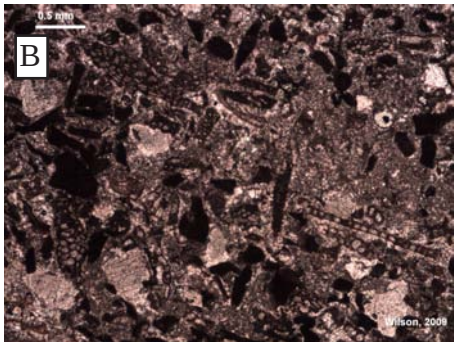
B
0.5 mm
Wilson, 2008

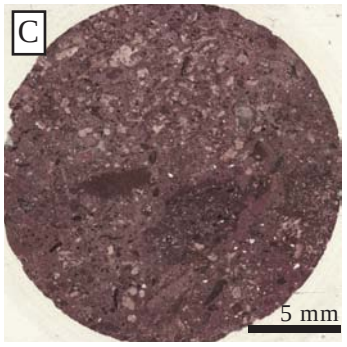
C
5 mm

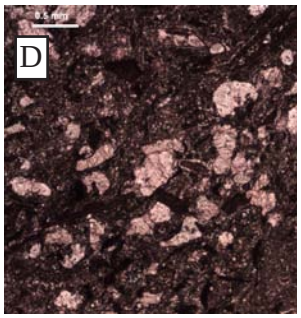
D

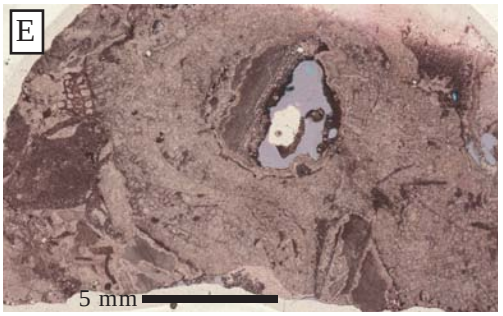
E
5 mm

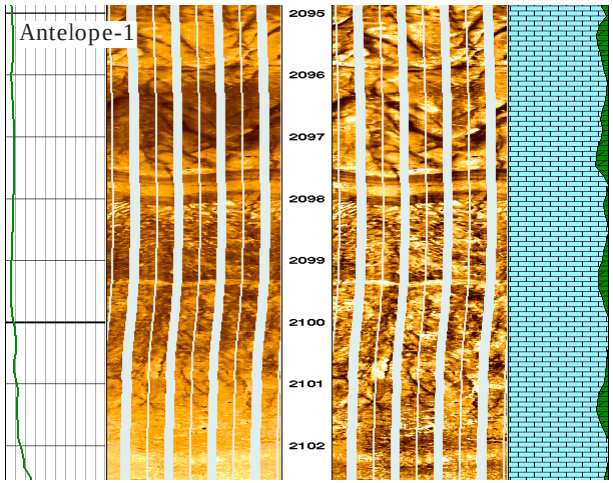

Centimetre- to sequence-scale variations

Image analysis (FMI)

Petrology

Iterative comparison to better evaluate & understand:

1) Mineralogical, depositional diagenetic & pore system controls on electrical image (FMI) features and textures.
2) Relationship between microfacies and FMI facies. Some FMI facies may have non-unique origins, but sample data may 'help train' FMI characterisation & interpretation.
3) Readjustment of sequence boundaries, understanding their nature and better evaluating and interpreting sequence trends.
4) Fill knowledge gaps when one type of data is unavailable, or of poor quality, e.g. when downhole conditions such as borehole rugosity or gas result in reduced quality electrical images, in areas of tool malfunction, or in regions of poor sidewall core recovery (perhaps porosity related).

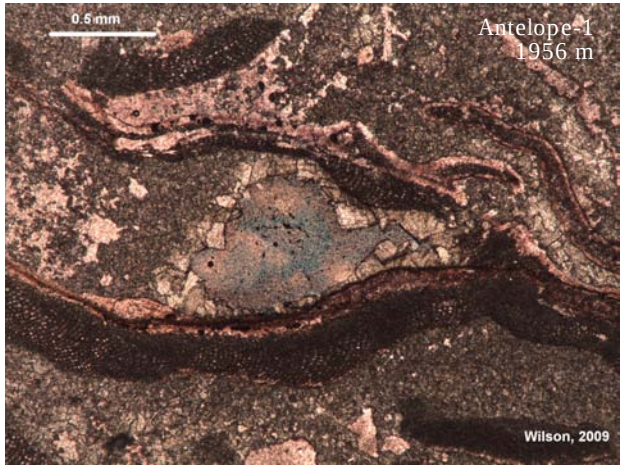

Micro- to centimetre-scale variations

Observations

1) Electrical conductivity versus resistivity response (indirectly reflecting mineralogical, pore systems and fluid variations)
2) 'Coarse' textures and fabrics (reflecting combined depositional and diagenetic fabrics)
3) 'Clast' & Vug characterisation, shape, size & distribution
4) Structures & their orientations (sedimentary and or others, e.g. fractures)
5) Boundary (bed and/or sequence) location and nature Sequence trends (individual stratal units/beds & large-scale sequences)

Inferences

1) Mineralogy (particularly when in combination with other techniques, e.g. FEQL)
2) Depositional environments, processes and sequence trends (for environments & processes inferences may be similar to those possible from petrology, but less certainty due to potential diagenetic overprints affecting FMI textures).
3) Diagenesis and post-depositional alteration, e.g. commonly used for fracture characterisation/interpretation, but diagenetic features, environments and processes (unless related to very specific fabrics) may prove difficult to recognise and interpret.

Inferences

1) Depositional environments & processes:
   marine versus non-normal marine, energies, water depths, local environments, proximity to potential reefs or platform margins
2) Diagenesis:
   Diagenetic environments & processes, relative timing of events, impacts on depositional textures, controls on diagenesis (particularly when integrated with other petrography & geochemistry results)

Observations

1) Components and their grain sizes
2) Bioclast morphologies, fragmentation & abrasion
3) Primary depositional textures
4) Diagenetic features and their relative timing
5) Mineralogies
6) Pore system types, sizes, morphologies, abundances, distribution & potential connectivity

Characterisation & Classification of FMI facies

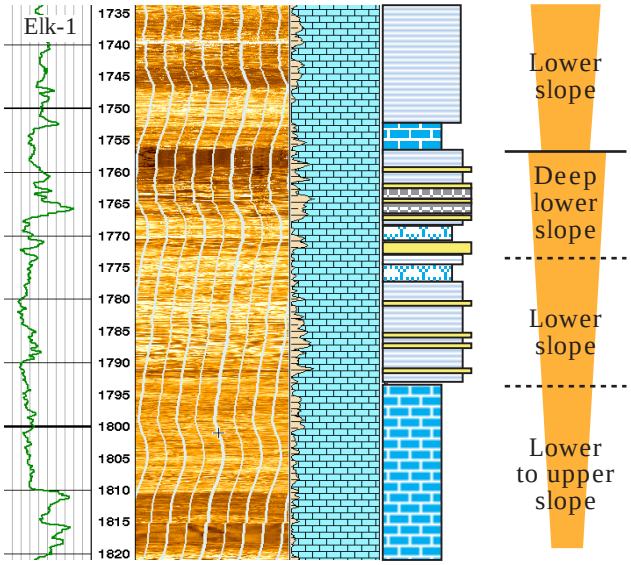

Characterisation & Classification of microfacies

Reservoir quality observations:

1) Pore sizes, morphologies, distribution and abundances.
2) Downhole trends in porosity
3) Potential pore connectivity.

Characterisation & Classification of Pore systems and in combination with other dataset (e.g. Core Plug Permeametry) Reservoir Rock Types (RRTs)

Reservoir quality inferences and predictions:
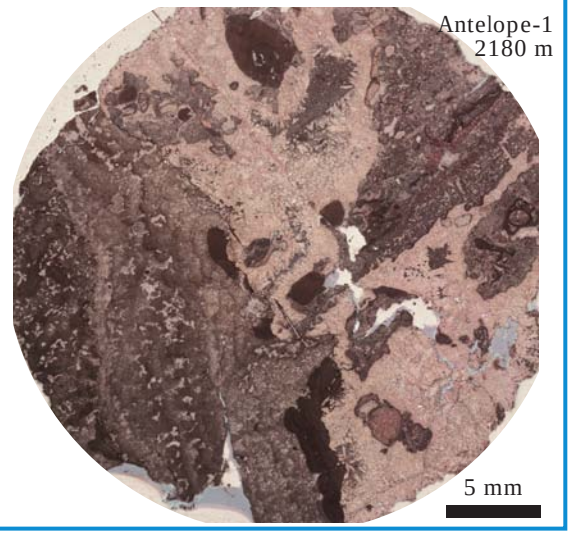
1) Pore systems development and downhole distribution controls.
2) Combined depositional & diagenetic impact on reservoir quality.
3) Understanding and predicting RRT distribution in the carbonate system near, and away from, the wells.
4) Providing rigorously researched inputs for reservoir modelling and prediction.